

# Sacred Ecology

Neha Deopa\*<sup>1</sup> and Daniele Rinaldo<sup>†1</sup>

<sup>1</sup>University of Exeter and Land, Environment, Economics and Policy Institute

November 1st, 2025

## Abstract

Can religions shape ecosystems? We explore the role religious beliefs play in human-environment interactions by studying African Traditional Religions (ATR), which place forests within a sacred sphere. We focus on the unique case of Benin, whose history is deeply intertwined with traditional religions and where adherence is reliably reported. By exploiting three sources of exogenous variation in Benin's exposure to Charismatic Pentecostalism, we find that increase in ATR adherence yields positive changes in both forest and tree canopy cover. This increase is driven by sustainable land use policies rather than cooperation and shared governance mechanisms. To understand how ATR beliefs shape the way individuals combine the sacred and the ecology in their preferences, we build a theoretical framework of deforestation with heterogeneous pro-environmental attitudes driven by ATR adherence. Bringing the model to the data, we estimate that without any ATR adherence Benin would experience a loss of 10% of its tree canopy area, and would exhibit unsustainable deforestation rates. Our results show how ATR beliefs can play a fundamental role in forest and ecosystem conservation.

**JEL Codes:** Z12, Z13, Q5, O13

**Keywords:** African Traditional Religions, Deforestation, Pro-Environmental Attitudes, Benin

---

\*Corresponding author: n.deopa@exeter.ac.uk.

University of Exeter, Department of Economics, Rennes Drive, EX4 4PU Exeter, United Kingdom

<sup>†</sup>d.rinaldo@exeter.ac.uk

Acknowledgements: We are thankful to Alex Farrant at CloudRF for his precious insights on radio transmission modeling. We are also thankful for the comments and discussions with Ethan Addicott, Jean-Louis Arcand, Andrew Balmford, Ben Balmford, Ian Bateman, Nicolas Berman, Yann Bramoullé, Yannick Dupraz, Sam Engle, Romain Ferrali, Piergiuseppe Fortunato, Ben Groom, Jérémy Laurent-Lucchetti, Aakriti Mathur, Ugo Panizza, Max Posch, Kritika Saxena, Lore Vandewalle and Sarah Vincent, as well as seminar, workshop and conference attendees at PSE, AMSE, Montpellier, Cambridge, Trinity College Dublin, NEUDC, CSAE, EAERE and the Econometric Society.

# 1 Introduction

*Open your eyes, stranger, and know where to step. Here, a tree is not a tree, a spring is not a spring. Everything is mysterious and mystical.*

– Eustache Prudencio, *Vents du Lac*

Religion is a powerful means by which societies shape worldviews, knowledge systems and ultimately human behaviour. The influence religious beliefs can have on individual attitudes such as prosocial behaviour, interpersonal relationships and economic outcomes is well established (Guiso et al., 2006; Iannaccone and Bainbridge, 2009; Iyer, 2016). What is less known, however, is how religion can shape human interactions with nature. The ecological and anthropological literatures provide several examples of systems of indigenous people and local communities whose ecological knowledge is embedded within spiritual or religious beliefs and where nature is imbued with sacredness (Taylor et al., 2016; Berkes, 2017). This phenomenon is especially conspicuous on the African continent where sacredness of common pool resources is prevalent among communities that adhere to African Traditional Religions (ATR) (Fairhead and Leach, 1996; Sheridan and Nyamweru, 2008).

ATR are religions that are indigenous to Africa and are based on the fundamental belief that the sacred and the everyday are inseparable, making religious life indistinguishable from daily experience (Amanze, 2024). An important feature of the ATR worldview is that divinities are the personification of natural phenomena and spirits are known to inhabit rivers, streams, forests, mountains, and other natural occurrences on the African landscape. Forests, distinctly, have defined the physical and spiritual environment of ATR communities. Sacred forests and groves feature in all aspects of ATR culture: history, art, worship, medicine, and social structure (Koppell and Falconer, 1990; Aderibigbe and Falola, 2022). Despite the significant role belief systems play in shaping human behaviour, there is limited evidence and understanding of how religious beliefs drive human-ecosystem interactions, particularly for non-Abrahamic religions such as ATR.

This knowledge gap has important implications for global conservation policy and decision-making as there is a burgeoning interest in the conservation discourse to reformulate the people–nature relationship by recognizing the heterogeneous values of traditional belief systems (Anderson et al., 2022; Ives et al., 2024). Current environmental governance overwhelmingly ignores the cultural and spiritual ways in which people around the world understand, value, and relate to nature. According to IPBES (2022), this narrowness underpins the current biodiversity crisis. Religion, therefore, provides a relevant lens to understand the socio-ecological process that shapes nature values at both individual and collective levels. Leveraging these values will therefore allow global policy to achieve sustainable and more equitable conservation outcomes (Dasgupta, 2021).

Our study explores how adherence to ATR, a religion that facilitates a unique worldview where forest is a fundamental sacred symbol, impacts forest-related environmental outcomes in the Republic of Benin

in West Africa.<sup>1</sup> The inquiry of traditional religions commonly poses an empirical challenge: widespread under-reporting of ATR in national surveys, rooted in colonial missionary efforts that stigmatized these belief systems (Claffey, 2007; Stoop et al., 2019). Self-reported ATR adherence, therefore, tends to be a weak proxy for actual beliefs and practices. As a result, reported ATR affiliation often shows little variation across communities. We are able to overcome these challenges by leveraging the distinctive features of Benin’s history as the cradle of Vodun, the most prominent ATR. These features include traditional religions being explicitly recognized in the constitution, being granted their own national holiday and enjoying the same legal status as Christianity and Islam. Since ATR is not stigmatized, adherence is therefore freely and reliably reported, and shows considerable local heterogeneity which is consistent with Benin being amongst the countries with the highest religious diversity (Pew Research Center, 2014). To identify the link between ATR adherence and environmental outcomes, land-use change must be locally driven i.e. ecosystems should be shaped by individual and community decisions, which is the case in Benin as well as most sub-Saharan African countries. In Benin forests continue to play vital social roles as sites for cultural and religious practices (World Bank, 2020). The country is estimated to contain approximately 3,000 sacred forests and groves, frequently used for traditional rituals. This makes Benin an ideal scenario for us to investigate if indeed ATR beliefs can impact forest outcomes.

We study the problem by means of an instrumental variable approach, an exploration of channels and a theoretical framework that formalises ATR-driven pro-environmental attitudes, fit to data and used to obtain forest density counterfactuals. We use the latest three waves of the population census from 1992, 2002, and 2013, providing us with arrondissement-level (administrative division 3) information on socio-economic and demographic characteristics, including religion. The resulting dataset is a panel of 546 arrondissements observed over a period of 3 census years. We define ATR adherence as the percentage of individuals living in an arrondissement that self-report as following ATR. We identify the impact of ATR on three remotely sensed environmental outcomes: forest cover, tree canopy cover (TCC) and the decadal annual rate of change of TCC.

Our data allows for the econometric specification to incorporate a comprehensive set of environmental and socio-economic covariates, as well as a rich set of fixed effects. We first include arrondissement-level fixed effects, thus isolating the effect of ATR adherence from any time-invariant arrondissement-specific characteristics potentially associated with forests: geographic conditions such as proximity to rivers and baseline ecological endowments, historical exposure to conflict and colonial-era land policies. Second, and most crucially, we include department(state) $\times$ agro-ecological zone $\times$ year fixed effects, which forces identification to come from within agro-ecological zone comparisons inside a state in the same year. These fixed effects ensure that the estimates are not confounded by agro-ecological zone-wide shocks in a given state-year, such as targeted conservation and agricultural extension programmes, land suitability and weather anomalies specific to each zone-year. Additionally, they account for state-level shocks in a given year, such as political cycles and environmental policy shifts, and for cultural patterns shared within the state and zone such as land use customs and commodity booms and busts experienced due to agro-ecological suitability.

---

<sup>1</sup>Although ATR refers to African Traditional Religions, in all that follows we will refer to the acronym ATR as singular.

The OLS results support our hypothesis that high ATR adherence positively impacts forest outcomes. A remaining potential concern with the analysis is endogeneity, as ATR adherents may not be randomly distributed. For example, because of their beliefs and worldview adherents may choose to live in places that already have high forest cover. In this case ATR adherence would not cause improved forest cover; instead, forested areas would attract ATR adherents. We address the potential endogenous distribution of adherents using a novel instrument that exploits the introduction, rise and expansion of African Charismatic and Born Again Pentecostalism.

We build an arrondissement-year index instrument by exploiting three key sources of variation. First, the cultural and physical proximity of Benin to the earliest adopters of Pentecostal movement in West Africa i.e. the Yoruba ethnic group who in the 1970s facilitated the emergence of the holiness revival underpinning the present day Charismatic Pentecostalism (Peel, 1977; Marshall, 2019). Second, the dominance of Nigeria as the Pentecostal Republic and its aggressive role in the evangelisation of West Africa (Obadare, 2018). Third, the introduction of religious radio broadcasters due to the liberalization of the Benin radio broadcasting sector in 1997, post which the religious market in Benin saw a boom of new Born Again Pentecostals (Grätz, 2011). The first two sources capture the “Nigeria exposure” and utilize the linguistic distance between the ancestral language group of an arrondissement and the Yoruba language, the geographic (haversine) distance between each arrondissement and the Yoruba ethnic homeland, and the population density of Pentecostal adherents in Nigeria in each census year. The third source focuses on “within Benin exposure” and exploits the staggered introduction and variation in signal strength of the two extremely influential Pentecostal radio stations, Radio Maranatha and Radio Alléluia.

Using a combination of the Nigeria and Benin exposure we construct and assign to each arrondissement an index  $Z_{it}$  that increases with ATR adherence by being inversely linked to arrondissement-level exposure to Charismatic Pentecostalism. The idea behind the instrument is the following. As Charismatic churches across Africa strongly oppose traditional religions, often portraying them as sources of malevolent spiritual forces and expend considerable effort in proselytizing ATR, arrondissements which have high exposure (lower index  $Z_{it}$ ) will have a lower ATR adherence.

Consistently, the first stage documents a positive association between the instrument index and ATR adherence. Our 2SLS results show that on moving from a low ATR adherence arrondissement (25th percentile, 5% share of ATR) to a high ATR adherence one (75th percentile, 54% share of ATR) leads to an increase of approximately 59% of forest cover and 76% of TCC relative to the sample mean. We also find that a 1 percentage point increase in adherence slows the decadal average annual rate of canopy decline by around 40%. We address concerns to identification through a battery of robustness tests which show that our 2SLS results are unlikely to be spurious due to omitted variables or outliers. Crucially, our findings are robust when including ethnic homeland×agro-ecological zone×year fixed effects which account for differential trends arising from exposure to slavery which was at the ethnic group level, cultural norms and social structure. Moreover, placebo tests further show that neither exposure to a non-Yoruba ethnic group nor reception of a religious, but non Pentecostal, radio station affected forest outcomes. This indicates that the Yoruba-specific religious influence is central, and that simple access to religious radio, regardless of content, does not drive our results.

Given this evidence, we explore possible mechanisms underlying the positive impact ATR adherence has on forest outcomes. The first two channels we investigate are the presence of shared enforcement and governance of common pool resources within ATR communities (Ostrom, 2000), and the role played by ethnic fractionalization which affects cooperation and trust thus impacting resource use (Alesina et al., 2019). We do not find strong evidence supporting the relevance of these channels. Inspired by qualitative evidence given by Kraus (2012), Malapane et al. (2024) and Chief Atawé Akôyi A. (2025), which highlight that traditional religion adherents often tend to engage in activities that align with environmental stewardship and sustainable land use, we investigate if high ATR adherence arrondissements tend to display evidence of sustainable land use policies and practices. Despite data limitations on this dimension, we find a negative correlation between ATR and cropland expansion of rain-fed agriculture, the primary driver of deforestation in Benin. We also find that ATR is negatively related to two key land cover transitions responsible for environmental degradation: forests to agriculture, and savanna to agriculture. Finally, we show evidence that ATR adherence mediates the negative impact of cropland expansion on forest cover. The evidence suggests the use of sustainable land practices in ATR communities, and how ATR adherence might be conducive to a *spirit of sustainability*.

Based on this evidence, we want to better understand how ATR adherence shapes the preferences that generate the interplay between individual beliefs and the environment that we observe in the data. One cannot conclude from the reduced form alone whether the differences in forest use we observe stem from a sacralization of one’s own lived environment, where an adherent believes one’s own sacred forest needs to be protected, or from ATR-driven pro-environmental attitudes. These attitudes would then be reflected in individual preferences such that *all* of the forest, and not simply one’s own available stock, should be conserved. ATR adherence will therefore impact how the state of forests contributes to individual welfare over the long run. To explore this channel and to analyse counterfactual conservation policies that do not account for ATR, we build a theoretical framework for a large population of individuals (a mean-field game) who interact with each other and draw utility from the extraction of forest resources, calibrated by their level of adherence. We introduce two key features: heterogeneity in ATR adherence and pro-environmental attitudes. The latter are represented by the value that adherents assign to the state of the forest across the population, constantly determined by collective deforestation. We therefore model the effect of ATR adherence on individual preferences as the degree of substitutability between one’s own consumption of natural resources and the importance given to the global state of the resource.

Solving for the equilibrium strategy, we highlight three crucial model implications. First, we find that for any given population distribution of ATR beliefs, a higher individual adherence implies a lower individual deforestation rate, which fits the OLS/2SLS evidence. Second, a decline in the population ATR adherence (i.e. a change in the adherence distribution) will also decrease individual deforestation rates, proportional to one’s adherence. This result is driven by the fact that adherents, *ceteris paribus*, substitute to a greater degree individual forest use with conservation outcomes. This insight explains how a population with a low average adherence to traditional beliefs and a low average forest cover, such as Benin in 2013, can exhibit rich forest hotspots within local communities. Lastly, an increase in ATR adherence can switch unsustainable deforestation trends to sustainable ones *only* if adherents harbour

pro-environmental attitudes.

Bringing the model to the data, we use its estimates to build a counterfactual spatial tree canopy distribution where we assume a uniformly zero ATR adherence across the population. We obtain a canopy cover distribution which is first-order dominated by both the predicted and observed ones, yielding an average counterfactual canopy loss of approximately 10%. We find that if there had been no ATR adherents between 2002 and 2013, the deforestation rate would have been unsustainable, depleting all forest resources across the country in the long run. Furthermore, we find that areas in the southwestern and northwestern departments of Benin exhibit a sustainable estimated forest use policy due to their higher number of ATR adherents, which proves the salience of ATR-driven pro-environmental attitudes in the population's deforestation decisions.

Our results contribute to a burgeoning literature in economics that focuses on African Traditional Religions (Alonso et al., 2016; Alidou and Verpoorten, 2019; Stoop et al., 2019; Alidou, 2021; Le Rossignol et al., 2022; Butinda et al., 2023) and refines our understanding of the impact of religions beyond the Abrahamic faiths and within the developing world context (Iyer, 2016). There is also a parallel growing literature on the social impact of witchcraft and supernatural beliefs (Gershman, 2016; Nunn and Sanchez de la Sierra, 2017; Araújo et al., 2022). Such beliefs are not mutually exclusive to traditional religions in Africa, and can cut across social status, education, gender and ethnic and religious affiliations (Falen, 2018). Our paper also broadly contributes to the larger work on the economics of religion, both empirical and theoretical (Iannaccone, 1998; Bisin and Verdier, 2001; Guiso et al., 2003; McCleary and Barro, 2006; Becker and Woessmann, 2009; Iyer, 2016; Carvalho et al., 2019; Alesina et al., 2023; Becker and Voth, 2023; Espín-Sánchez et al., 2023; Ciscato et al., 2024; Montero et al., 2025), the role played by culture in public goods provision (Owen and Videras, 2007; Alesina et al., 1999, 2019; Bisin et al., 2024) and the political economy of deforestation (Pfaff, 1999; Burgess et al., 2012; Ferraro and Simorangkir, 2020; Baragwanath et al., 2023). In particular, our research focuses on the environment, something that the literature on religion has not yet systematically studied either within a quantitative or theoretical framework. To our knowledge, our paper is the first systematic empirical and theoretical evidence on the effect of religious beliefs on environmental outcomes. Our results have real-world policy relevance: land use policies that include salient local spiritual institutions can achieve more legitimate and effective environmental outcomes than purely market-based instruments. Our results also indicate that the lessons of traditional knowledge codified in religious beliefs, especially of the ecological kind, can have substantial significance for conservation efforts.

The paper proceeds as follows. Section 2 provides background on African Traditional Religions, and the historical and contemporary overview of Benin. Section 3 introduces the data and descriptive evidence. Section 4 presents our empirical strategy and the instrumental variable. Sections 5 and 6 discuss results and potential channels. Section 7 presents the model, the structural estimates and counterfactuals. Finally, section 8 concludes.

## 2 Background

### 2.1 African Traditional Religions & Forests

African Traditional Religions refer to the indigenous religions of the African continent and encapsulate a significant belief system, thought patterns, and ritual practices reflective of the culture and geography unique to Africa. The term “African Traditional Religions” has been used as a nomenclature by scholars such as [Idowu \(1973\)](#) and [Mbiti \(1970, 1990, 2015\)](#) to distinguish it from other *imported* religions practiced in Africa today such as Christianity and Islam. Although ATR varies widely from region to region and does not have sacred scriptures, and is without an all-encompassing founder or central historical figure, there are several common features that unify the traditional religions on the continent under the term ATR ([Aderibigbe and Falola, 2022](#)).

One such characteristic is the belief and veneration of divinities with expression in natural phenomena. These divinities are usually spirits that are associated with natural forces like rivers, lakes, trees, mountains and forests, which become central to communal rituals and are regarded as sacred. This is especially true for West Africa where nature’s sacred element has led to large pantheons of spirits and divinities. For example, in the coastal regions of West Africa, the water deity Mami Wata (Mother of Water) is highly revered and celebrated ([Drewal, 2008](#)).

Of particular interest within the ATR cosmology are trees and forests: from the Congo basin to the forests of Western Africa, they are thought of as a sacred place which is revered in the traditional belief systems as they are intimately linked with ancestry and cultural heritage. The value of forests go beyond utilitarian purposes and they are often seen as a natural boundary between the living and the spirit world. Forest trees can represent the links between the sky and earth, often symbolising links between the spiritual world of ancestors and people. For example, the *Iroko* tree (*Milicia excelsa*), also known as African teak, holds a significant place in West African culture and for Vodun adherents is one of the most important trees in Dahomey’s history with significant natural and traditional wealth. The deciduous characteristic of the trees give it an ambiguous image which reflects the tree’s power to give life and rebirth as well as to bring about death. In many African myths and stories, the tree is portrayed as an ancestral symbol of wisdom, authority and custom, providing a bond between the dead and the living ([Koppell and Falconer, 1990](#); [Juhé-Beaulaton, 2010](#); [Inyang, 2015](#)).

The inseparable link between religion and nature pervades traditional African religious life, and ATR worldview often advocates for preserving the harmony between humans and nature. This insight alludes to the possibility that ATR cosmology can represent a blueprint for ecological principles and adaptation that endeavours to maintain an equilibrium between natural resources and consumption, and is in line with studies in ecology and anthropology that demonstrate this result ([Reichel-Dolmatoff, 1976](#); [Taylor et al., 2016](#); [Berkes, 2017](#)). Considering the salient nature of forests and trees in ATR beliefs, it is of interest to further explore this relationship.

## 2.2 Benin: The Cradle of Vodun

The Republic of Benin is a combination of several distinct historical entities which continue to influence the socio-cultural and political dimensions of the country today. Appendix Figure A1 illustrates the contemporary and historical boundaries of the nation: the south-east is mainly composed of the Yoruba cultural group, who have historically been influenced by the Oyo Empire, and in present times by the social and political movements in Nigeria. The south-west was historically home to the hegemonic Kingdom of Dahomey which came about in the late seventeenth century and continues to remain culturally relevant in contemporary Benin.

Dahomey was defined to a great extent by its role in the Atlantic slave trade, and the consistent wars and slave raiding in the neighbouring regions resulted in a fusion of diverse religious beliefs and practices leading to the development of Vodun, one of the best known ATR (Manning, 2004; Claffey, 2007). The kingdom had a fierce reputation of being defiant to the introduction of Christianity and the constant efforts to resist evangelization was most evident in the fact that prior to colonisation most missionary efforts could not move beyond the port cities, rendering it almost impenetrable (Dupuis, 1998). In fact, converting to Christianity was an offense punishable by death in Dahomey. On the contrary, the neighbouring regions were embracing Christianity. This was especially true for the Yoruba hinterland as the destruction of the Old Oyo Kingdom and the presence of a significant number of established missionary posts led to a remarkable rise in Christianity while Vodun continued to flourish under Dahomey (Vaughan, 2016).

In the nineteenth and twentieth centuries, under colonial rule and the subsequent post independence communist dictatorship under Mathieu Kérékou, Vodun and other ATR in Benin were marginalized. In 1976, as a part of the sweeping modernization scheme, the Kérékou regime established anti-witchcraft laws and the risk of persecution and intimidation led to a sharp decline in ATR practices and a promotion of Christianity and Islam (Kahn, 2011). After the dismantling of the dictatorship in 1991, the new democratic leadership promoted ATR as part of a new Béninois national identity and Vodun was officially recognized as a religion within the constitution (Tall, 1995). In 1992, the president declared “Ouidah ’92”, a festival for embracing all ATR within the country, which continues to be celebrated today. The unique revival and acceptance of ATR in Benin allows one to safely surmise that self-reported ATR adherence in Benin is a reasonably good proxy for ATR beliefs.

Within the context of its environmental profile, Benin is located in the dry sub-humid zone of the Guinean forest-savanna mosaic, an important habitat for biodiversity. According to World Bank (2020) forest ecosystems in the country remain vastly underutilized. Aside from providing key ecosystem services, and representing a means for food security and poverty alleviation, forests in Benin also serve as a place for social, cultural and religious activities. For example, in Forêt Sacrée de Kpassè (Sacred Forest of Kpassè), a key location of Vodun worship which is located in Ouidah, the followers care for the forest, understanding that they are caring for their ancestors, whose spirits are reincarnated into Loko (Iroko) trees. Similarly, literature and poetry in Vodun often reference the importance and sacredness of forests.

Ossito Midiohouan (1999) provides an insightful example when discussing Béninoises singer-poets whose god, Aziza Nubodé, also god of hunters, inventor of music and composer of the first song which goes as follows:

*Aziza kun kwe bo malan gbé è*  
*Azwi gbé na nyo*  
*Aziza vi Nubodé kun kwe bo malan gbé è*  
*Azwi gbé na nyo ni*

which translates to:

*Aziza plays the flute to give homage to the forest*  
*Hare, the hunt will be fruitful*  
*Nubode, the young son of Aziza, plays the flute to give homage to the forest*  
*Hare, the hunt will be favorable.*

Although no official database exists, the Government of Benin estimates that the country has about 3000 sacred forests and groves covering 0.16 percent of the national territory. Benin is the only country in Africa that has implemented a national legislation, in 2013, aiming to recognize sacred natural sites as a category of Benin’s protected areas to maintain important ecological clusters. Consistent with the rest of the region, the highest rates of deforestation and agricultural expansion were observed in Benin during the 1970s and 1980s, in fact under the Kérékou regime the country experienced rampant destruction of several sacred forests and groves (Juhé-Beaulaton, 2006). Today, Benin continues to struggle with high forest loss due to smallholder and shifting agriculture, and according to Global Forest Watch (2025) between 2000 and 2023 the country’s tree cover decreased by 28%. For the interested readers who might be seeking more visual evidence, we refer to the excellent works of the art historian Dana Rush (Rush, 2001, 2010).

### 3 Data

**Measuring ATR Adherence:** We leverage data from the three latest waves of the Republic of Benin population census conducted in 1992, 2002 and 2013.<sup>2</sup> The census provides information on individual and household socio-demographic characteristics, including religion. Benin is subdivided into 12 departments with 77 communes, 546 arrondissements and 5,295 villages and cities, and our unit of empirical analysis is administrative division three i.e. arrondissements. We measure ATR adherence as the percentage or share of individuals living in an arrondissement  $i$  in census year  $t$  that self-report as following ATR.<sup>3</sup>

---

<sup>2</sup>The individual and household microdata consists of a random sample of 10% of person and household records from the censuses. The household file allows linkage between individuals in the same family and the same household.

<sup>3</sup>Whilst the 1992 census has a single category representing Traditional religions, the remaining two waves make a distinction between Vodun and “other Traditional religions”. For our analysis, we use ATR to encapsulate both categories, allowing comparability across the censuses.

Panel (a) of Appendix Figure A2 presents the adherence to different religions in Benin over time, and one can observe that while ATR was the dominant religion in 1992, its share dropped considerably by 2013. On the contrary, we observe the incredible rise of “Other Christianity” which is indicative of the booming African Pentecostalism phenomenon in West Africa and primarily consists of Charismatic Churches which emphasize the “Born Again” identity. The extent and the spatial distribution of ATR adherence within arrondissements changed significantly over time, as illustrated in Figure 1. The high adherence hotspots continue to be concentrated in the south west overlapping the old boundaries of the historical Dahomey Kingdom, and in the north west which is home to the Tammari people. Despite regional differences, all religions are practiced throughout the country and Benin ranks as one of the world’s highest in religious diversity index (Pew Research Center, 2014). This religious heterogeneity is evident in our sample as seen in panel (b) of Appendix Figure A2 which shows the religious fractionalization index across arrondissements over years.

**Environmental Data:** We study three environmental outcomes and rely on two separate datasets. In 2009 the European Space Agency (ESA) launched their Climate Change Initiative (CCI) programme aimed at providing high quality satellite-derived products of Essential Climate Variables (ECV), including global land cover (LC) as suggested by the Global Climate Observing System. The ESA-CCI-LC dataset presents consistent multi-temporal global LC maps at 300m spatial resolution covering 1992 to 2015 with one-year intervals. The data is binary as each pixel represents one type of LC classification. Unlike other remote sensing products that are based on single-year and single-sensor approaches, this dataset is generated using multiple sensors: Advanced Very High Resolution Radiometer (AVHRR), Systeme Probatoire d’Observation de la Terre Vegetation (SPOT-VGT), and PROBA-V. A total of 37 original LC types are presented using the LC Classification System developed for FAO with an overall global accuracy of about 71% (Defourny et al., 2009). However, classes such as cropland, forests, urban and bare areas have higher accuracy, while others such as mosaic classes have lower accuracy, making ESA-CCI-LC product especially useful for monitoring changes in forest cover and cropland expansion.

As defined in ESA (2017), Appendix Table A1 shows the land classifications relevant to this study, and for our main analysis we focus on the “forest” class. Appendix Figure A3 shows the spatial distribution of forests across Benin which is primarily dominated by broadleaved deciduous tree cover. The year 1992 has a low forest distribution relative to 2002 and 2013 which is consistent with the fact that in West Africa the largest phase of conversion of natural vegetation such as forests and other wooded land to agriculture occurred before the 1990s (Gibbs et al., 2010). The main land transition observed during our sample period is open deciduous forest regrowth (indicating secondary forest regrowth) and agricultural expansions (represented by rain-fed croplands), both at the expense of shrublands or savanna ecosystems as seen in Appendix Figures A4 and A5 (Tappan et al., 2016).

These trends are consistent with the second dataset we use which is NASA’s Making Earth System Data Records for Use in Research Environments (MEaSUREs) Vegetation Continuous Fields Version 1 data product (VCF5KYR) created by Song et al. (2018) and has been recently used in studies such as Sanford (2023) and Baragwanath et al. (2023). The data provides historical annual global fractional vegetation cover (FVC) during the time of the local peak growing season, for the time period 1982 - 2016. Each pixel

is characterized by the percentage of tree canopy cover ( $\geq 5$  metres in height) at  $5.6 \text{ km} \times 5.6 \text{ km}$  spatial resolution. FVC is a primary means for measuring global forest cover change and is a key parameter for a variety of environmental and climate-related applications. The dataset is derived from a bagged linear model algorithm using Long Term Data Record (LTDR version 4) compiled from AVHRR observations.

Unlike the ESA-CCI-LC dataset which is binary, VCF5KYR is continuous, providing an estimated percentage of tree cover in a given pixel. Moreover, as this data product starts 10 years prior to the first census wave in 1992 it allows us to also explore the annual rate of change of tree cover.<sup>4</sup> The first outcome studied, forest cover, uses the ESA-CCI-LC data to calculate the share of pixels in each arrondissement  $i$  in year  $t$  that are of forest class i.e. percentage share of forest cover. Second, using the VCF5KYR continuous dataset we aggregate and calculate the mean percentage of tree canopy cover (TCC) for arrondissement  $i$  in year  $t$ . Finally, following FAO guidelines and Puyravaud (2003), we study the annual change rate of TCC over approximately a decade-long period, calculated as  $r_{it} = (1/\Delta t) \times \ln(\text{TA}_{it}/\text{TA}_{it-1}) \times 100$  where TA is total area of tree canopy cover.<sup>5</sup> This gives the average annual growth rate that would compound to the total 10-year change and capture sustained, long-term effects rather than short-term fluctuations.

## 4 Empirical Strategy

This section presents the main empirical strategy, sub-section 4.1 discusses its identification challenges and 4.2 gives insights into the instrument. For our baseline results we use the following specification:

$$Y_{idzt} = \beta \text{ATR}_{it} + \boldsymbol{\theta} \mathbf{X}_{it} + \alpha_i + \phi_{dzt} + \epsilon_{idzt} \quad (1)$$

where  $Y_{idzt}$  denotes forest cover, TCC and annual rate of change of TCC in arrondissement  $i$ , department  $d$  and agro-ecological zone  $z$  in census year  $t$ , as defined in section 3. We note that the eight agro-ecological zones of Benin cut across administrative departmental boundaries. Specification (1) includes a rich set of fixed effects. The arrondissement-level  $\alpha_i$  fixed effects absorb any time-invariant characteristics that may correlate with both the outcomes studied and ATR adherence, such as the historical or initial stock of forests and protected areas, distance to rivers and the Atlantic coastline, baseline proximity to markets and road access, precolonial structures, historical exposure to conflict, as well as colonial-era land policies. Crucially, by including department (state)  $\times$  agro-ecological zone (aez)  $\times$  year time fixed effects  $\phi_{dzt}$  we can isolate several sources of shocks. We account for state-level shocks in a given year such as policy and governance changes that may trigger or impede deforestation, aez-wide shocks in a given state-year such as weather anomalies and climate trends affecting crop viability, profitability and timber production, aez-specific pressure of pastoralist migration and other traditional land managements systems in an ecological corridor in given year, and targeted conservation and agricultural programmes that often operate at a state-aez level. The fixed effects  $\phi_{dzt}$  thus absorb time-varying shocks affecting outcomes of

<sup>4</sup>Further technical details about the procedure used in building VCF5KYR data is provided in the documentation provided by NASA at [https://cmr.earthdata.nasa.gov/search/concepts/C1452975608-LPDAAC\\_ECS.html](https://cmr.earthdata.nasa.gov/search/concepts/C1452975608-LPDAAC_ECS.html)

<sup>5</sup>Since the census are spaced approximately 10 years apart,  $\Delta t$  for the year 1992 is the difference taken from the year 1982.

arrondissements within the same aez in the same department in a common fashion. Appendix Figure A6 visually presents the various boundaries of the fixed effects for the readers to get a better understanding of their geography.

Finally, to further pin down the effect of ATR and to account for differential trends in local conditions and determinants of change in the dependent variables that are correlated with ATR adherence, we include arrondissement level covariates  $\mathbf{X}_{it}$ . These include socio-economic characteristics such as rate of illiteracy, share of poorest households, share of informal employment, population density, nighttime lights intensity, and to account for trends in agricultural practices for the main crops harvested: maize, cassava and cotton soil suitability interacted with a linear time trend. Our specification also controls for share of catholic adherents as the Catholic church has been important in Benin’s socio-political space with Catholic elites being powerful political players in the development of the country (Claffey, 2007). Additionally, climatic and geographic controls include precipitation, minimum and maximum temperature, elevation and the latitude and longitude of the arrondissement centroid interacted with a linear time trend to capture change in access and built environment. Summary statistics of the controls are provided in the Appendix Table A2 and a discussion of the data sources used is provided in the Appendix Section B. The coefficient of interest  $\beta$ , therefore, captures the marginal impact of an increase in the adherence of ATR. Finally, standard errors are clustered at the arrondissement level and shown within parentheses.

#### 4.1 Identification and relevance

Let us now consider the effect of the two main sources of bias separately. First, attenuation bias, since ATR may be measured with error, particularly due to syncretism in the population. Although the choice of Republic of Benin mitigates this issue to a large extent, the trend across the African continent is that individuals tend to under-report ATR adherence. Therefore, if increasing ATR has a positive impact on the environmental outcomes, as we will find, this would cause us to understate the effect of ATR by estimating a positive coefficient but smaller in magnitude than the true effect. Second, and most importantly, endogeneity may exist due to the potential non-random allocation of ATR adherents across space and time, as it may be the case that due to the importance of forests within the ATR cosmology, adherents may have a preference to settle in areas with pre-existing high forest cover. To address this bias, we rely on an instrumental variable approach. We exploit the spatial and temporal variation in the rise of new denominations of Christianity, specifically Charismatic and Born Again Pentecostal Christianity across Benin.

The relevance of our instrument hinges on three important facts: first, the Yoruba ethnic group were early adopters of the Pentecostal movement in West Africa and have played a key role in its spread. The origin of independent Christianity in the region can be traced back to 19th century in the Oyo - Yoruba empire due to the early presence of the English Church Missionary Society (Gaiya, 2002). In 1916 as a result of a religious revival very similar to the evangelical revivals in Europe and America in the 18th century, Yorubaland (present day southwestern Nigeria) saw an emergence of Aladura churches which

emphasized prayer, performance of miracles and their leaders tended to display a charisma unseen in traditional churches. By the 1930s Aladura Churches began to further integrate elements of Pentecostal discourse and practices, and in the 1970s the “holiness revival” resulted in a substantial surge of new followers where the messages of revival and born-again conversion played an important role (Marshall, 2019). Peel (1977) highlights that on introduction of Christianity to the Yoruba, they were creative in transforming their new religion by becoming more evangelical, more spiritual, incorporating elements of what is today referred to as African Pentecostalism and more aggressive in spreading the movement.

Second, Charismatic churches across Africa vehemently reject indigenous and traditional religions which they diabolize and construe as harbingers of evil spirits. This fact is evidenced in Benin by President Mathieu Kérékou, the former military-Marxist dictator between 1972 and 1991 who returned to power via democratic elections in 1996, and used Pentecostal discourse as a political discourse, specifically presenting himself as a Born Again Christian. He thus distanced himself from his Marxist-military past associated with the “occult forces” of Vodun (Camilla, 2005). Simultaneously, the country experienced an unprecedented growth in new Christian churches and Charismatic Pentecostalism became a very visible part of the public sphere. According to the 2001 census conducted by the Christian project ARCEB (Action pour la recherche et la croissance des Églises au Bénin) the country saw nearly 4000 local congregations of new Pentecostal denominations (Mayrargue, 2005). This increase was in a large part due to Benin’s media sector undergoing liberalization, and from 1997 onward enabling the establishment of independent radio and television networks. The liberalization led to an enormous proliferation of religious radio broadcasting in various forms, from establishing independent stations to contracting broadcasting hours on local stations. In 2013, the main licensed Christian broadcasters in the country were Radio Immaculée Conception (established in 1998), the broadcaster of the Roman Catholic Church, and the two Charismatic Pentecostal broadcasters: Radio Maranatha (established in 1998) and Radio Alléluia (established in 2003) (Grätz, 2011). The latter two’s media strategy was to Christianize popular culture for consumption by Born Again Christians which involved persistent efforts to evangelize and portray a negative view of ATRs in Christian dominated media (Hackett, 1998; Asamoah-Gyadu, 2009). We observe the success of this phenomenon in our data, as seen in Panel (a) of Appendix Figures A2 and A7 which show the spatial distribution and rise of other denominations of Christianity in Benin contrasted with the decline of ATR in Figure 1.

The last relevant fact is Nigeria’s key role in establishing trans-national religious networks to facilitate the expansion of Pentecostalism from Nigeria into other West African countries. Ojo (2005) attributes the rise of Nigerian Pentecostalism to the creation of mega-churches with multi-ethnic congregations that are dynamic religious enterprises building extensive cross-border networks, engaging in missionary campaigns, and shaping a regional Christian identity. These churches have strategically expanded into neighboring countries through transnational mobility of pastors and members, and aggressive media outreach. Most importantly, Ojo (2005) emphasizes the ideological convictions among Nigerian Pentecostals that God has entrusted the evangelisation of Africa in their hands, positioning Nigeria as a Pentecostal hub in the sub-region. This is accompanied by the flourishing trade and exchange of Pentecostal products, such as recorded audio and video cassettes, home video films on religious themes and devotional literature

which are produced mainly in Nigeria and distributed widely in the West African region (Ukah, 2005). Furthermore, Mayrargue (2002, 2005) highlights the role of Nigeria in influencing the religious makeup of Benin and how it is primarily churches which originated in Nigeria that propagated the Christian renewal of the 1990s in Benin. For example, Kérékou’s pastor and spiritual advisor who converted him, underwent pastoral training first in Nigeria at the Foursquare Pastoral School.

## 4.2 Building the instrument

Drawing on these three observations, we construct an instrument that leverages both Nigeria’s historical and ongoing influence, as well as Benin’s domestic exposure to Pentecostalism that emerged in the mid-1990s. We create an index  $Z_{it}$  that increases with ATR adherence by being inversely linked to arrondissement-level exposure to Charismatic Pentecostalism:

$$Z_{it} = \underbrace{\frac{\text{HD}_i^{\text{YORUBA}} \times \text{LD}_i^{\ell, \text{YORUBA}}}{\text{Density of Pentecostals in Nigeria}_t}}_{\text{Exposure from Nigeria}} \times \underbrace{\text{RP}_{it}^c}_{\text{Within-Benin exposure}} \quad (2)$$

**Exposure from Nigeria:** The first term in the numerator,  $\text{HD}_i^{\text{YORUBA}}$ , is the haversine distance of each arrondissement  $i$  from the ethnic homeland of the Yoruba group as given by Murdock (1967) and illustrated in Appendix Figure A8. We use the haversine distance (a particular type of geodesic distance) in order to account for the Earth’s curvature by measuring the shortest arc (great-circle) between each point. The second term in the numerator,  $\text{LD}_i^{\ell, \text{YORUBA}}$ , is a measure of linguistic distance to the language Yoruba. In order to compute this term, we first assign each arrondissement  $i$  to a language group  $\ell$  based on the language map in Ethnologue using the data provided by Giuliano and Nunn (2018). We then calculate  $\text{LD}_i^{\ell, \text{YORUBA}}$  as the measure of linguistic distance that represents how different is the language group  $\ell$ , to which arrondissement  $i$ ’s language belongs, from the Yoruba language.

As is standard in the literature, we use linguistic trees in the Ethnologue database and for each language, the Ethnologue provides a classification starting with the language family followed by nodes, that is, the branching points of the linguistic tree (Desmet et al., 2012; Guarnieri, 2025). Following Guarnieri and Tur-Prats (2023), we calculate the distance between the arrondissement language  $\ell$  and the Yoruba language, based on the number of common nodes in the tree, as follows:

$$\text{LD}_i^{\ell, \text{YORUBA}} = 1 - \left( \frac{\# \text{ of common nodes between languages } \ell \text{ and Yoruba}}{\frac{1}{2} \times (\# \text{ of nodes for language } \ell + \# \text{ of nodes for language Yoruba})} \right)^\lambda \quad (3)$$

For example, the language Baatonum is classified as: Niger-Congo, Atlantic-Congo, Volta-Congo, North,

Gur, Bariba. The Yoruba language is classified as: Niger-Congo, Atlantic-Congo, Volta-Congo, Benue-Congo, Defoid, Yoruboid, Edekiri. These two languages have three nodes in common (Niger-Congo, Atlantic-Congo, Volta-Congo) and using (3) the linguistic distance between the two languages is 0.321. Languages originating from different families have no nodes in common, and their distance will be equal to 1. The parameter  $\lambda$  ranges between 0 and 1 and is used to attribute higher weight to earlier common nodes, as early separations in the language tree are likely to signify larger cultural divergence on average than later separations. In practice, we follow Fearon (2003) in assuming  $\lambda = 0.5$ .

$LD_i^{\ell, \text{YORUBA}}$  captures frictions to the diffusion of Pentecostalism as religious ideas diffuse more easily between linguistically close groups (translations, preaching and networks). The Charismatic Pentecostal movement is especially known for the use of local languages in both audio and visual media as a tool for evangelization. As Nigeria is the biggest exporter of such products, they are primarily in Yoruba or English, while translations to French and local productions can take significant time (Mayrargue, 2005; Ojo, 2005). Therefore, linguistic proximity to Yoruba language is predictive of Pentecostal adoption/intensity. Similarly, the haversine distance from the Yoruba homeland, origin point of Charismatic Pentecostal movement in the region, captures its diffusion as communication and missionary frictions rise with distance, and predict exposure to Pentecostalism in Benin. Both  $LD_i^{\ell, \text{YORUBA}}$  and  $HD_i^{\text{YORUBA}}$  capture plausibly relevant channels of diffusion, adoption of new denomination of Christianity and displacement of traditional religions. Therefore, the greater are these distances, the higher is adherence to ATR. Finally, this is inversely weighed by the density of Pentecostal population in Nigeria at time  $t$ , capturing how over time Pentecostalism has become a major cultural force in Nigeria and the country’s prominent role in the aggressive exporting of Pentecostalism to Benin.

**Within-Benin exposure:** The second part of the instrument focuses on the domestic exposure that only began post 1997. To capture this we exploit the staggered introduction of the only two Pentecostal radio broadcasters that existed in Benin up until 2013. Radio Maranatha (RM), which was established by a union of several evangelical churches in Benin, the Conseil des Églises Protestantes et Évangéliques du Bénin (CEPEB), and whose first station opened in Cotonou in 1998. Today, the station continues to broadcast in French, Dendi, Yoruba and Fongbé languages, and offers a wide range of programmes featuring music, Bible teachings and call-in shows. One of its most popular programmes is *Témoignages* where believers and converts testify to their religious lives and spiritual experiences. RM’s second station opened in 2003 as a regional branch in Parakou to establish a closer relationship with listeners in the north of Benin, and instantly became popular among regional pastors as an important part of their proselytisation efforts. Grätz (2014) analyzed RM Parakou’s programming structure, discursive tendencies and the motives of the actors involved. Below we provide excerpts from his March 2013 interviews with Pastors who hosted shows on the station:

*“I reach more people with the radio broadcasts, including those far away from my parish. Furthermore, many people prefer to listen to radio programmes instead of attending church services. My programme is another kind of evangelisation, and I think a very effective one.”*

*“My father is originally from Nigeria, so I have family I frequently visit. On these occasions, I always*

*purchase some of the latest gospel hits in Yoruba, which I subsequently use during my shows – they are especially liked by my listeners.”*

These excerpts emphasize the significance of Radio Maranatha as one of the most prominent Charismatic Christian radio stations in Benin and the role it played in shaping contemporary Pentecostal and evangelical life. It also highlights the relevance of Yoruba language in evangelization. The second broadcaster, Radio Alléluia (RA) was founded in 2003 by one of the rapidly growing Charismatic Pentecostal churches in Benin *Chrétianisme Céleste*, and is situated in the country’s capital Porto-Novo. Majority of their members are converted Christians and the church imposes a strict code of conduct and worship, practices spiritual healing and argues strongly against traditional religions. The station programmes promote hopes of deliverance, spiritual assistance along with a wide range of developmental and entertainment shows, keeping in line with the values of the church (Grätz, 2011).

Following Olken (2009) and Wang (2021), we use data on transmitter characteristics of the three stations of RM and RA to calculate the signal strength or received power  $RP_{it}$ , measured in decibel-milliwatts (dBm), for each transmitter-arrondissement pair using a radio propagation modelling software which utilizes the Longley-Rice or Irregular Terrain Model (ITM).<sup>6</sup> ITM is the standard framework used in the telecommunication industry, and factors in electromagnetic theory, terrain features, diffraction and radio measurements to predict the attenuation of a radio signal at a given point on the earth. The International Telecommunication Union (ITU), whose standards are used by several African broadcasting regulators, indicates that usable FM reception typically begins at signal levels between  $-70$  dBm and  $-60$  dBm (ITU, 1998). Therefore, the signal strength for 1992, when no religious broadcasting existed in Benin, is assumed to be  $-90$  dBm reflecting significant transmission loss and effectively zero exposure. In 2002, RM’s first transmitter in Cotonou was operational, and by 2013 all three stations had been established. For 2013, the coverage of each arrondissement is defined by the maximum signal strength among all transmitters i.e. by the transmitter providing the strongest reception.

The key concern here is that  $RP_{it}$  depends by construction on the terrain configuration of the arrondissement, which in turn may be correlated with the drivers of forest cover. Whereas Olken (2009), Yanagizawa-Drott (2014) and Wang (2021) deliberately exploit the topographical variation, our objective is to obtain a measure of signal strength which is purged of these terrain-related influences. Although our specification (1) controls for elevation, a better approach is to first partial out terrain characteristics from signal strength and obtain  $\widetilde{RP}_{it} = RP_{it} - \hat{\varphi}(\text{terrain}_i)$  where  $\varphi$  is estimated using a generalized linear model in order to account for nonlinearities between the two, shown in Appendix Figure A9. For accuracy we use the same terrain data as inputted by the software in modelling the radio propagation.<sup>7</sup> However, even after residualizing terrain from signal strength, we may still not be able to capture all unobservable characteristics that jointly drive radio transmission, terrain and forest cover. We address this by following Borusyak and Hull (2023), and generate a measure of “expected” signal strength  $\overline{RP}_{it} = \frac{1}{K} \sum_{k=1}^K (RP_{it} - \hat{\varphi}(\text{terrain}_i^k))$ , now residualized over  $K = 1000$  terrain permutations, in

<sup>6</sup>In consultation with a radio engineer, we used “CloudRF” software. For more information refer to <https://cloudf.com/about/>

<sup>7</sup>CloudRF uses Shuttle Radar Topography Mission (SRTM) Global 30m resolution data

which we calculate the average counterfactual signal strength for each arrondissement over all possible terrain features. We then obtain a re-centered residualized measure of radio exposure  $RP_{it}^c = \widetilde{RP}_{it} - \overline{RP}_{it}$ . Although radio signal strength is negatively related to ATR adherence due to greater exposure to Charismatic Pentecostalism, to understand the direction of the effect for the re-centered and residualized signal strength, we regress the arrondissement-level ITM-based signal strength  $RP_{it}$  on our measure  $RP_{it}^c$  with year fixed effects which yields a coefficient of  $-13.93$  (s.d.  $0.63$ ). This confirms that  $RP_{it}^c$  is positively related to ATR adherence, and we normalize it to be between 0 (perfect signal, full exposure) and 1 (no signal, zero exposure), which is consistent with both distance measures in the numerator of  $Z_{it}$ .

Appendix Figure A10 illustrates the distribution of the three sources of exogenous variation used in building the instrument:  $LD_i^{\ell, \text{YORUBA}}$ ,  $HD^i$  and  $RP_{it}^c$ . For the 2SLS estimation, the first stage equation is specified as:

$$\text{ATR}_{it} = \omega Z_{it} + \delta \mathbf{X}_{it} + \alpha_i + \phi_{dzt} + \nu_{it} \quad (4)$$

where  $Z_{it}$  is given by (2) and the intuition is that greater is  $Z_{it}$ , the lower is the exposure to Charismatic and Born Again Pentecostalism, and higher is the ATR adherence. The second stage takes the instrumented ATR as a regressor, and the specification becomes:

$$Y_{idzt} = \beta \widehat{\text{ATR}}_{it} + \theta \mathbf{X}_{it} + \alpha_i + \phi_{dzt} + \epsilon_{idzt} \quad (5)$$

With  $Z_{it}$  we are able to identify the exogenous variation in ATR. The validity of the IV estimates rest on the assumption that the differential exposure to Charismatic Pentecostalism affects the environmental outcomes today only through its impact on ATR, conditional on the covariates included in the regression.

## 5 Results

Panel A of Table 1 presents the OLS results, confirming our hypothesis that an increase in ATR adherence has a positive impact on forest cover, tree canopy cover and the annual rate of change in TCC. Tackling the endogeneity concerns, Panel D reports the first-stage estimate from equation (4) showing a strong and significant relationship between the instrument and ATR adherence. Consistent with the discussion in sections 4.1 and 4.2, we find that greater is  $Z_{it}$ , indicative of a low exposure to Pentecostalism, and higher is ATR adherence. The [Olea and Pflueger \(2013\)](#) effective F-statistic of 29, with a critical value of 10% bias of 23.1, gives us further confidence that the instrument is sufficiently strong.<sup>8</sup> In Panel C, we find that there is a positive reduced-form effect of  $Z_{it}$  on the outcomes, which is reassuring for the validity of the instrument. Finally, Panel B reports the 2SLS estimates with the square brackets showing the 95% Anderson-Rubin (AR) confidence intervals which are robust to weak identification and are efficient in the just-identified case ([Andrews et al., 2019](#)). We find that a 1 percentage point increase in ATR adherence increases forest and tree canopy cover by 0.17 and 0.25 percentage points. This implies that

<sup>8</sup>In a just-identified model the effective F statistic reduces to robust F and thus coincides with the [Kleibergen and Paap \(2006\)](#) Wald statistic.

if an arrondissement moves from low ATR adherence levels (25<sup>th</sup> percentile, 5% ATR share) to high ATR adherence (75<sup>th</sup> percentile, 54% ATR share) it leads to an increase of approximately 59% forest cover and 76% TCC relative to the mean. Panel B column (3) shows that ATR has a positive impact on the annual rate of change in TCC. As the sample mean is -0.42%, the average arrondissement is experiencing deforestation. We find that a 1 percentage point increase in adherence reduces tree canopy loss by approximately 40% or, equivalently, slows the average annual rate of canopy decline by 0.172 percentage points.

We find that the magnitude of the coefficients increase significantly compared to the OLS specification, indicating that the original coefficients were biased downwards. This may be due to attenuation bias or simply because the 2SLS estimates reflect the average effect for observations that comply with the instrument, i.e., a local average treatment effect. In our setting, compliers are the arrondissements where ATR adherence is sensitive to the Pentecostal exposure. This includes arrondissements where adherents are more likely to convert if exposed to high levels of evangelizing forces (linguistic and physical distances, radio signal) that displace traditional religions, less likely to convert if exposed to low levels of Pentecostalism, but does not include arrondissements whose ATR adherence levels are unaffected by the diffusion of Pentecostalism over time. The IV estimate is therefore a local average treatment effect of ATR adherence on forest outcomes for those arrondissements whose ATR share moves when Pentecostal exposure shifts.

## 5.1 Threats to identification

A unique advantage of using the linguistic distance from the Yoruba language is that it is plausibly exogenous to ecological characteristics that could impact environmental outcomes today such as forests and tree canopy. A potential issue here may be that language proximity might correlate with conflict or trade, which in turn can impact deforestation (Burgess et al., 2015; Abman and Lundberg, 2020). However, these are not particularly concerning issues in our case. For the conflict related channel, we find that during our sample period Benin experienced very low levels of conflict and was relatively stable as seen in Appendix Figure A11. The event with highest frequency was of type “peaceful demonstrations” compared to events which are likely to impact forest outcomes such as “armed clash” and “attacks” which occurred far less frequently. Second, if this channel was in play, we would expect greater linguistic distance from Yoruba to indicate greater likelihood of conflict between Yoruba and local groups, thereby leading to higher deforestation. In contrast, our data shows that higher  $LD_i^{\ell, \text{YORUBA}}$  is associated with improved forest outcomes, which mitigates concerns that conflict could be driving the observed relationship.

Regarding the trade channel, we note that Melitz and Toubal (2014) show that the primary source of linguistic influence on bilateral trade is information rather than ethnicity, our instrument only uses the linguistic distance from the language Yoruba, while the commonly spoken languages (CSL) relevant for trade in Nigeria are English and Hausa, therefore  $LD_i^{\ell, \text{YORUBA}}$  is less likely to be capturing the trade relations between the two countries. However, while technically Nigeria is not Benin’s largest export

partner (it's China, followed by India for 2013), there continues to exist extensive informal trade between the two. Benin is referred to as the 'entrepôt state' vis-à-vis its neighbours, particularly Nigeria and aims to expand its role as a transit trading hub, importing goods and re-exporting them to Nigeria, thus profiting from the distortions in Nigeria's economy (Golub, 2012). Linguistic distance might then relate to deforestation via the necessity of clearing forests for the creation of trade-improving road networks. Any effect and spillovers coming in through this channel should be accounted for by our fixed effects, and controls such as household income and employment. Furthermore, we use data from Bensassi et al. (2019), who map all the informal trading hubs in Benin, defined as the most commonly used border crossings or port access for informal trade with Nigeria by arrondissement. We estimate the 2SLS specification by interacting  $ATR_{it}$  with an indicator variable equal to one if the arrondissement has any of such trading hubs, zero otherwise. In Table 2 Panel A we find that the impact of ATR is not significantly different for arrondissements with and without informal trading hubs.

The use of haversine distance from the historical Yoruba homeland boundary, which is outside of the modern day Republic of Benin and overlapping contemporary state borders in Nigeria, is unlikely to be correlated with political characteristics influencing forest policies within Benin. Even though our specification controls for a plethora of environmental and geographical characteristics, there may still be some concern that this distance might correlate with unobservables that determine forest cover dynamics. Therefore, in Table 2 Panel B we drop  $HD_i^{YORUBA}$  and simply use  $Z'_{it} = \frac{LD_i^{\ell, YORUBA}}{\text{Density of Pentecostals in Nigeria}_t} \times RP_{it}^c$  as an instrument. We find that although the estimates are weaker in significance they are still positive and the magnitudes are similar. The final concern for identification is that the location of the radio transmitters may be endogenous to environmental outcomes. It is important to highlight that unlike the Catholic Church which has been historically a wealthy institution, the new wave of Pentecostal churches had limited budget and their transmitter placement decision was driven purely by convenience and to reach as many people as possible (Claffey, 2007; Grätz, 2011). Indeed, the three transmitters were located in the three largest cities of Benin: Cotonou (RM1), Porto Novo (RA) and Parakou (RM2). Therefore, while transmitter placement may be jointly determined by population and economic density, our specification controls for all of these. To this avail, we build our instrument using only the exposure from Nigeria  $Z''_{it} = \frac{LD_i^{\ell, YORUBA}}{\text{Density of Pentecostals in Nigeria}_t}$  and obtain equivalent, if slightly larger, estimates with a weaker F-stat, shown in Panel C of Table 2.

**Placebo test:** We provide additional evidence for the validity of our identification strategy by undertaking a placebo test and estimating the reduced-form equation using two placebo instruments. For the first placebo, as opposed to the Yoruba-Pentecostal relation we examine the impact of the Gurma ethnic group whose homeland overlaps with Northern Benin, and who did not play a role in the diffusion of Pentecostalism and displacement of ATR. The Gurma ethnic group primarily consists of a mix of traditional and Islamic adherents due to the proximity to the sub-Saharan trade routes, and historically Islam has not been involved in targeted proselytizing of ATR adherents in Benin during our sample period. Appendix Figure A8 highlights the Gurma homeland relatively to the Yoruba homeland. Therefore, if our identification strategy is valid, then constructing the following placebo instrument:  $\tilde{Z}_{it} = \frac{HD_i^{Gurma} \times LD_i^{\ell, Gourmanché}}{\text{Density of Pentecostals in Nigeria}_t} \times RP_{it}^c$  should not have a significant impact on the environmental

outcomes as the original instrument in (2) does.

For the second placebo, we focus on the within-Benin exposure but instead use data on the transmitters of Radio Immaculée Conception, the broadcaster of the Roman Catholic Church. As discussed in Section 4.2, we calculate the re-centered and residualized signal strength  $RIC_{it}^c$  from the eight stations of Radio Immaculée Conception that were installed between 1998 and 2003. Appendix Figure A12 shows the locations of the transmitters. If our instrument is valid, then constructing the placebo instrument  $\tilde{Z}_{it} = \frac{HD_i^{YORUBA} \times LD_i^{\epsilon, YORUBA}}{\text{Density of Pentecostals in Nigeria}_t} \times RIC_{it}^c$  which focuses on religious broadcasting but not one that is actively targeting and displacing ATR, should have no effect on the outcomes. The results of the placebo test are reported in Figure 2, which reproduces the baseline reduced-form estimates from Panel C of Table 1 for comparison. Unlike  $Z_{it}$ , using the two placebo instruments, we do not estimate a statistically significant relationship between the placebo index and the dependent variables. Overall, the estimates provide confirmation of the validity of our estimation strategy.

## 5.2 Robustness

As our instrument exploits diffusion of Pentecostalism, there is the possibility of local spillovers and it may be likely that residuals are spatially correlated across arrondissements in a way that decays with distance, and simple clustering isn't appropriate. Appendix Figure A13 shows that the 2SLS estimates are robust to computing spatial HAC errors. In Table 3 we examine the sensitivity of the 2SLS estimates to the use of alternative specifications. Column (1) shows the baseline estimates for reference and in column (2) we adjust for two-way clustering within departments and within agro-ecological zones to account for within-group correlation of the residuals. Columns (3) and (4) calculate the linguistic distance with the parameter  $\lambda = 0.25$  and  $\lambda = 0.75$  and we continue to find our results robust to these checks. An additional concern may be the historical exposure to the Atlantic slave trade which may have impacted the baseline ecological characteristics of regions or evolution of social characteristics such as trust, which is known to have an impact on governance of common pool resources (Nunn and Wantchekon, 2011; Alesina et al., 2019). Although our specification controls for differential state trends through department  $\times$  aez  $\times$  year time fixed effects, one can argue that exposure to slavery was at the ethnic group level rather than an administrative division such as department. Therefore, in column (5) of Table 3 we replace the above with Murdock ethnic homeland  $\times$  aez  $\times$  year fixed effects. We find the 2SLS estimates continue to be robust. In section 4.2 we build  $RP_{it}^c$  assuming -90dBm as effectively indicating zero exposure, therefore, in column (6) we change this to -100dBm and find our results remain consistent. Finally, in column (7) we also show the robustness of our results to using non-re-centered radio signal strength, and instead use the free space radio propagation model which assumes the earth is smooth and without any geographic or topographic obstacles, thus making the signal strength independent of the terrain characteristics. This model can be considered the theoretical maximum for the received power.<sup>9</sup>

<sup>9</sup>The free space received power/signal strength is straightforward to calculate given the effective radiated power (ERP) which is converted to the Equivalent Isotropic Radiated Power (EIRP). The basic transmission loss in free space is calculated from the ITU-R P.525 (ITU Recommendation, 2019) given by  $Loss = 32.45 + 20 \log_{10}(f_{MHz}) + 20 \log_{10}(d_{km})$  where  $f_{MHz}$  is frequency and  $d_{km}$  is the distance of the arrondissement centroid to the transmitter location. Then the signal strength in

## 6 Channels

These results raise the intriguing question of why adherence to ATR leads to a positive environmental impact. In this section we explore the potential mechanisms at play behind the evidence we have shown so far.

### 6.1 Shared governance and ethnic fractionalization

Baland and Platteau (1996) and Ostrom (2000) have shown that users of common-pool resources can and often do self-govern effectively, including enforcement through monitoring and graduated sanctions, when certain institutional conditions are met. One can therefore ask whether the positive relation between ATR and environmental outcomes is generated by preferences or by stricter enforcement of regulations within the ATR community on common land. Libois (2022) shows theoretically that in order for this mechanism to hold there should be threshold levels of enforcement (sanctions) at which conservation efforts become unfeasible. Agrawal and Goyal (2001) and Poteete et al. (2010) discuss evidence showing that such thresholds are related to the size of the adherent population as very small groups benefit from dense information and social sanctions. Whilst larger communities can still succeed, compliance can be eroded by anonymity and coordination problems, since enforcement typically shifts to formal monitors and committees, written records, and nested tiers. Smaller groups, on the other hand, often enforce rules well because everyone knows each other, information is inexpensive, and social sanctions bite. Such a mechanism would be observed in the data if such effects vary over the distribution of ATR, yielding substantial nonlinearities (for example, if most of the effect is driven by arrondissements with high ATR adherence, or if the positive effect that we observe is only driven by specific group sizes). If this was the case, community governance, rather than preferences, may be one of the drivers of the positive ATR/forest cover nexus. We therefore investigate the presence of nonlinearities in the marginal effects of adherence to ATR.

We do so by estimating a semiparametric fixed effects model using a procedure by Baltagi et al. (2002) for a specification similar to (1) but allowing for a fully flexible functional form in the relationship between ATR and the outcomes. Figure 3 shows the nonparametric fit with arrondissement fixed effects and alternating between department-year fixed effects and department-aez-year fixed effects. The top left panel of Figure 3 estimated using forest cover as the dependent variable shows hints of evidence for such a phenomenon, since the effect of ATR is higher for both very low and very high adherence levels, and linearly increasing in between. However, this result is not robust to different choices of fixed effects. Furthermore, we find that the estimated nonparametric relationships between the other main environmental outcomes (tree canopy cover and tree canopy annual change rate) and ATR appear monotonically and linearly increasing. Another way to explore this channel is to see how the level of ethnic fractionalization moderates the impact of ATR, as lower fractionalization may reduce transaction costs of working together and facilitate cooperation leading to positive impact on forests and resource use

---

free space is EIRP - Loss.

(Alesina et al., 2019). To do so we re-estimate specification (1) with the interaction term  $ATR_{it} \times \text{Frac}_{it}$  where  $\text{Frac}_{it}$  is an ordered categorical variable identifying the quartile of the ethnic fractionalization distribution to which each observation belongs. Columns (1)–(3) of Table 4 show that, across all three outcomes, the effect of ATR does not vary with different levels of ethnic fractionalization. We therefore do not find strong evidence for governance or cooperation-based mechanisms. Building on the Weberian view that the unique feature of religion is its potential influence on beliefs that reinforce particular traits and values, thereby reshaping behavior, we turn to the possibility that pro-environmental attitudes embedded in individual preferences may be driving our results (Weber, 1904).

## 6.2 Spirit of sustainability

In Benin, agricultural expansion is the primary driver of forest loss resulting in increasing pressure on land and soil quality and the subsequent environmental degradation. The pattern of deforestation in Benin indicates a more local interaction where it is dominated by smallholder-driven and shifting agriculture characterized by small, temporally dynamic patches of cultivated land interspersed with natural vegetation (Pendrill et al., 2022). As an initial step, we examine how ATR adherence relates to the expansion of rainfed agriculture (RainAg), using data from the ESA-CCI-LC dataset. Column (4) of Table 4 presents the OLS estimate from specification (1) with  $\text{RainAg}_{it}$  as the dependent variable. We find a negative association between ATR adherence and cropland expansion over the sample period.

To investigate this mechanism more directly, we re-estimate the 2SLS specification including an interaction term between ATR and a binary variable  $\text{RainAgDummy}_{it}^{[>Q_1]}$ , which equals one for observations above the 25th percentile of rain-fed agricultural expansion. The intuition is that although cropland expansion typically worsens environmental outcomes, ATR may mitigate this effect. Consistent with this interpretation, we find the interaction between ATR and  $\text{RainAgDummy}_{it}^{[>Q_1]}$  to be positive and statistically significant. Figure 4 plots the marginal effects, showing the estimated difference in outcomes between high and low cropland-expansion areas across quartiles of ATR adherence. The predicted outcomes are higher and statistically significant for high-expansion arrondissements at higher levels of ATR adherence, indicating that ATR reduces the environmental costs of cropland proliferation.

Associated with agricultural expansion is the considerable fragmentation of Benin’s natural landscapes, especially the diverse remaining savannas that range from open tree savannas in the north to wooded savannas in the south. Savanna area decreased by 23 percent between 1975 and 2013, but continues to remain the dominant land cover type in Benin (Tappan et al., 2016). Using the ESA-CCI-LC dataset we are able to account for the percentage share of an arrondissement that underwent land cover transitions, between census waves, from savanna to agriculture ( $\text{SavannaAg}_{it}$ ) and forests to agriculture ( $\text{ForestAg}_{it}$ ). Columns (5) and (6) of Table 4 indicate that ATR adherence is negatively related to the two primary land transitions responsible for environmental degradation and forest loss in the country. These results suggest that areas with high ATR adherence tend to engage in more sustainable interactions with the natural environment. Based on this evidence, we hypothesize that deep-seated ATR beliefs, which place high

value on forests, trees and foster a profound connection to land, can help generate the *spirit* conducive to sustainable behaviour and environmental stewardship.

## 7 Combining the Sacred and the Ecology

The evidence we have obtained so far shows that higher ATR adherence yields an increase in local forest cover, both in levels and in annualized growth rates, across Benin. We also find that ATR adherence correlates with pro-environmental behaviours, such as lower agricultural expansion and reduced land conversion. What remains to be explored, however, is how ATR adherence shapes individual preferences. In particular, one cannot distinguish whether the difference in ecosystem use is a consequence of the sacralization of individuals’ local environment or stems from ATR beliefs being conducive to more environmentally conscious economic behaviours. In other words, is it a sacred grove that drives such behaviours, or is it an interest in the state of forests in general? Do ATR beliefs shape the importance given to local forests and groves, or does ATR generate genuine concerns for the overall state of the environment and the sustainability of ecosystem use policies? The answer is likely to be a combination of both, the sacred and the ecology. If ecology indeed plays a role, ATR adherence should then affect how the overall state of the forest, and not just one’s own available stock, impacts individual utility. To this aim, we build a model of forest use under ecosystem uncertainty that explicitly incorporates these aspects.

### 7.1 Theoretical framework

Let us present a framework where  $N$  individuals indexed by  $i \in [1, \dots, N]$  draw utility continuously in  $t \in [0, T]$  from extracting / consuming a quantity  $q_{it}$  of the forest cover  $X_{it}$  available for individual  $i$ , assumed to evolve according to the following dynamics:

$$dX_{it} = (\mu X_{it} - q_{it}) dt + \sigma X_{it} dW_{it}, \quad (6)$$

where every  $i$ -th  $W_{it}$  is an independent Brownian motion. The ecological parameters  $\mu$  and  $\sigma$  are respectively the growth rate of the forest cover and the standard deviation of the increments of each Brownian motion<sup>10</sup>. We retain the same index  $i$  for individuals that we have used in the previous sections to identify Benin arrondissements, since in estimating the model we will associate an “individual” as a representative agent of each arrondissement in the data.

Individuals maximize the following objective function:

---

<sup>10</sup>We assume the technical requirements of a triple  $(\mathbb{R}^+, P, \mathcal{F}_t)$  comprised by the positive real domain - forest cover cannot be negative - a probability measure  $P$  and a filtration (an information set)  $\mathcal{F}_t$ . We could extend the model, adding some complexity, to one in which each individual has their own  $\mu_i$  and  $\sigma_i$ . However, such a framework would not allow us to identify  $\mu_i$  from the Benin data we have, a point we will discuss at length in the following section, and thus we leave such a model for future extensions.

$$J^i(X_{it}, q_{it}, t) = \mathbb{E}_t \int_t^T e^{-\rho s} u(q_{is}, v(p(x, s)); a_i) ds + b(X_{iT}; a_i), \quad (7)$$

where  $a_i \in A \subseteq [0, 1]$ ,  $a_i \sim p_0(a)$ , normalized between 0 (“not believing at all”) and 1 (“fully adherent”). This term parametrises the role played by heterogeneous ATR beliefs, defined within a bounded set  $A$  and is distributed across the population according to a measure  $p_0(a)$ , assumed to be known by the individuals. The utility function includes the spatial (“cross-sectional”) empirical distribution of the resource *across* individuals  $p(x, t)$  where  $x = [X_{1t}, \dots, X_{Nt}]$ , defined as  $p(dx, t) = \frac{1}{N} \sum_{i=1}^N \delta_{X_{it}}(dx)$ , where  $\delta_x$  is a unit mass function at each  $X_{it}$ . This distribution maps the state of the resource for all the  $N$  individuals at any time  $t$  into a real-valued quantity via a function  $v : \mathbb{R}^+ \rightarrow \mathbb{R}$ , a signal that individuals are able to observe which captures all available information on the overall state of the resource. This term represents the utility individuals draw due to *pro-environmental attitudes*<sup>11</sup>. The function  $v$  therefore captures the interactions across all individuals, since the distribution  $p(x, t)$  is continuously determined for each  $t$  by everyone’s resource use policies. Each adherence level  $a_i$  calibrates how both  $q$  and  $p$  generate utility for each individual  $i$ . We consider utility functions  $u(q, v; a)$  such that  $u_q \geq 0$ ,  $u_{qq} \leq 0$ ,  $u_v \geq 0$ ,  $u_{vv} \leq 0$ . Lastly, the function  $b$  is a bequest function which depends on individual adherence levels such that  $b_a \geq 0$ .

We now assume that the signal  $v := v(p(x, t))$  that individuals observe to gauge the overall state of the forest cover is the *geometric mean* of the forest distribution. This quantity is formalised naturally by  $v(p) = \exp \mathbb{E}^p[\log X_{it}^q] := \bar{X}_t$ , where the expectation is with respect to the joint measure of forest cover and ATR beliefs induced by  $X_{it}^q$  (the forest cover  $X_{it}$  associated with any feasible extraction policy  $q$ ) defined as  $p := p^a(x, t)$ . We thus augment our information set to include the information available to all individuals at time 0 over the initial state of both forest and adherence<sup>12</sup>. Note that for a discrete number  $j = 1, \dots, n$  of observations  $x_j$ ,  $p^a(x, t)$  is the empirical measure associated to the realizations  $x_j$  and  $\bar{X}_t$  becomes the familiar expression for the geometric mean  $(\prod_j x_j)^{1/n}$ . Individuals, therefore, observe the *median* forest cover across the population. The choice of the geometric mean is one of convenience, as one can derive explicitly the dynamics of the median forest cover and characterize precisely the model solution. In Appendix Section C we show all the formal details, where we also show how the median state of the forest depends not only on the ecological parameters  $\mu$  and  $\sigma$ , but also on the heterogeneity in beliefs within the population, which shape global deforestation.

The presence of  $\bar{X}_t$  in the utility function of each individual represents the role that the state of the environment, and in particular its scarcity, plays in determining pro-environmental attitudes, and ultimately shaping their ecosystem use policies. The term shows how populations may be concerned about a collapsing ecosystem, a consequence of global, rather than individual, actions. What matters for individual welfare is the overall state of forests, beyond what is available for one to exploit, as decreasing aggregate levels of forest reduce individual utility. The term is endogenous as it depends on the probability measure

<sup>11</sup>We note that the model setup is general, in which  $x$  can be any renewable resource and  $a$  can represent a wide variety of preferences over the overall resource distribution  $p(x, t)$ . For the purpose of this paper and to understand the implications within the context of religion and ecology we restrict our attention to  $a_i$  as individual ATR adherence,  $X_{it}$  as the forest area managed by individual  $i$  at time  $t$  and  $p(x, t)$  is the (empirical) forest cover distribution.

<sup>12</sup>In more technical terms, we augment the filtration  $\mathcal{F}_t$  to  $\mathcal{F}_t^a$ , which includes all information on ATR beliefs across the population.

$p^a(x, t)$  which identifies the spatial distribution of the resource  $x$  at time  $t$ . We will assume the scarcity term to enter the utility function as  $\bar{X}_t^{g_2(a)}$  and the forest consumption term as  $q^{g_1(a)}$ , where we impose  $g'_1 \leq 0, g'_2 \geq 0$ .<sup>13</sup>

In our framework, therefore, individual  $i$  draws utility from a composite good given by  $q_{it}^{g_1(a_i)} \bar{X}_t^{g_2(a_i)}$ , which is expressed in forest cover units and is a combination of individual consumption  $q_{it}$  and overall median forest state  $\bar{X}_t$ . This combination is calibrated by one's own individual adherence  $a_i$ . The intuition of this formalisation is as follows:  $g_1$  (the sacred) determines how ATR adherence affects individual deforestation utility, which defines the value individuals give to *their* forest cover. This local environment can be specific trees or groves considered sacred, where spirits may lie. The function  $g_1$  is decreasing in ATR adherence, so the more individuals are adherent, the less utility they will draw from consuming forest products from their own local stock. The pro-environmental attitudes are calibrated by  $g_2$  (the ecology), which controls how individuals care about the *global* environment, rather than individual / specific parts of forest, via its scarcity. Individual belief levels  $a_i$ , therefore, calibrate the *degree of substitutability* between individual consumption  $q$  and the state of the resource across all individuals. If  $g_1 + g_2 = 1, \forall a \in A$ , then individual resource use and pro-environmental attitudes are perfect substitutes.<sup>14</sup>

We now assume a continuum of individuals, which is equivalent to assuming a large number  $N$  of individuals. In this limit, the interactions across agents generated by the presence of scarcity in the utility function yield an example of a mean-field game. It has been shown rigorously in the mathematics literature (Lasry and Lions, 2007) how under fairly general assumptions the infinite-population / continuum limit can effectively approximate the equilibrium of a finite- $N$  game, and the system can be fully characterized by a single representative agent interacting with a distribution of states. In short, the large  $N$  limit allows us to switch from solving for *all* deforestation interactions  $q_{it}$  in the formation of  $\bar{X}_t$ , to the interaction between the deforestation  $q_t$  by a representative individual with adherence  $a$ , the endogenous spatial forest distribution  $p^a(x, t)$  and the adherence distribution  $p_0(a)$  across the population.<sup>15</sup>

The equilibrium deforestation policy  $q_t^{MFE}$  is obtained by solving the following problem:

---

<sup>13</sup>We note that by using  $\bar{X}_t$  as the signal of the global state of the environment observed by individuals we implicitly choose not to include peer effects in our framework, since pro-environmental attitudes involve drawing utility from observing an aggregate state, rather than observing an aggregate quantity which is chosen by other individuals. In other words, individuals do not react directly to what others *do* (cutting trees), but rather observe a wider outcome. We however note that including peer effects is something that would be entirely possible using our framework, for example by using  $1/\bar{q}_t$  (i.e. the median deforestation policy) instead of  $\bar{X}_t$ . We leave this aspect to potential future extensions.

<sup>14</sup>We do not mandate that local forest consumption and global forest scarcity should be perfect substitutes: all we require is  $g'_1 \leq 0, g'_2 \geq 0$ , both continuous.

<sup>15</sup>On the technical side, the large- $N$  limit problem is now equipped with the augmented filtration  $\mathcal{F}_t^a$  which now has to be set as the smallest filtration such that the beliefs “type” vector  $[a_i]$  drawn from  $a \sim p_0(a)$  is  $\mathcal{F}_0$ -measurable and to which every Brownian motion  $W_{it}$  remains adapted.

$$q_t^{MFE} \rightarrow \sup_{q \in Q} \mathbb{E}_t \int_t^T e^{-\rho s} u \left( q^{g_1(a)} \bar{X}_t^{g_2(a)} \right) ds + b(X_T; a) \quad (8)$$

$$dX_t = (\mu X_t - q) dt + \sigma X_t dW_t, \quad X_0 = x_0$$

$$\bar{X}_t = \exp \int_{[0, \infty)} \int_A \log x p^a(dx, t) p_0(da). \quad (9)$$

For all details on deriving the setup of the problem (8) and the associated coupled partial differential equations we refer to Appendix Section C. In the large  $N$  limit, the problem (8) can be reduced to solving a system of two coupled partial differential equations instead of  $N$  (one for each  $i$ ). The key feature of this system is the forward/backward dimension, essential characteristic of mean-field games. The optimality equation of the representative individual (the mean field) is solved backwards starting from an endpoint condition. The relevant information over the actions of all agents is captured over the observation of  $p^a(x, t)$ , which represents the actual dynamics of the resource implied by individual behaviours. This information is then internalized via the pro-environmental attitudes  $\bar{X}_t$  in (9) and calibrated by the effect of adherence  $g_2(a)$ , yielding the optimal deforestation policy  $q_t^{MFE}$ . Forest consumption thus directly affects the overall forest resources in  $dt$  via the agents' heterogeneity  $p_0(a)$  and consequently the spatial distribution of forest cover  $p^a(x, dt)$ . The spatial distribution therefore keeps being updated forward via the probability evolution equation, starting from an initial resource distribution  $p^a(x, 0)$ , and agents form their forward-looking expectations based on their anticipation of what  $p^a(dx, dt)$  will be like. Lastly, rational expectations imply that for all agents there must be self-consistency between the anticipated  $p^a$  and the actual (realized)  $p^a$ , and thus we will have to prove the existence of a fixed point.

We now assume functional forms such that we can obtain explicit solutions. We choose a CRRA utility function of the form  $u(z) = \frac{z^{1-\gamma}}{1-\gamma}$ , with  $\gamma > 0$ . We impose  $\rho > \mu(1-\gamma) - \frac{\sigma^2}{2}\gamma(1-\gamma)$ , a standard assumption that allows the problem to be well-defined at the baseline  $g_1 = 1, g_2 = 0$ . We then can state the following Proposition:

**Proposition 1.** *An equilibrium exists for all  $T$ . For  $T \rightarrow \infty$ , the equilibrium deforestation rate  $q^{MFE} := q^*(a)/X_t$  for the problem (8) is given for every  $a \sim p_0(a)$  by*

$$\begin{aligned} q^{MFE} &= \epsilon_q \left( \rho - \mu(\nu_q + \nu_{\bar{x}}) - \frac{\sigma^2}{2} \left( \frac{\nu_q}{\epsilon_q} + \nu_{\bar{x}} \right) + \nu_{\bar{x}} \tilde{q}^* \right) \\ \tilde{q}^* &= \left( \rho \bar{\epsilon}_q - \mu \overline{(1 - \epsilon_q)} - \frac{\sigma^2}{2} (1 - \gamma) \bar{g}_1 - \left( \mu - \frac{\sigma^2}{2} \right) \frac{\sigma^2}{\epsilon_q \nu_{\bar{x}}} \right) (1 - \bar{\epsilon}_q \nu_{\bar{x}})^{-1} \end{aligned} \quad (10)$$

where  $\bar{\omega} = \int_A \omega p_0(da)$  for any  $\omega$ ,  $\epsilon_q := \epsilon_q(a) = -\frac{u_q}{u_{qq}} \frac{1}{q}$  is the elasticity of intertemporal substitution for forest use,  $\nu_q := \nu_q(a) = q \frac{u_q}{u}$  is the (point) elasticity of utility with respect to forest consumption  $q$ , and similarly  $\nu_{\bar{x}} := \nu_{\bar{x}}(a) = \bar{x} \frac{u_{\bar{x}}}{u}$  is the elasticity of utility with respect to the median forest cover  $\bar{x}$ .

**Proof:** See Appendix Section D, which also shows the solution for the finitely-lived case, proves the

existence of a mean-field equilibrium for all  $t$  and discusses the finite-time evolution of the equilibrium spatial forest distribution. Note that all the expectations with respect to  $p_0(da)$  exist and are bounded for all continuous distributions, since  $\epsilon_q(0)$  is bounded and  $a \in [0, 1]$ .

We can now state the key characteristics of the equilibrium deforestation policy, which allow us to better map the model to the data. We define as *unsustainable deforestation* a deforestation policy such that  $q^{MFE} > \mu - \frac{\sigma^2}{2}$  for some  $a \in A$ , since in each  $dt$  individuals with adherence  $a$  consume an amount of forest resource which is greater than its “natural” growth rate  $\mu - \frac{\sigma^2}{2}$ , and thus leading to an almost sure (in the probability sense) forest depletion. Conversely, we define as *sustainable deforestation* a policy such that  $q^{MFE} < \mu - \frac{\sigma^2}{2}$  for all  $a$ . We can now state the following proposition, which summarises the key characteristics of the optimal equilibrium deforestation policy, and will help map the model to the patterns that we observe in the data.

**Proposition 2:** *(i) Local deforestation decreases with increasing individual ATR adherence and with increasing global deforestation. (ii) Decreasing global ATR adherence yields decreased individual deforestation rates, proportional to one’s individual adherence. (iii) Unsustainable deforestation can occur in low ATR adherence areas, and can become sustainable as the population ATR adherence increases only for individuals with pro-environmental attitudes.*

**Proof:** See Appendix Section E.

Proposition 2 describes the key characteristics of the equilibrium deforestation policy. Characteristic (i) implies that a greater individual adherence yields a lower deforestation rate, as also evidenced by the reduced form. Characteristic (ii) can be inferred from noticing in (10) that the equilibrium individual deforestation rate is shaped by the interaction between individual adherence to ATR and the population’s median forest cover, which in turn depends continuously on the median deforestation rate  $\tilde{q}^*$  and the global distribution of ATR beliefs. The intuition behind (ii), which might seem counterintuitive, is that decrease in overall ATR adherence yields a global average increase in deforestation, since there are less adherents across the population with less pro-environmental concerns. In turn, individuals with nonzero adherence who have not been impacted by the change in ATR population distribution (i.e. it wasn’t them who changed adherence) observe this change, and as a response in  $dt$  decrease their own deforestation policy based on their own adherence  $a$ . Then, the median deforestation policy across all levels of adherence (the mean-field) adjusts and the system remains in equilibrium. Lastly, (iii) yields the key insight that an increase in ATR adherence can change unsustainable deforestation rates to sustainable ones only if adherents harbour pro-environmental attitudes, and provides a useful prediction to be mapped to our data. Figure 5 presents an illustration of the optimal deforestation rates under different functional choices.

## 7.2 Estimation: beliefs, preferences and optimal deforestation

In this section we fit the model to the data and estimate its parameters. In all that follows we will assume infinitely-lived agents, as having a fully explicit solution of the problem simplifies identification

and estimation considerably. Furthermore, the dataset on ATR beliefs does not have information over the individuals’ lifecycle, and thus the time-invariant nature of the optimal deforestation rate  $q^{MFE}/X_t$  given by (10) is better suited for our estimation requirements. We first estimate the beliefs distribution  $p_0(a)$  from the Benin census data. Since we have information on ATR adherence only at the arrondissement level, we associate each arrondissement to an agent  $i$  in our model, and assume that the reported ATR adherence is representative of all individuals in the arrondissement. This choice directly maps to the model primitives  $g_1$  and  $g_2$ , as in our data ATR adherence is the percentage of adherents and thus naturally falls between 0 and 1 as is the case for the functions  $g_1, g_2$ . The model heterogeneity in agents’ beliefs, therefore, is mapped directly to the observed heterogeneity across Benin arrondissements. We find that a Beta distribution with shape parameters  $\alpha_a = 0.55, \beta_a = 1.24$  (s.d. 0.01 and 0.04, such that the distribution mean is given by  $\frac{\alpha}{\alpha+\beta}$ ) yields an excellent fit (see Appendix Section F for details). Estimating the parameters for each sample year yields equivalent model fit results.

For our estimations we use tree canopy cover area (TA) as our  $X_{it}$ , expressed in square kilometers. We choose TA because forest cover is a specific, much more narrow LC type, with a lot more zeroes than tree canopy cover. More importantly, we want to look at trees in general since ATR sacralize trees as much as forests, as discussed in Section 2.1. A first issue we encounter in identifying the model’s parameters is how to disentangle the “uncontrolled” drift parameter  $\mu$  from the deforestation policy  $q_t$ , function of all model parameters, in the evolution equation of the tree canopy. Estimating the drift from individual trajectories in (6) for TA in each arrondissement  $i$  or alternatively estimating it from the country-level geometric mean (the median), whilst perfectly feasible computationally, does not allow one to identify separately  $\mu$  from  $q^{MFE}$  or  $\tilde{q}^*$ . Since we assume  $\mu$  to be constant across individuals, one would like to look in our data for an area where  $q_t = 0$  for all times, in order to exploit “untouched” areas to capture the natural rate of canopy growth. Benin, however, is a narrow, key-shaped country, measuring about 2.9 latitude degrees at its widest point (around 325 km) and is highly densely populated, making the search for such an area difficult. As a solution to this challenge, we focus on regions where it is plausible to assume that human forest consumption is zero, or at least negligible. We turn our analysis towards the W-Arly-Pendjari (WAP) Complex which is a transnational park shared between the Republic of Niger, Burkina Faso and the Republic of Benin and has been a part of the UNESCO World Heritage List since 1996, shown in Appendix Figure A14. The park covers a major expanse of intact Sudano-Sahelian savannah, with vegetation types including grasslands, shrub lands, wooded savannah and extensive gallery forests.<sup>16</sup>

We first obtain the canopy data for areas of WAP falling within Benin corresponding to the W and Pendjari national parks. We then estimate the parameters based on the construction of a likelihood function derived from the transition probability density of the discretely sampled data, based on the uncontrolled version of (6). Given that we only have access to yearly data, we bootstrap the maximum likelihood estimator (3000 repetitions) to get robust confidence bands for our estimate. We report all details of both data building and estimations in Appendix Section F. We obtain an estimate of  $\hat{\mu} = 0.0482$  (s.d. 0.004), i.e. a annual “untouched” growth rate of 4.82%, for the forests in the WAP area, which

<sup>16</sup>For additional information refer to <https://whc.unesco.org/en/list/749/>

we consider to be a reasonable estimate of the natural growth rate of the forest resources  $\mu$  for Benin. Similarly, we estimate  $\sigma^2$  by an equivalent procedure over the entire canopy cover of Benin since the diffusion coefficient is assumed to be constant across arrondissements. We obtain an estimate of  $\hat{\sigma} = 0.258$  (s.d. 0.032), corresponding to a yearly variance of 6.5%. We assume  $\rho = 0.0487$ , an estimate provided by Hyman et al. (2021) for ecological (forest) goods obtained with surveys of Fulani people in Benin, and thus perfectly suited for our purposes. This estimate is similar to the 4.27% average Benin Central Bank discount rate between 2010 and 2024.<sup>17</sup>

Having identified  $\mu$ , we can now obtain from the data the optimal forest consumption policy  $q^{MFE}$  implied by our framework. We exploit variation for ATR adherence across the arrondissements and the three census years available, and we use the linearity in  $X_{it}$  of the optimal policy (10). The form of each dynamic equation (6), together with a time discretization  $\Delta t$ , imply that the equilibrium deforestation rate  $q^{MFE}$  can be recovered as the following conditional moment condition<sup>18</sup>:

$$\mathbb{E}_{p^a}[X_{it+\Delta t} - X_{it} - \mathbb{E}_{p_0}[(\hat{\mu} - q^{MFE}(a_i))X_{it}]\Delta t | \mathcal{F}_t^a] = 0. \quad (11)$$

Furthermore, the term  $\mathbb{E}_{p_0}[\hat{\mu} - q^{MFE}(a)]$  is time-invariant. From the data across all arrondissements  $i$  and given the annual nature of the TCC dataset such that  $\Delta t = 1$ , the moment condition (11) implies that  $\frac{X_{it+1} - X_{it}}{X_{it}}$  can identify  $q^{MFE}$  unconditionally, where  $X_{it}$  is the TA for arrondissement  $i$  in year  $t$  and  $a_i$  is arrondissement-level ATR adherence. For each of the three census years ( $t = 1992, 2002, 2013$ ), we use the following year's TA ( $t + 1 = 1993, 2003, 2014$ ) and calculate the yearly growth rate of tree canopy cover area necessary for computing (11). The moments of  $g_2$  with respect to the distribution  $p_0$  are recovered by numerical integration, using the Beta PDF at the estimated parameters  $\hat{\alpha}_a, \hat{\beta}_a$ . Figure 5 shows how a choice of  $g_1 = 1$  and  $g_2 = a$  yields deforestation rates linear in the canopy stock. Guided by the linearity shown by the semiparametric estimates of  $r$  in Figure 3, we focus our estimation effort to the modeling choice of  $g_1 = 1$ . We can then estimate  $\gamma$ , the CRRA parameter which drives the mean-field interactions in our model, using a two-step generalized method of moments method over the condition (11) induced by the optimal extraction (10). The estimation is straightforward, uses the Brent method with an optimal weighting matrix for computing standard errors, which converges easily and yields an estimate of  $\hat{\gamma} = 2.272$  (std. dev. 0.856) for a linear choice  $g_2(a) = a$ .<sup>19</sup> We refer to Appendix F for all details and robustness checks for our estimates.

<sup>17</sup>Source: Central Bank of West African States (BCEAO).

<sup>18</sup>We note that using (11) to estimate the parameters is internally consistent, as it incorporates naturally the error structure of (6) in the moment condition, unlike simply matching  $q^{MFE}$  with the data “plus an error term” (by nonlinear least squares, for example).

<sup>19</sup>As a further justification for this choice, we do not find any statistical significance of upper-order terms fitting a polynomial in  $ATR_{it}$  in our reduced form specification using  $r_{it}$  as outcome. We also estimate nonparametrically the relationship between  $\frac{X_{it+1} - X_{it}}{X_{it}}$  and  $a_i$  implied by 11 in the data (with year dummies) and we get essentially a straight line, shown in Appendix Figure F3. Increasing  $k$  yields estimates of  $\gamma$  that are slightly increasing in magnitude but not statistically different than  $k = 1$ , and yields negligible changes in root mean squared error.

### 7.3 Counterfactuals and sustainable deforestation

Using the 2013 data, the predicted arrondissement-level TA is obtained via the closed-form solution of the dynamic equations (6) with each optimal policy  $q^{MFE}$  evaluated at the parameters shown in Table 5, assuming  $k = 1$  and heterogeneous over the distribution  $p_0(a)$ . As a final exercise, we can now obtain the counterfactual canopy area distribution resulting from setting all adherence levels uniformly to zero. This distribution is obtained by setting  $a = 0$  in  $q^{MFE}$ , removing all heterogeneity in beliefs and obtaining a counterfactual no-ATR deforestation rate  $\hat{q}_0^{MFE}$ . We then predict the trajectories of each dynamic equation between 2002 and 2013 using the no-ATR deforestation rates. Figure 6 maps the three distributions, counterfactual (no ATR), observed and predicted for Benin in 2013. The left panel of Figure 7 plots density estimates showing how the observed and predicted TA distribution match closely, and how the counterfactual distribution is clearly first-order dominated by the other two. The right panel of Figure 7 further clarifies this point, showing the density of the difference between observed and predicted TA to be centered on zero (mean: 0.02, median: 0.082, std. dev: 10.68)

The average difference between observed and counterfactual 2013 TA is  $-3.32 \text{ km}^2$  per arrondissement, which corresponds to a canopy loss of 9.88%. We find the largest counterfactual tree canopy losses in the southern departments of Mono and Kouffo, which is consistent with these departments exhibiting the highest numbers of ATR adherents. We conclude with an interesting observation: evaluated at our estimated parameters, the counterfactual no-ATR deforestation rate is not sustainable, as  $\hat{q}_0^{MFE} = 0.0451$ , a yearly deforestation rate of 4.51%. Given our estimates of  $\hat{\mu} = 0.0482, \hat{\sigma} = 0.258$ , it's clear that  $\hat{q}_0^{MFE} dt > (\hat{\mu} - \hat{\sigma}^2/2)dt$ , and the “effective” growth rate of (6) is negative, which means that in absence of any ATR beliefs, the forest resources in Benin will eventually be depleted. On the other hand, there exist departments in Benin that show a sustainable (estimated) deforestation policy, all of which are high-adherence areas and are concentrated in the southwestern department of Kouffo and in the north-eastern department of Atakora, bordering the WAP protected areas. This result is consistent with Proposition 2: the fact that deforestation switches from unsustainable to sustainable rates for arrondissements above a certain adherence threshold proves both presence and salience of pro-environmental attitudes in the decision-making of the adherent population.

## 8 Conclusion

Our paper provides evidence that African Traditional Religions matter for environmental outcomes. Drawing on three waves of Benin’s census linked to remote-sensing measures of forest cover and tree-canopy change, and exploiting variation generated by the spread of Charismatic Pentecostalism, we show that higher ATR adherence is associated with greater forest cover, denser tree canopy, and substantially slower decadal rates of canopy loss. These associations survive extensive fixed-effects controls, robustness checks, placebo tests and alternative specifications, and the IV estimates strengthens a causal interpretation by addressing concerns about endogenous sorting of adherents into forested areas.

Contrary to a pure commons-governance story, we find limited evidence that collective enforcement, ethnic fractionalization, or Ostrom-style self-governance drive the results. Instead, the balance of quantitative and qualitative evidence points toward ATR-shaped individual preferences and value systems: adherents appear more likely to behave in pro-environmental ways (less cropland expansion, lower conversion of forests and savannas), and these behaviours plausibly mediate the positive ATR–forest relationship. We formalise this channel with a theoretical framework, showing how heterogeneity in ATR adherence alters individuals’ valuation of the global forest stock, shifting equilibrium deforestation rates. Counterfactual exercises suggest that absent ATR adherence Benin’s forests would be measurably poorer, and that pockets of sustainable forest use align with higher ATR prevalence.

We acknowledge that the mechanisms we identify are only partially uncovered: syncretism, variation in belief intensity, and heterogeneity within communities require deeper empirical investigation. Future work should combine household surveys, ethnography and experimental designs to unpack belief-behavior links, and test how traditional values interact with modern interventions. Nevertheless, our results have substantive real-world policy relevance. First, culturally embedded value systems can yield durable conservation outcomes, and environmental valuation frameworks should include non-market, spiritual and cultural dimensions to avoid systematically underestimating nature’s worth. Understanding these intersections could expand the toolbox for sustainable, equitable conservation in West Africa and beyond.

## References

- Abman, R. and C. Lundberg (2020). Does free trade increase deforestation? the effects of regional trade agreements. *Journal of the Association of Environmental and Resource Economists* 7(1), 35–72.
- Achdou, Y., J. Han, J.-M. Lasry, P.-L. Lions, and B. Moll (2022). Income and wealth distribution in macroeconomics: A continuous-time approach. *The Review of Economic Studies* 89(1), 45–86.
- Aderibigbe, I. S. and T. Falola (2022). The palgrave handbook of african traditional religion.
- Agrawal, A. and S. Goyal (2001). Group size and collective action: Third-party monitoring in common-pool resources. *Comparative Political Studies* 34(1), 63–93.
- Alesina, A., R. Baqir, and W. Easterly (1999). Public goods and ethnic divisions. *The Quarterly journal of economics* 114(4), 1243–1284.
- Alesina, A., C. Gennaioli, and S. Lovo (2019). Public goods and ethnic diversity: Evidence from deforestation in indonesia. *Economica* 86(341), 32–66.
- Alesina, A., S. Hohmann, S. Michalopoulos, and E. Papaioannou (2023). Religion and educational mobility in africa. *Nature* 618(7963), 134–143.
- Alidou, S. (2021). Beliefs and investment in child human capital: case study from benin. *The Journal of Development Studies* 57(1), 88–105.

- Alidou, S. and M. Verpoorten (2019). Only women can whisper to gods: Voodoo, menopause and women's autonomy. *World Development* 119, 40–54.
- Alonso, E. B., R. Houssa, and M. Verpoorten (2016). Voodoo versus fishing committees: The role of traditional and contemporary institutions in fisheries management. *Ecological Economics* 122, 61–70.
- Amanze, J. N. (2024). African approaches to the protection and conservation of the environment: The role of african traditional religions. *Religion and Development* 2(3), 445–462.
- Anderson, C. B., S. Athayde, C. M. Raymond, A. Vatn, P. Arias-Arévalo, R. K. Gould, J. Kenter, B. Muraca, S. Sachdeva, A. Samakov, et al. (2022). Conceptualizing the diverse values of nature and their contributions to people. In *The Methodological Assessment Report on The Diverse Values and Valuation of Nature*, pp. 31–122. Zenodo.
- Andrews, I., J. H. Stock, and L. Sun (2019). Weak instruments in instrumental variables regression: Theory and practice. *Annual Review of Economics* 11(1), 727–753.
- Araújo, D., B. Carrillo, and B. Sampaio (2022). Economic production and the spread of supernatural beliefs.
- Asamoah-Gyadu, J. K. (2009). African traditional religion, pentecostalism and the clash of spiritualities in ghana. *Fundamentalism and the Media*, 161–178.
- Baland, J.-M. and J.-P. Platteau (1996). *Halting degradation of natural resources: is there a role for rural communities?* Food & Agriculture Org.
- Baltagi, B. H., D. Li, et al. (2002). Series estimation of partially linear panel data models with fixed effects. *Annals of economics and finance* 3(1), 103–116.
- Baragwanath, K., E. Bayi, and N. Shinde (2023). Collective property rights lead to secondary forest growth in the brazilian amazon. *Proceedings of the National Academy of Sciences* 120(22), e2221346120.
- Becker, S. O. and H.-J. Voth (2023). From the death of god to the rise of hitler.
- Becker, S. O. and L. Woessmann (2009). Was Weber wrong? a human capital theory of protestant economic history. *The Quarterly Journal of Economics* 124(2), 531–596.
- Bensassi, S., J. Jarreau, and C. Mitaritonna (2019). Regional integration and informal trade in africa: Evidence from benin's borders. *Journal of African Economies* 28(1), 89–118.
- Berkes, F. (2017). *Sacred ecology*. Routledge.
- Bisin, A., J. Rubin, A. Seror, and T. Verdier (2024). Culture, institutions and the long divergence. *Journal of Economic Growth* 29(1), 1–40.
- Bisin, A. and T. Verdier (2001). The economics of cultural transmission and the dynamics of preferences. *Journal of Economic Theory* 97(2), 298–319.

- Borusyak, K. and P. Hull (2023). Nonrandom exposure to exogenous shocks. *Econometrica* 91(6), 2155–2185.
- Brown, D. and P. James (2018). The religious characteristics of states: Classic themes and new evidence for international relations and comparative politics. *Journal of Conflict Resolution* 62(6), 1340–1376.
- Burgess, R., M. Hansen, B. A. Olken, P. Potapov, and S. Sieber (2012). The political economy of deforestation in the tropics. *The Quarterly journal of economics* 127(4), 1707–1754.
- Burgess, R., E. Miguel, and C. Stanton (2015). War and deforestation in sierra leone. *Environmental Research Letters* 10(9), 095014.
- Butinda, L. D., A. A. Lameke, N. Nunn, M. Posch, and R. S. de la Sierra (2023). *On the importance of African traditional religion for economic behavior*. National Bureau of Economic Research.
- Camilla, S. (2005). Les nouveaux réseaux évangéliques et l'état: le cas du bénin. *Laurent Fourchard, André Mary, Entreprises religieuses transnationales en Afrique de l'Ouest, Paris, Karthala*, 223–241.
- Carvalho, J.-P., S. Iyer, and J. Rubin (2019). *Advances in the Economics of Religion*. Springer.
- Chernozhukov, V. and C. Hansen (2008). The reduced form: A simple approach to inference with weak instruments. *Economics Letters* 100(1), 68–71.
- Chief Atawé Akôyi A., O. L. (2025). The forest is life: Restoring the health of people and place in benin. Available online at: <https://rooted-magazine.org/2025/04/14/the-forest-is-life-restoring-the-health-of-people-and-place-in-benin-2/>, last accessed on 05.12.2025.
- Ciscato, E., Q.-A. Do, and K.-T. Nguyen (2024). Astrology and matrimony: Social reinforcement of religious beliefs on marriage matching in vietnam.
- Claffey, P. (2007). *Christian churches in Dahomey-Benin: a study of their socio-political role*. Brill.
- Dasgupta, P. (2021). *The economics of biodiversity: the Dasgupta review*. Hm Treasury.
- Defourny, P., L. Schouten, S. Bartalev, S. Bontemps, P. Caccetta, A. De Wit, C. M. Di Bella, B. Gérard, P. Giri, V. Gond, et al. (2009). Accuracy assessment of a 300 m global land cover map: The globcover experience. In *Conference Proceedings: 33rd International Symposium on Remote Sensing of Environment, Sustaining the Millennium Development Goals*.
- Desmet, K., I. Ortuño-Ortín, and R. Wacziarg (2012). The political economy of linguistic cleavages. *Journal of Development Economics* 97(2), 322–338.
- Di Gregorio, A. (2005). *Land cover classification system: classification concepts and user manual: LCCS*, Volume 2. Food & Agriculture Org.
- Drewal, H. J. (2008). Mami wata: Arts for water spirits in africa and its diasporas. *African arts* 41(2), 60–83.

- Dupuis, P. P.-H. (1998). Histoire de l'église du Bénin, tome 1, le temps des semeurs (1494–1901).
- ESA (2017). Land cover cci product user guide version 2. technical report. Available online at: [https://maps.elie.ucl.ac.be/CCI/viewer/download/ESACCI-LC-Ph2-PUGv2\\_2.0.pdf](https://maps.elie.ucl.ac.be/CCI/viewer/download/ESACCI-LC-Ph2-PUGv2_2.0.pdf), last accessed on 16.03.2025.
- Espín-Sánchez, J.-A., S. Gil-Guirado, and N. Ryan (2023). Praying for rain. Technical report, National Bureau of Economic Research.
- Fairhead, J. and M. Leach (1996). *Misreading the African landscape: society and ecology in a forest-savanna mosaic*. Number 90. Cambridge University Press.
- Falen, D. J. (2018). *African science: Witchcraft, vodun, and healing in Southern Benin*. University of Wisconsin Press.
- Fearon, J. D. (2003). Ethnic and cultural diversity by country. *Journal of economic growth* 8, 195–222.
- Ferraro, P. J. and R. Simorangkir (2020). Conditional cash transfers to alleviate poverty also reduced deforestation in Indonesia. *Science Advances* 6(24), eaaz1298.
- Gabaix, X., J.-M. Lasry, P.-L. Lions, and B. Moll (2016). The dynamics of inequality. *Econometrica* 84(6), 2071–2111.
- Gaiya, M. A. (2002). *The pentecostal revolution in Nigeria*. Centre of African Studies, University of Copenhagen Occasional paper. Copenhagen.
- Gershman, B. (2016). Witchcraft beliefs and the erosion of social capital: Evidence from sub-Saharan Africa and beyond. *Journal of Development Economics* 120, 182–208.
- Gibbs, H. K., A. S. Ruesch, F. Achard, M. K. Clayton, P. Holmgren, N. Ramankutty, and J. A. Foley (2010). Tropical forests were the primary sources of new agricultural land in the 1980s and 1990s. *Proceedings of the National Academy of Sciences* 107(38), 16732–16737.
- Giuliano, P. and N. Nunn (2018). Ancestral characteristics of modern populations. *Economic History of Developing Regions* 33(1), 1–17.
- Global Forest Watch (2025). Benin forest atlas. Accessed on April 7, 2025. URL: <https://gfw.global/3TAhNi4>.
- Golub, S. S. (2012). Entrepot trade and smuggling in West Africa: Benin, Togo and Nigeria. *The World Economy* 35(9), 1139–1161.
- Grätz, T. (2011). 'Paroles de vie': Christian radio producers in the Republic of Benin. *Journal of African Media Studies* 3(2), 161–188.
- Grätz, T. (2014). Christian religious radio production in Benin: The case of Radio Maranatha. *Social Compass* 61(1), 57–66.

- Guarnieri, E. (2025). Cultural distance and ethnic civil conflict. *American Economic Review* 115(4), 1338–1368.
- Guarnieri, E. and A. Tur-Prats (2023). Cultural distance and conflict-related sexual violence. *The Quarterly Journal of Economics* 138(3), 1817–1861.
- Guiso, L., P. Sapienza, and L. Zingales (2003). People’s opium? religion and economic attitudes. *Journal of monetary economics* 50(1), 225–282.
- Guiso, L., P. Sapienza, and L. Zingales (2006). Does culture affect economic outcomes? *Journal of Economic perspectives* 20(2), 23–48.
- Hackett, R. I. (1998). Charismatic/pentecostal appropriation of media technologies in nigeria and ghana. *Journal of religion in Africa*, 258–277.
- Hyman, A. A., O. G. Gaoue, C. Tamou, and P. R. Armsworth (2021). How pastoralists weight future environmental benefits when managing natural resources. *Conservation Letters* 14(2), e12770.
- Iannaccone, L. R. (1998). Introduction to the economics of religion. *Journal of economic literature* 36(3), 1465–1495.
- Iannaccone, L. R. and W. S. Bainbridge (2009). Economics of religion. In *The Routledge Companion to the Study of Religion*, pp. 475–489. Routledge.
- Idowu, E. B. (1973). *African traditional religion: A definition*. Orbis Books.
- Inyang, E. (2015). *The Forest: An African Traditional Definition*. Langaa RPCIG.
- IPBES (2022). Summary for policymakers of the methodological assessment report on the diverse values and valuation of nature of the intergovernmental science-policy platform on biodiversity and ecosystem services. Technical report.
- ITU (1998). Itu-r planning standards for terrestrial fm sound broadcasting at vhf. Available online at: [https://www.itu.int/dms\\_pubrec/itu-r/rec/bs/R-REC-BS.412-9-199812-I!!PDF-E.pdf](https://www.itu.int/dms_pubrec/itu-r/rec/bs/R-REC-BS.412-9-199812-I!!PDF-E.pdf), last accessed on 11.11.2025.
- ITU Recommendation (2019). 525-4: Calculation of free-space attenuation. *Geneva, Switzerland: ITU*.
- Ives, C. D., J. Kidwell, C. B. Anderson, P. Arias-Arévalo, R. K. Gould, J. Kenter, and R. Murali (2024). The role of religion in shaping the values of nature. *Ecology and Society* 29(2), 10.
- Iyer, S. (2016). The new economics of religion. *Journal of Economic Literature* 54(2), 395–441.
- Juhé-Beaulaton, D. (2006). Enjeux économiques et sociaux autour des bois sacrés et la «conservation de la biodiversité», bénin, burkina faso et togo.
- Juhé-Beaulaton, D. (2010). *Forêts sacrées et sanctuaires boisés: des créations culturelles et biologiques (Burkina Faso, Togo, Bénin)*. KARTHALA Editions.

- Kahn, J. (2011). Policing ‘evil’: state-sponsored witch-hunting in the people’s republic of bénin. *Journal of Religion in Africa* 41(1), 4–34.
- Kleibergen, F. and R. Paap (2006). Generalized reduced rank tests using the singular value decomposition. *Journal of econometrics* 133(1), 97–126.
- Koppell, C. R. and J. Falconer (1990). *Major Significance of” Minor” Forest Products: The Local Use and Value of Forests in the West African Humid Forest Zone*. Food and Agriculture Organization of the United Nations.
- Kraus, E. B. (2012). *People and forests: a case study from Benin, West Africa*. Ph. D. thesis, University of Kansas.
- Lasry, J.-M. and P.-L. Lions (2006). Jeux à champ moyen. i–le cas stationnaire. *Comptes Rendus Mathématique* 343(9), 619–625.
- Lasry, J.-M. and P.-L. Lions (2007). Mean field games. *Japanese journal of mathematics* 2(1), 229–260.
- Le Rossignol, E., S. Lowes, and N. Nunn (2022). The social consequences of traditional religion in contemporary africa. Technical report, National Bureau of Economic Research.
- Li, X., Y. Zhou, M. Zhao, and X. Zhao (2020). A harmonized global nighttime light dataset 1992–2018. *Scientific data* 7(1), 168.
- Libois, F. (2022). Success and failure of communities managing natural resources: Static and dynamic inefficiencies. *Journal of Environmental Economics and Management* 114, 102671.
- Lovejoy, H. B. (2013). Redrawing historical maps of the bight of benin hinterland, c. 1780. *Canadian Journal of African Studies/La Revue canadienne des études africaines* 47(3), 443–463.
- Lucas, R. E. and B. Moll (2014). Knowledge growth and the allocation of time. *Journal of Political Economy* 122(1), 1–51.
- Malapane, O. L., W. Musakwa, and N. Chanza (2024). Indigenous agricultural practices employed by the vhavenda community in the musina local municipality to promote sustainable environmental management. *Heliyon* 10(13).
- Manning, P. (2004). *Slavery, colonialism and economic growth in Dahomey, 1640-1960*. Number 30. Cambridge University Press.
- Marshall, R. (2019). *Political spiritualities: the Pentecostal revolution in Nigeria*. University of Chicago Press.
- Mayrargue, C. (2002). *Dynamiques religieuses et démocratisation au Bénin. Pentecôtisme et formation d’un espace public*. Ph. D. thesis, Institut d’études politiques de Bordeaux; Université Montesquieu-Bordeaux IV.
- Mayrargue, C. (2005). 9. dynamiques transnationales et mobilisations pentecôtistes dans l’espace public béninois. In *Entreprises religieuses transnationales en Afrique de l’Ouest*, pp. 243–265. Karthala.

- Mbiti, J. S. (1970). *Concepts of god in Africa*. New York : Praeger Publishers.
- Mbiti, J. S. (1990). *African religions & philosophy*. Heinemann.
- Mbiti, J. S. (2015). *Introduction to African religion*. Waveland Press.
- McCleary, R. M. and R. J. Barro (2006). Religion and economy. *Journal of Economic perspectives* 20(2), 49–72.
- Melitz, J. and F. Toubal (2014). Native language, spoken language, translation and trade. *Journal of International Economics* 93(2), 351–363.
- Montero, E., D. Yang, and T. Yentzen (2025). The price of faith: Economic costs and religious adaptation in sub-saharan africa. Technical report, National Bureau of Economic Research.
- Murdock, G. P. (1967). Ethnographic atlas: a summary. *Ethnology* 6(2), 109–236.
- Nunn, N. and R. Sanchez de la Sierra (2017). Why being wrong can be right: Magical warfare technologies and the persistence of false beliefs. *American economic review* 107(5), 582–87.
- Nunn, N. and L. Wantchekon (2011). The slave trade and the origins of mistrust in africa. *American Economic Review* 101(7), 3221–52.
- Obadare, E. (2018). *Pentecostal republic: Religion and the struggle for state power in Nigeria*. Bloomsbury Publishing.
- Ojo, M. A. (2005). 15. nigerian pentecostalism and transnational religious networks in west african coastal regions. In *Entreprises religieuses transnationales en Afrique de l'Ouest*, pp. 395–415. Karthala.
- Olea, J. L. M. and C. Pflueger (2013). A robust test for weak instruments. *Journal of Business & Economic Statistics* 31(3), 358–369.
- Olken, B. A. (2009). Do television and radio destroy social capital? evidence from indonesian villages. *American Economic Journal: Applied Economics* 1(4), 1–33.
- Ossito Midiohouan, G. (1999). Vodoun et littérature au bénin. *Présence Francophone: Revue internationale de langue et de littérature* 53(1), 10.
- Ostrom, E. (2000). Collective action and the evolution of social norms. *Journal of economic perspectives* 14(3), 137–158.
- Owen, A. L. and J. R. Videras (2007). Culture and public goods: The case of religion and the voluntary provision of environmental quality. *Journal of Environmental Economics and Management* 54(2), 162–180.
- Peel, J. D. Y. (1977). Conversion and tradition in two african societies: Ijebu and buganda. *Past & Present* (77), 108–141.

- Pendrill, F., T. A. Gardner, P. Meyfroidt, U. M. Persson, J. Adams, T. Azevedo, M. G. Bastos Lima, M. Baumann, P. G. Curtis, V. De Sy, et al. (2022). Disentangling the numbers behind agriculture-driven tropical deforestation. *Science* 377(6611), eabm9267.
- Pew Research Center (2014). Global religious diversity: Half of the most religiously diverse countries are in asia-pacific region. Technical report, Washington, D.C.
- Pfaff, A. S. (1999). What drives deforestation in the brazilian amazon?: Evidence from satellite and socioeconomic data. *Journal of environmental economics and management* 37(1), 26–43.
- Poteete, A. R., M. A. Janssen, and E. Ostrom (2010). *Working together: collective action, the commons, and multiple methods in practice*. Princeton University Press.
- Puyravaud, J.-P. (2003). Standardizing the calculation of the annual rate of deforestation. *Forest ecology and management* 177(1-3), 593–596.
- Reichel-Dolmatoff, G. (1976). Cosmology as ecological analysis: a view from the rain forest. *Man*, 307–318.
- Rush, D. (2001). of ouidah, benin. *African Arts* 34(4), 32–47.
- Rush, D. (2010). Ephemerality and the “unfinished” in vodun aesthetics. *African Arts* 43(1), 60–75.
- Sanford, L. (2023). Democratization, elections, and public goods: the evidence from deforestation. *American Journal of Political Science* 67(3), 748–763.
- Sheridan, M. J. and C. Nyamweru (2008). African sacred groves: ecological dynamics & social change.
- Song, X.-P., M. C. Hansen, S. V. Stehman, P. V. Potapov, A. Tyukavina, E. F. Vermote, and J. R. Townshend (2018). Global land change from 1982 to 2016. *Nature* 560(7720), 639–643.
- Stoop, N., M. Verpoorten, and K. Deconinck (2019). Voodoo, vaccines, and bed nets. *Economic Development and Cultural Change* 67(3), 493–535.
- Tall, E. K. (1995). De la démocratie et des cultes voduns au Bénin (on democracy and voodoo in benin). *Cahiers d'études africaines*, 195–208.
- Tappan, G. G., W. M. Cushing, S. E. Cotillon, J. A. Hutchinson, B. Pengra, I. Alfari, E. Botoni, A. Soulé, and S. M. Herrmann (2016). *Landscapes of West Africa: A window on a changing world*. United States Geological Survey.
- Taylor, B., G. Van Wieren, and B. D. Zaleha (2016). Lynn white jr. and the greening-of-religion hypothesis. *Conservation Biology* 30(5), 1000–1009.
- Ukah, A. F. (2005). 11. the local and the global in the media and material culture of nigerian pentecostalism. In *Entreprises religieuses transnationales en Afrique de l'Ouest*, pp. 285–313. Karthala.
- UNDP et MEPN (2008). Programme d'action national d'adaptation aux changements climatiques du Bénin (pana-bÉnin). Technical report, Cotonou, République du Bénin.

- Vaughan, O. (2016). *Religion and the Making of Nigeria*. Duke University Press.
- Vestraeten, D. (2004). The conditional probability density function for a reflected brownian motion. *Computational Economics* 24(2), 185–207.
- Wang, T. (2021). Media, pulpit, and populist persuasion: Evidence from father coughlin. *American Economic Review* 111(9), 3064–3092.
- Weber, M. (1904). Die protestantische ethik und der geist des kapitalismus (the protestant ethic and the spirit of capitalism. new york, ny: Charles scriber’s sons. 1958).
- World Bank (2020). Benin country forest note. Technical report, Washington, D.C.
- Yanagizawa-Drott, D. (2014). Propaganda and conflict: Evidence from the rwandan genocide. *The Quarterly Journal of Economics* 129(4), 1947–1994.

Table 1: OLS and 2SLS results

Dep. Variables:	Forest (1)	TCC (2)	$r$ (3)	ATR (4)
Panel A:	<b>OLS</b>			
$ATR_{it}$	0.018 (0.009)	0.047 (0.019)	0.042 (0.019)	
Panel B:	<b>2SLS</b>			
$ATR_{it}$	0.165 (0.082) [0.01, 0.34]	0.254 (0.079) [0.11, 0.43]	0.172 (0.080) [0.03, 0.35]	
Panel C:	<b>Reduced form</b>			
$Z_{it}$	0.907 (0.461)	1.398 (0.430)	0.947 (0.433)	
Panel D	<b>First stage</b>			
$Z_{it}$				5.509 (1.019)
Mean of dep. variable	13.75	16.331	-0.428	
Standard F Stat				36.4
Effective/K-P F stat				29.2
Fixed effects	yes	yes	yes	yes
Controls	yes	yes	yes	yes
Observations	1,637	1,637	1,637	1,637
Arrondissements	546	546	546	546

Unit of analysis is arrondissement.  $Z_{it}$  is the instrument from (2) which inversely captures the exposure to Charismatic Pentecostalism in Benin. Column (1) outcome is the percentage of forest cover in an arrondissement  $i$  at time  $t$  from the ESA-CCI-LC data. Column (2) and (3) outcomes are the percentage of tree canopy cover (TCC) and the annual rate of change of TCC ( $r$ ) in an arrondissement  $i$  at time  $t$ , both from the VCF5KYR dataset. All specifications include the full set of fixed effects: arrondissement and department  $\times$  aez  $\times$  year. Socio-economic controls include rate of illiteracy, share of poorest households based on wealth index quintiles, share of informal employment, share of catholic adherents, mean population density, nighttime lights intensity and to control for agricultural practices maize, cassava and cotton soil suitability interacted with a linear time trend. Climatic controls include precipitation, minimum and maximum temperature. Geographic controls include elevation and the latitude and longitude of the arrondissement centroid - these are interacted with a linear time trend. Panel B shows the Anderson-Rubin 95% CI using the inversion method proposed by [Chernozhukov and Hansen \(2008\)](#). Robust standard errors are clustered at the arrondissement level.

Table 2: Threats to identification: 2SLS estimates

Dep. Variables:	Forest (1)	TCC (2)	$r$ (3)
Panel A:	<b>Informal Trading</b>		
$ATR_{it}$	0.177 (0.085)	0.253 (0.081)	0.181 (0.082)
$ATR_{it} \times \text{Inf.Hub}_i$	0.048 (0.036)	-0.003 (0.040)	0.036 (0.056)
K-P F Stat: 15.1			
Panel B:	<b>Dropping <math>HD_i^{\text{YORUBA}}</math></b>		
$ATR_{it}$	0.177 (0.108)	0.282 (0.098)	0.151 (0.087)
K-P F Stat: 27.3			
Panel C:	<b>Dropping <math>RP_{it}^c</math></b>		
$ATR_{it}$	0.195 (0.091)	0.286 (0.084)	0.210 (0.085)
K-P F Stat: 23.3			
Observations	1,637	1,637	1,637
Arrondissements	546	546	546

Unit of analysis is arrondissement. Column (1) outcome is forest cover from the ESA-CCI-LC data. Column (2) and (3) outcomes are tree canopy cover (TCC) and the annual rate of change of TCC ( $r$ ), both from the VCF5KYR dataset. In Panel A  $\text{Inf.Hub}_i$  is an indicator variable equal to one if the arrondissement has informal trading hubs, zero otherwise. In Panel B we estimate 2SLS with an instrument excluding  $HD_i^{\text{YORUBA}}$  which is the haversine distance of each arrondissement  $i$  from the ethnic homeland of the Yoruba group. In Panel C we estimate 2SLS with an instrument excluding  $RP_{it}^c$  which is the re-centered and residualized signal strength received by each arrondissement. All specifications include all baseline controls and the full set of fixed effects: arrondissement and department  $\times$  aez  $\times$  year. Socio-economic controls include rate of illiteracy, share of poorest households based on wealth index quintiles, share of informal employment, share of catholic adherents, mean population density, nighttime lights intensity and to control for agricultural practices maize, cassava and cotton soil suitability interacted with a linear time trend. Climatic controls include: precipitation, minimum and maximum temperature. Geographic controls include elevation and the latitude and longitude of the arrondissement centroid - these are interacted with a linear time trend. Robust standard errors are clustered at the arrondissement level.

Table 3: Robustness of 2SLS estimates to alternative specifications

Rob. checks:	Baseline	Two-way clustering	LD $\lambda = 0.25$	LD $\lambda = 0.75$	Ethnic home FE	-100 dBm	Free Space
	(1)	(2)	(3)	(4)	(5)	(6)	(7)
Panel A	<b>Forest</b>						
$ATR_{it}$	0.165 (0.082)	0.165 (0.076)	0.156 (0.073)	0.173 (0.088)	0.132 (0.072)	0.158 (0.084)	0.200 (0.107)
Panel B	<b>TCC</b>						
$ATR_{it}$	0.254 (0.079)	0.254 (0.086)	0.276 (0.073)	0.245 (0.085)	0.300 (0.095)	0.258 (0.080)	0.299 (0.101)
Panel C	$r$						
$ATR_{it}$	0.172 (0.080)	0.172 (0.086)	0.190 (0.086)	0.163 (0.080)	0.340 (0.094)	0.174 (0.082)	0.275 (0.125)
arrond FE	yes	yes	yes	yes	yes	yes	yes
dep-aez-year FE	yes	yes	yes	yes		yes	yes
eth-aez-year FE					yes		
Eff./K-P F stat	29.2	13.9	18.1	33.2	26.6	28.5	19.5
Observations	1,637	1,637	1,637	1,637	1,637	1,637	1,637

Unit of analysis is arrondissement. Panel A the dependent variable is forest cover from the ESA-CCI-LC data. For Panel B and C the outcomes are tree canopy cover (TCC) and the annual rate of change of TCC ( $r$ ), both from the VCF5KYR dataset. Col. (1) shows the baseline 2SLS estimates using the instrument in (2). Col. (2) has robust standard errors clustered over the 12 departments and 8 aez. Col. (3) and (4) calculate the linguistic distance with  $\lambda = 0.25$  and  $\lambda = 0.75$ . Column (5) replaces dep-aez-yr fixed effects with Murdock ethnic homeland-aez-year fixed effects. Finally, column (6) takes -100 dBm value for the no exposure signal strength and column (7) uses signal strength calculated from the free space propagation model. All baseline controls are included in the specification. With the exception of column (2) all standard errors are robust and clustered on arrondissements.

Table 4: Channels

Dep Variables:	Forest (1)	TCC (2)	$r$ (3)	RainAg (4)	SavannaAg (5)	ForestAg (6)
$ATR_{it}$	0.020 (0.009)	0.055 (0.022)	0.056 (0.024)			
$ATR_{it} \times \text{Ethnic Frac}_{it}^{Q_{1-2}}$	-0.002 (0.006)	-0.002 (0.018)	-0.023 (0.015)			
$ATR_{it} \times \text{Ethnic Frac}_{it}^{Q_{2-3}}$	-0.010 (0.007)	-0.017 (0.020)	-0.026 (0.020)			
$ATR_{it} \times \text{Ethnic Frac}_{it}^{[>Q_3]}$	-0.004 (0.011)	0.011 (0.027)	-0.007 (0.025)			
$ATR_{it}$				-0.041 (0.015)	-0.034 (0.017)	-0.021 (0.012)
Observations	1,637	1,637	1,637	1,637	1,092	1,092
Arrondissements	546	546	546	546	546	546

Unit of analysis is arrondissement. Column (1) the dependent variable is forest cover from the ESA-CCI-LC data. Column (2) and (3) the outcomes are tree canopy cover (TCC) and the annual rate of change of TCC ( $r$ ), both from the VCF5KYR dataset. Column (4) the dependent variable is the share of rainfed agriculture in an arrondissement, and columns (5) and (6) is the share of savanna to agriculture transition, and forest to agriculture transition.  $\text{Frac}_{it}$  is an ordered categorical variable identifying the quartile of the ethnic fractionalization distribution to which each observation belongs, with  $\text{Frac}_{it}^{[<Q_1]}$  as the reference category. All specifications include all baseline controls and the full set of fixed effects: arrondissement and department  $\times$  aez  $\times$  year. Robust standard errors are clustered at the arrondissement level.

Table 5: Model parameter estimates

Parameter	Estimate	Std. Dev.	Method
$\mu$	0.0482	0.003	MLE on TPD (only WAP data, 1982-2016)
$\sigma$	0.258	0.032	MLE on TPD (1982-2016)
$\alpha_a$	0.553	0.028	MLE
$\beta_a$	2.251	0.151	MLE
$\gamma$	2.272	0.856	GMM ( $g_2 = a$ )

MLE: maximum likelihood estimation. TPD: transition probability density. WAP: W-Arly-Pendjari complex. GMM: generalized method of moments.

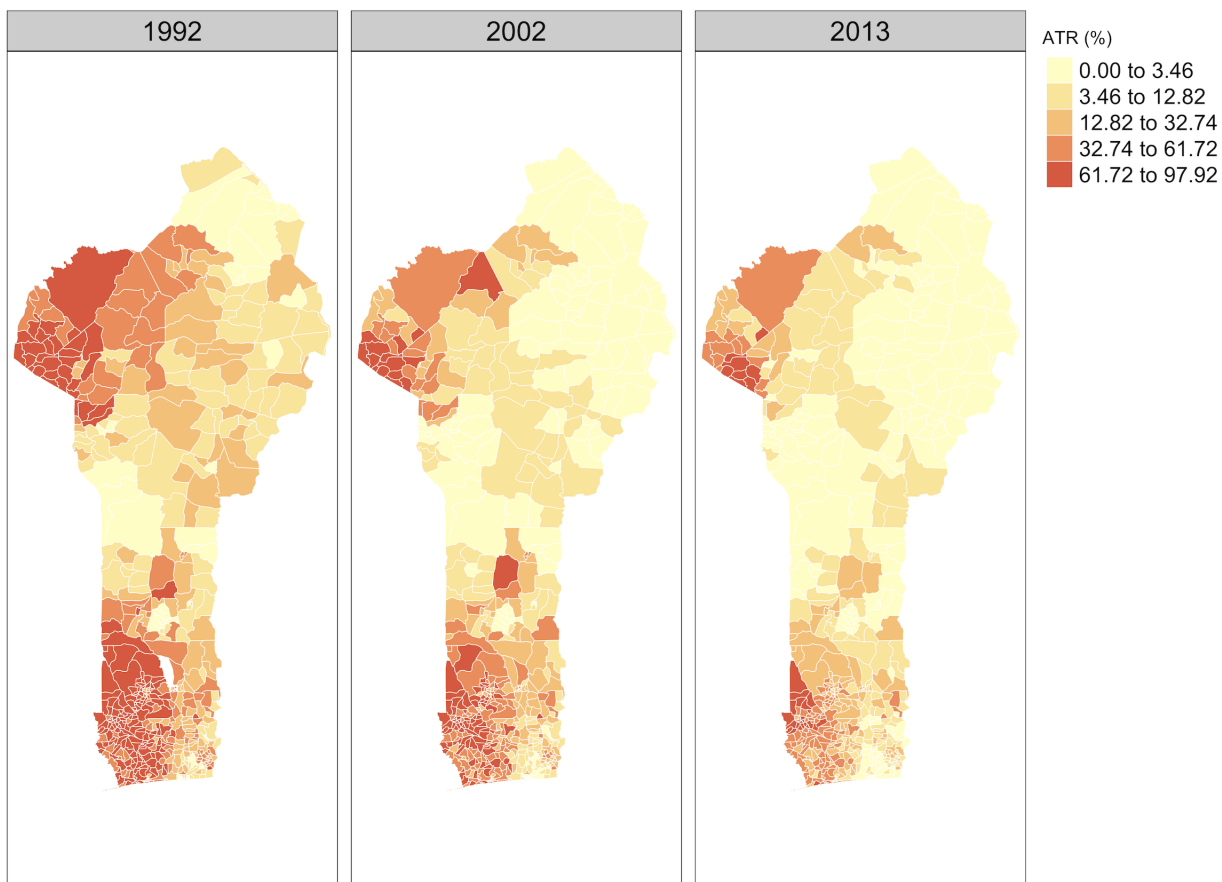


Figure 1: Evolution of ATR adherence across arrondissements over time. ATR adherence is measured as the percentage or share of individuals living in an arrondissement that self-report as following ATR, in a given census year.

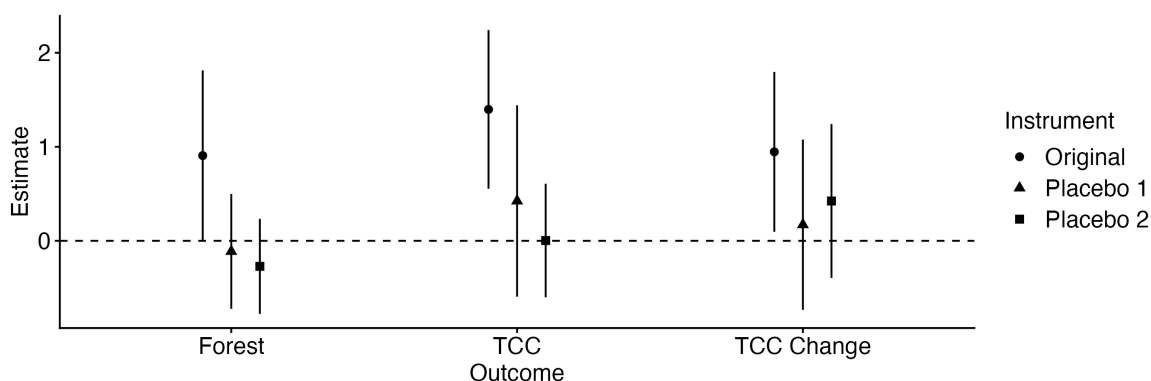


Figure 2: Reduced-form estimates of the effect of placebo instruments with 95% CIs. Original instrument is  $Z_{it} = \frac{HD_i^{YORUBA} \times LD_i^{\ell, YORUBA}}{\text{Density of Pentecostals in Nigeria}_t} \times RP_{it}^c$ , placebo 1 is  $\tilde{Z}_{it} = \frac{HD_i^{Gurma} \times LD_i^{\ell, Gourmanché}}{\text{Density of Pentecostals in Nigeria}_t} \times RP_{it}^c$  and placebo 2 is  $\tilde{\tilde{Z}}_{it} = \frac{HD_i^{YORUBA} \times LD_i^{\ell, YORUBA}}{\text{Density of Pentecostals in Nigeria}_t} \times RIC_{it}^c$

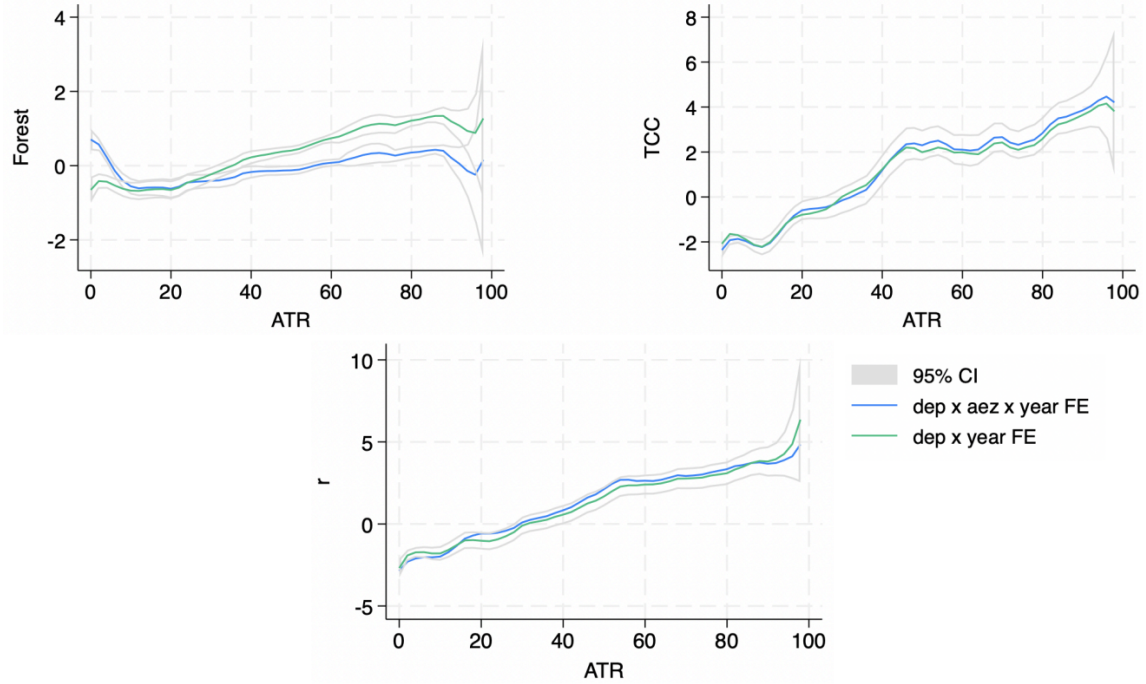


Figure 3: Baltagi et al. (2002) semiparametric regression of forest cover, TCC and TCC rate of change on ATR, department-year fixed effects (green solid line) and department-aez-year fixed effects (blue solid line). All specifications include baseline controls and arrondissement fixed effects. Local linear regressions with Epanechnikov kernel. Grey lines show 95 percent confidence interval, clustered by arrondissements.

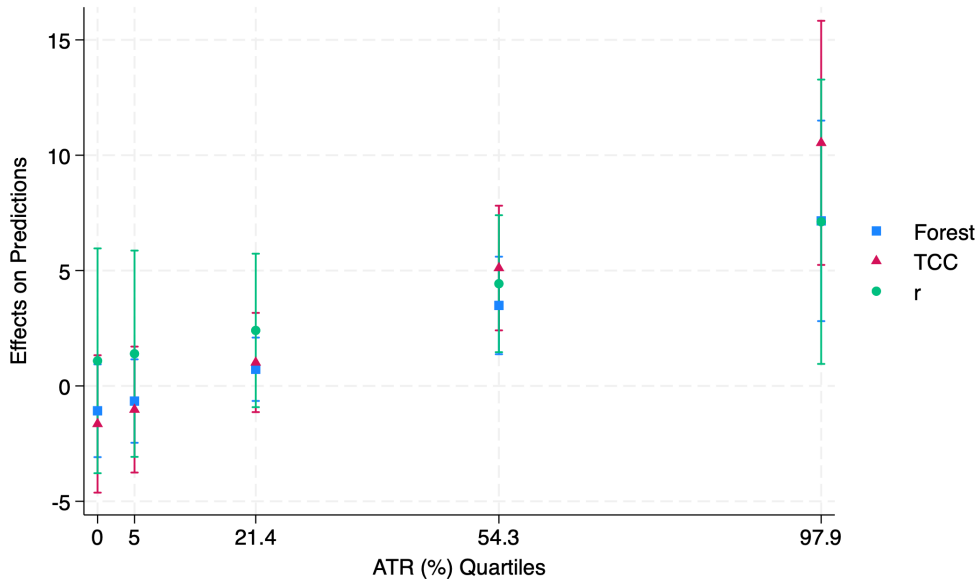


Figure 4: 2SLS estimation including an interaction between  $ATR_{it}$  and  $RainAgDummy_{it}^{>Q1}$ , a binary variable which equals one for observations above the 25th percentile of rain-fed agricultural expansion. The figure illustrated the average marginal effects of  $RainAgDummy_{it}^{>Q1}$  for ATR at 0, 25<sup>th</sup>, 50<sup>th</sup>, 75<sup>th</sup> and 100<sup>th</sup> percentile, with 95% CIs.

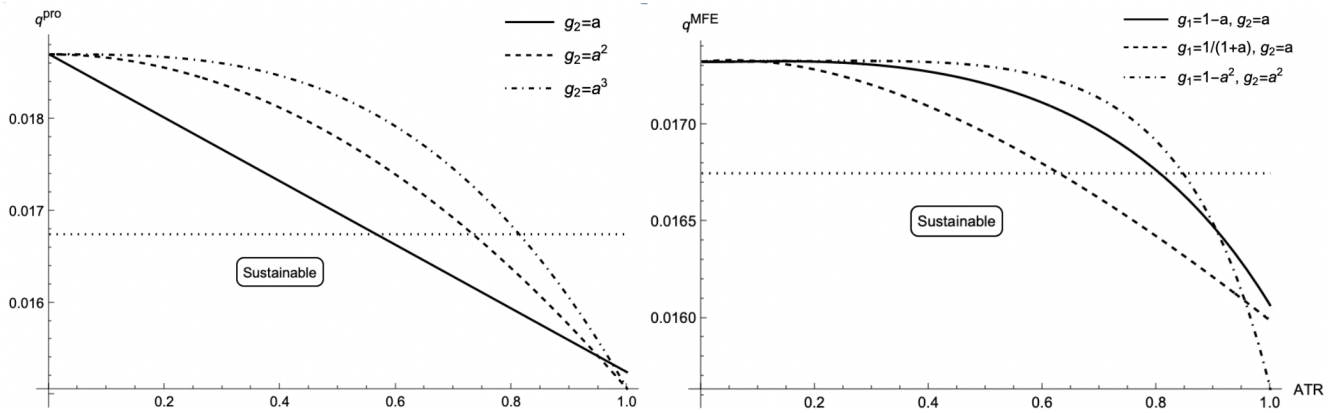


Figure 5: Optimal deforestation rates and ATR adherence. Left panel: model with only pro-environmental attitudes ( $g_1 = 0$ ) for different choices of  $g_2$  ( $\gamma = 1.5$ ). Right panel: model with adherence affecting both individual consumption and pro-environmental attitudes, for different choices of  $g_1$  and  $g_2$  ( $\gamma = 2.2$ ). Full and dot-dashed lines: local forest consumption and global scarcity are perfect substitutes. Other parameters:  $\rho = 0.02, \mu = 0.018, \sigma = 0.05$ . Beliefs distribution  $p_o(a) \sim \text{Beta}(0.55, 2.55)$ , estimated from the Benin census data.

### 2013 Tree Canopy Cover

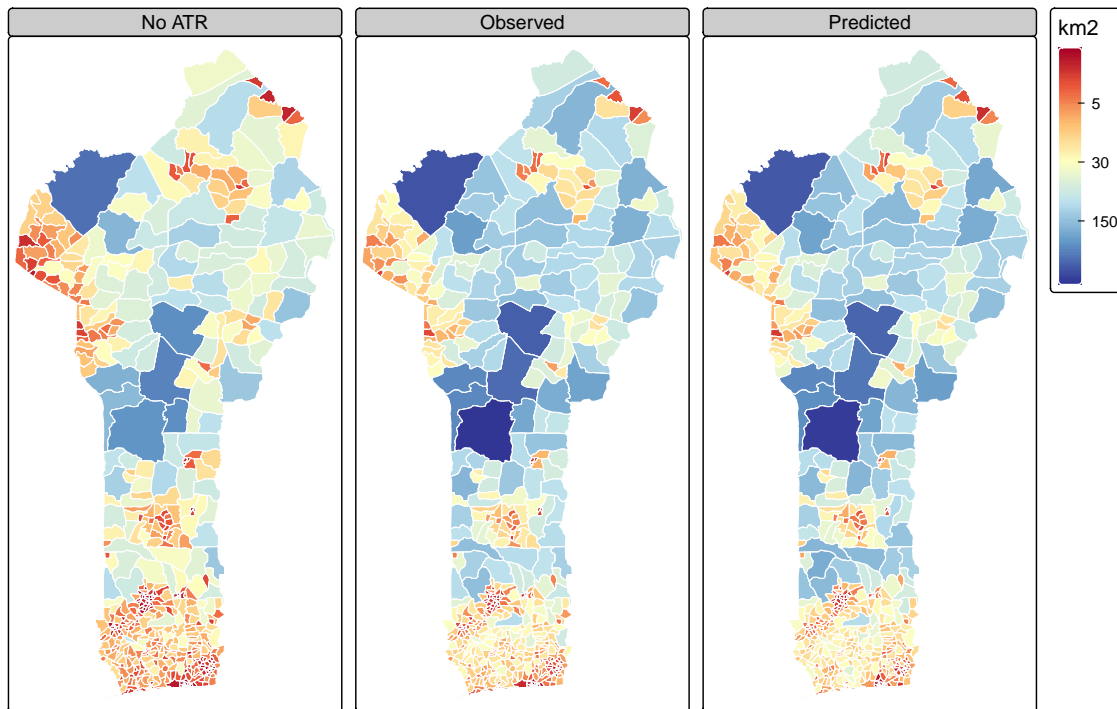


Figure 6: Counterfactual (no ATR), observed and predicted spatial tree canopy distributions in Benin for 2013.

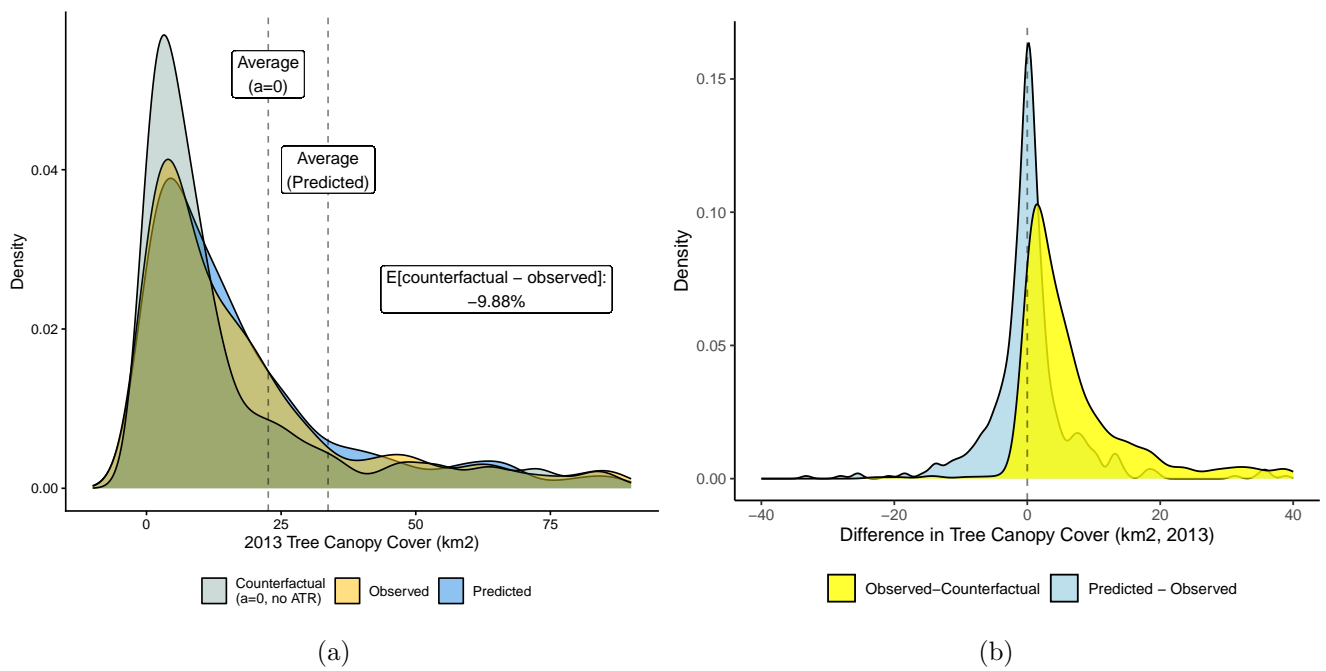


Figure 7: Panel (a): Counterfactual (no ATR), observed and predicted 2013 Benin tree canopy densities. Panel (b): difference between observed and predicted, and observed and counterfactual 2013 tree canopies.

# Sacred Ecology

## Online Appendix

<b>A Tables and Figures</b>	<b>48</b>
<b>B Data Sources</b>	<b>59</b>
<b>C Model Setup</b>	<b>61</b>
<b>D Proof of Proposition 1</b>	<b>63</b>
<b>E Proof of Proposition 2</b>	<b>70</b>
<b>F Estimation of the model parameters</b>	<b>72</b>

## A Tables and Figures

Table A1: ESA-CCI-LC dataset: Land Cover classifications used in the study

	Land Cover (LC) classification	LC type
Forests	Tree cover, broadleaved, evergreen, closed to open ( $\geq 15\%$ )	50
	Tree cover, broadleaved, deciduous, closed to open ( $\geq 15\%$ )	60, 61, 62
	Tree cover, needleleaved, evergreen, closed to open ( $\geq 15\%$ )	70, 71, 72
	Tree cover, needleleaved, deciduous, closed to open ( $\geq 15\%$ )	80, 81, 82
	Tree cover, mixed leaf type (broadleaved and needleleaved)	90
	Mosaic tree and shrub ( $> 50\%$ ) / herbaceous cover ( $< 50\%$ )	100
	Tree cover, flooded, fresh or brakish water	160
	Tree cover, flooded, saline water	170
Agriculture	Rain-fed Cropland	10
Savanna	Shrubland	120, 121, 122

Global land cover (LC) data from the European Space Agency (ESA) Climate Change Initiative (CCI) programme. The data is binary as each pixel represents one type of LC classification. A total of 37 original LC types are presented in the dataset based on the LC Classification System developed by [Di Gregorio \(2005\)](#) for FAO. The LC types used in the study are Forests, Agriculture and Savanna. For further details refer to Section 3 in the main paper and [ESA \(2017\)](#).

Table A2: Summary Statistics

Statistic	N	Mean	St. Dev.	Min	Max
ATR (%)	1,637	31.049	28.907	0.000	97.921
Share of forest (%)	1,637	13.750	20.488	0.000	96.830
TCC (%)	1,637	16.331	10.625	0.000	58.500
$r$ (%)	1,637	-0.428	5.404	-26.614	22.837
Illiteracy (%)	1,637	54.288	17.968	11.935	91.489
Catholic adherents (%)	1,637	22.495	17.830	0.000	88.908
Poorest households (%)	1,637	65.795	30.549	0.000	100.000
Informal employment (%)	1,637	39.618	10.237	14.903	72.131
Precipitation (mm)	1,637	87.188	11.476	58.438	123.422
Max temp (celsius)	1,637	32.487	1.137	30.124	36.000
Min temp	1,637	22.287	1.232	19.321	25.184
Population density	1,637	470.400	1,599.071	5.282	17,925.120
Nighttime lights	1,637	2.774	9.036	0.000	62.999
Elevation	1,637	158.899	134.480	0.002	573.609
Soil suitability: Maize	1,637	2,597.477	2,130.454	20.589	8,111.000
Soil suitability: Cotton	1,637	2,386.006	1,645.405	25.622	5,556.000
Soil suitability: Cassava	1,637	2,947.035	2,110.851	33.336	7,778.000
Ethnic fractionalization	1,637	0.406	0.265	0.000	0.914
Rainfed Agriculture (%)	1,637	44.855	33.906	0.000	100.000
Forest to Ag. (%)	1,092	0.714	2.532	0.000	29.023
Savanna to Ag. (%)	1,092	1.127	3.470	0.000	36.526
$LD_i^{\ell, \text{YORUBA}}$	1,637	0.308	0.152	0.000	1.000
$HD_i^{\text{YORUBA}}$	1,637	154.880	57.789	28.573	344.030
$RP_{it}^c$	1,637	0.567	0.308	0.000	1.000

Unit of observation is arrondissement. The sample consists of three census years 1992, 2002 and 2013. ATR refers to African Traditional Religions, TCC refers to Tree Canopy Cover,  $r$  refers to the annual rate of change of TCC over approximately a decade-long period, calculated as  $r_{it} = (1/\Delta t) \times \ln(\text{TA}_{it}/\text{TA}_{it-1}) \times 100$  where TA is total area of tree canopy cover.  $HD_i^{\text{YORUBA}}$ , is the haversine distance of each arrondissement from the ethnic homeland of the Yoruba group as given by [Murdock \(1967\)](#).  $LD_i^{\ell, \text{YORUBA}}$  is a measure of linguistic distance to the language Yoruba.  $RP_{it}^c$  is the re-centered and residualized signal strength received by each arrondissement.

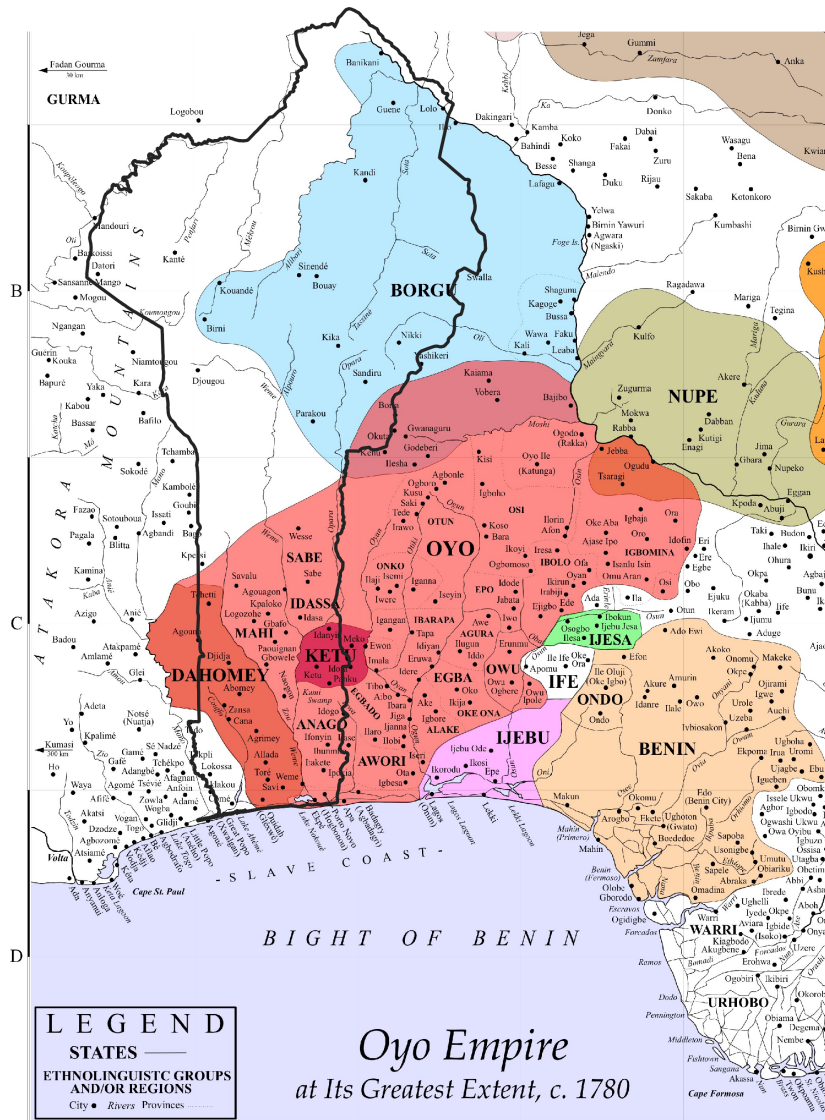


Figure A1: Bight of Benin: Dahomey, Oyo, Borgu and neighbouring kingdoms, 1780. The Kingdom of Benin is not to be confused with modern Republic of Benin. Today the former refers to Benin city in Nigeria and Dahomey refers to the nation state Benin. Solid black line represents modern day boundary of Republic of Benin. Source: [Lovejoy \(2013\)](#)

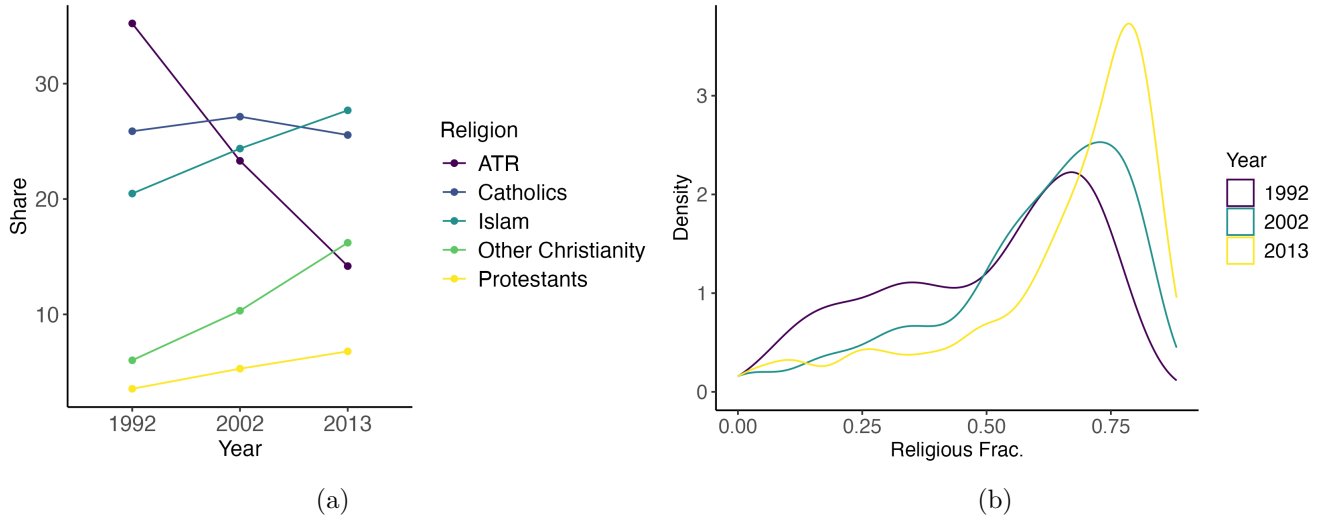


Figure A2: Panel (a) shows the share of adherents of major religions across the three censuses. Panel (b) shows the density estimation of the distribution of arrondissements by religious fractionalization over time.

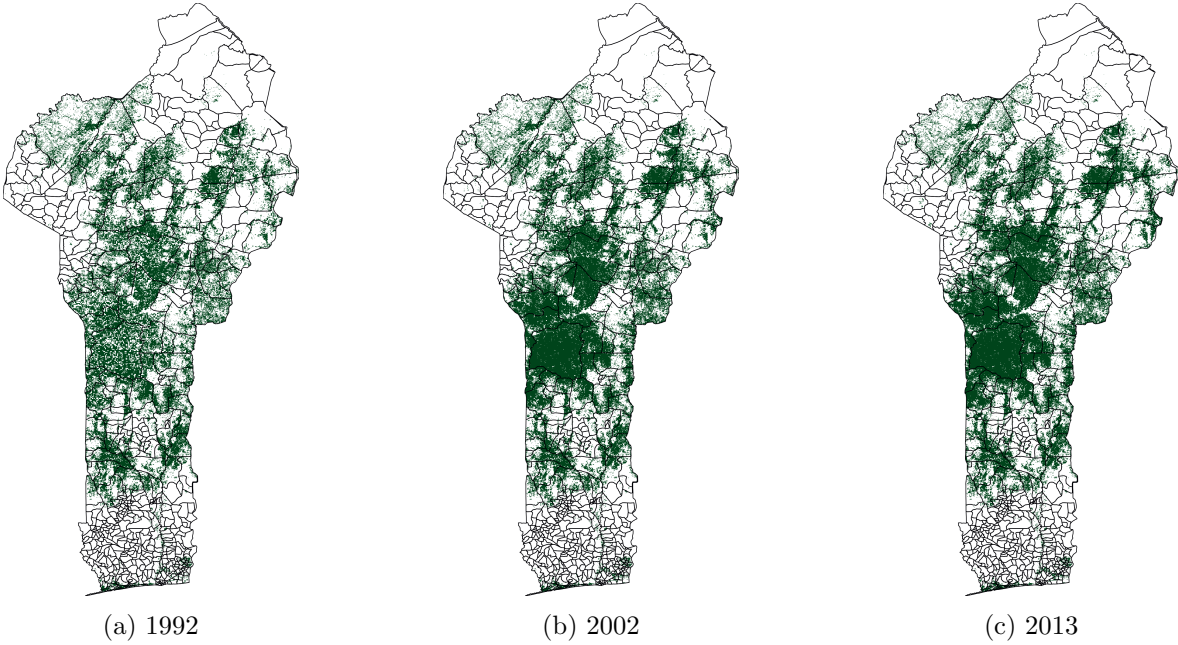


Figure A3: Spatial distribution of forest type land class based on ESA-CCI-LC maps.

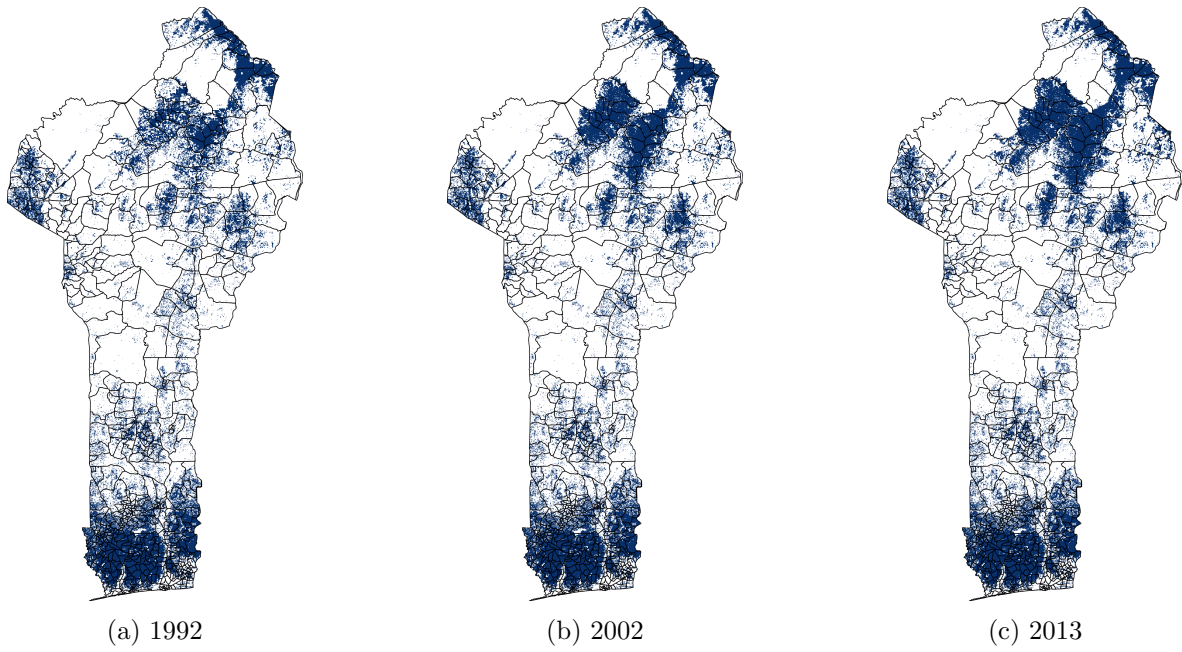


Figure A4: Spatial distribution of rainfed cropland type land class based on ESA-CCI-LC maps.

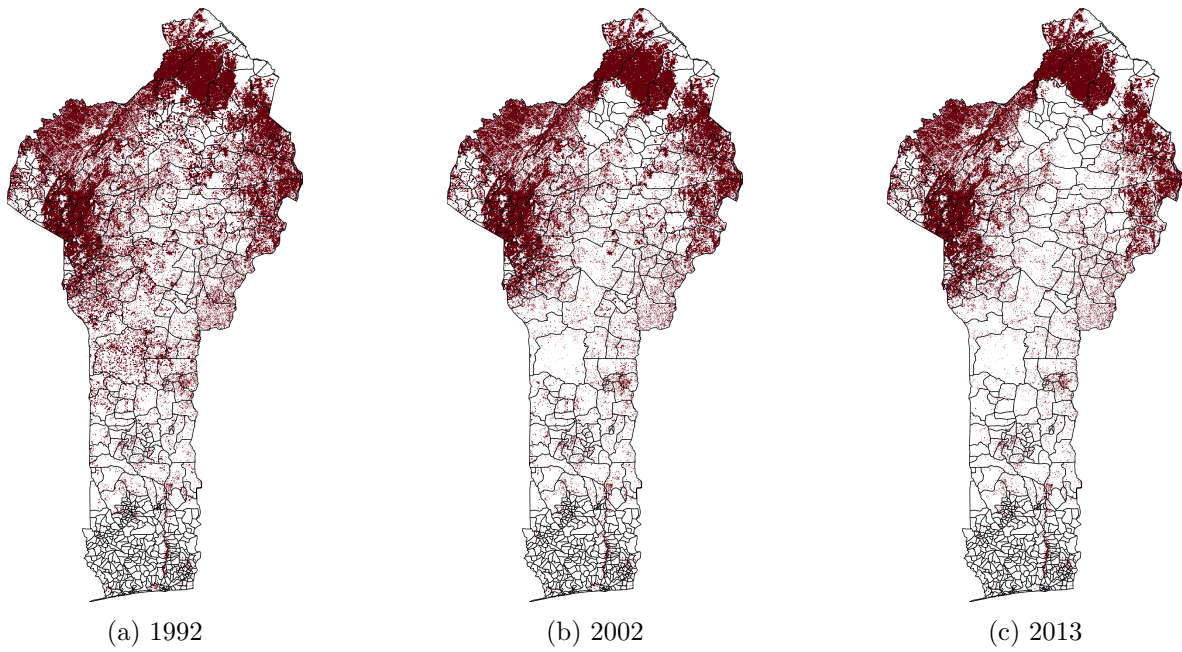


Figure A5: Spatial distribution of savannah type land class based on ESA-CCI-LC maps.

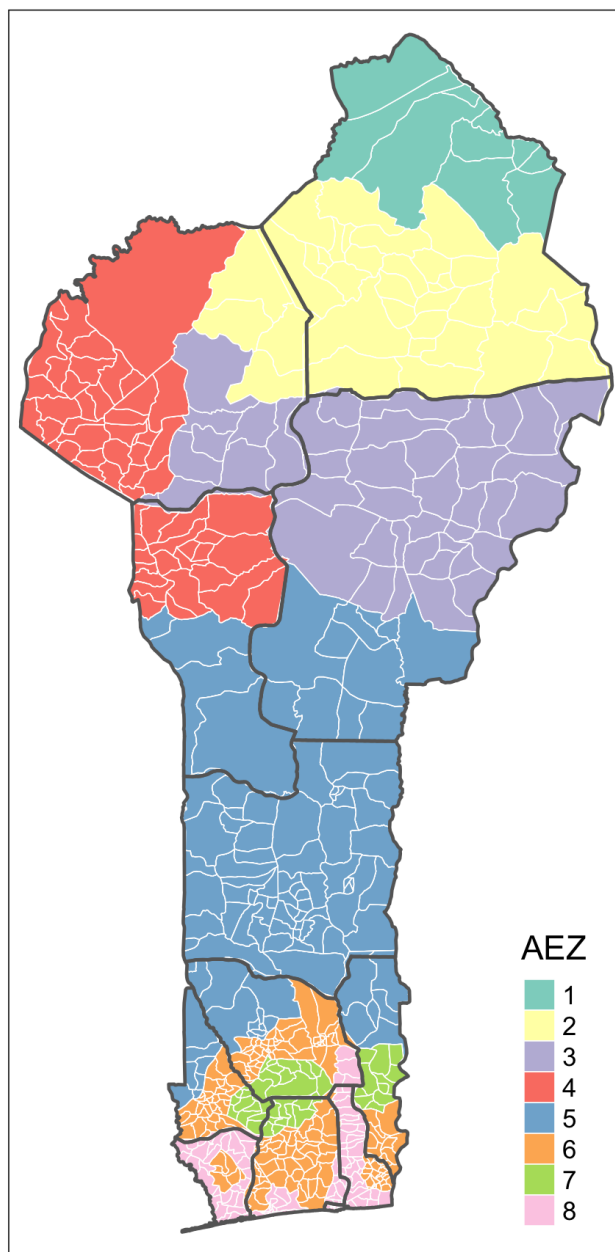


Figure A6: White lines represent the boundaries of the arrondissements and black lines represent the boundaries of the departments. The eight agro-ecological zones are: 1) Extreme North Zone, 2) North Cotton Zone, 3) South Borgou Crops Zone, 4) West Atacora Zone, 5) Centre Benin Cotton Zone, 6) Clayey Earth Zone, 7) Depression Zone and 8) Fisheries Zone (UNDP et MEPN, 2008).

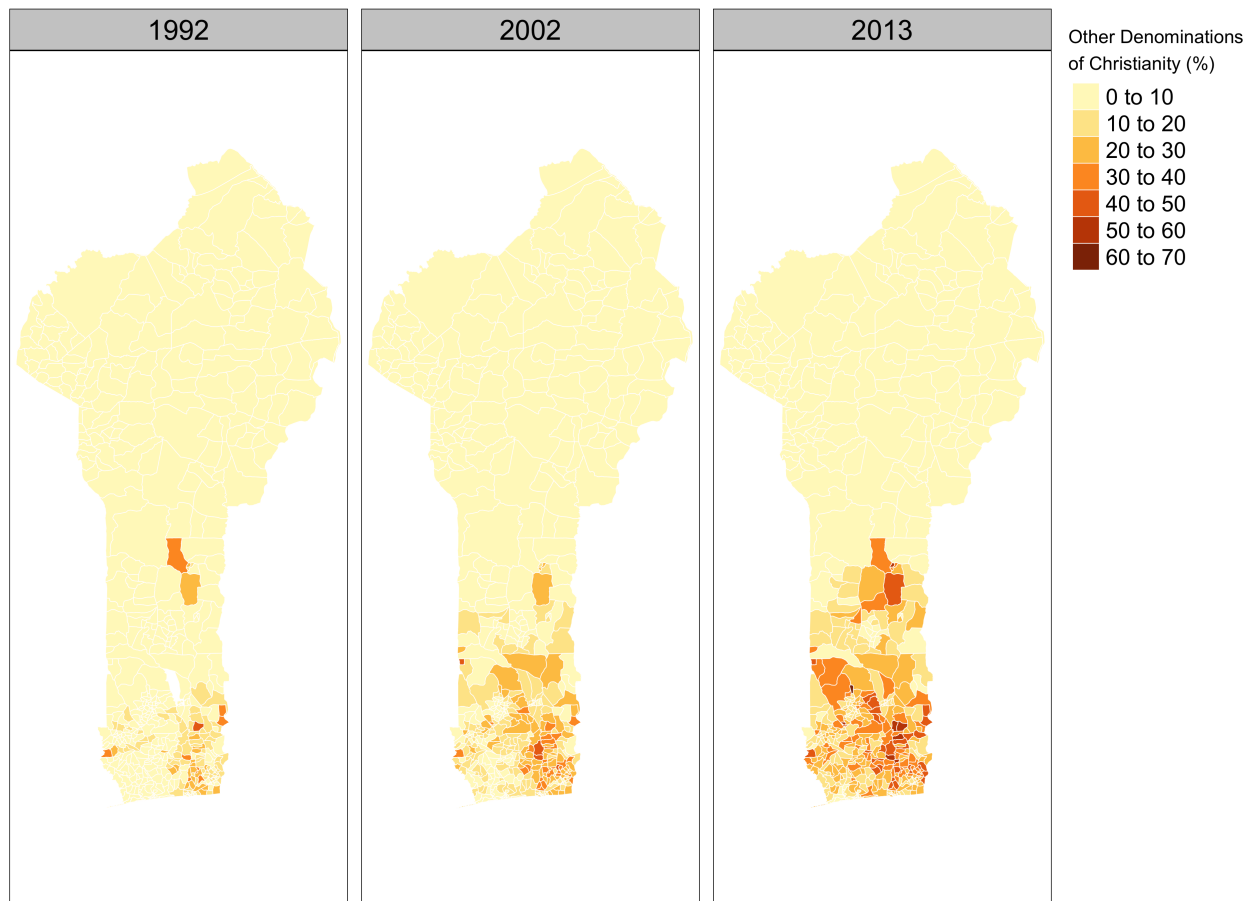


Figure A7: Evolution of other denominations of Christianity across arrondissements over time.

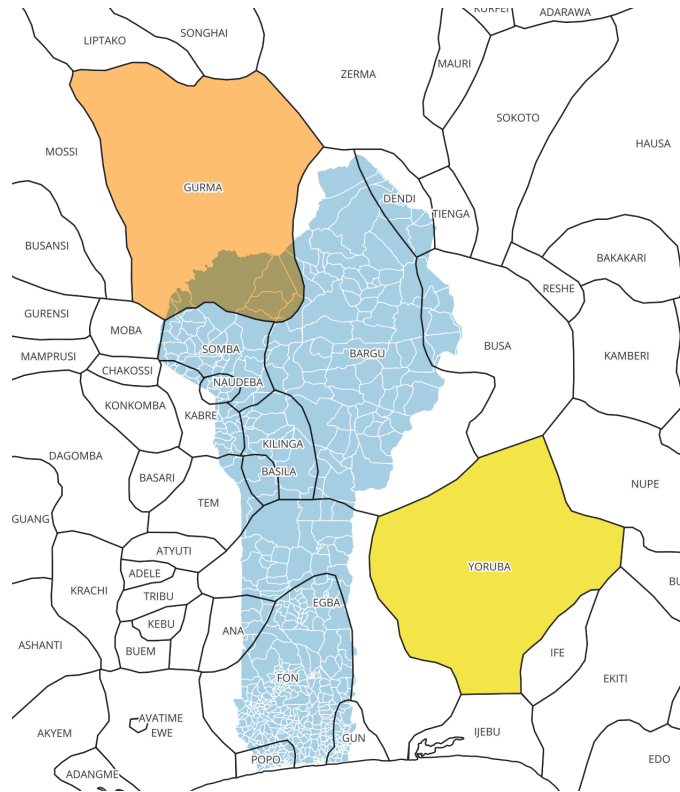


Figure A8: The solid white lines represent the boundaries of the 546 arrondissements in Benin, the solid black lines represent the ethnic homeland boundaries as given by [Murdock \(1967\)](#). The yellow polygon represents the Yoruba homeland and the orange polygon represents the Gurma homeland.

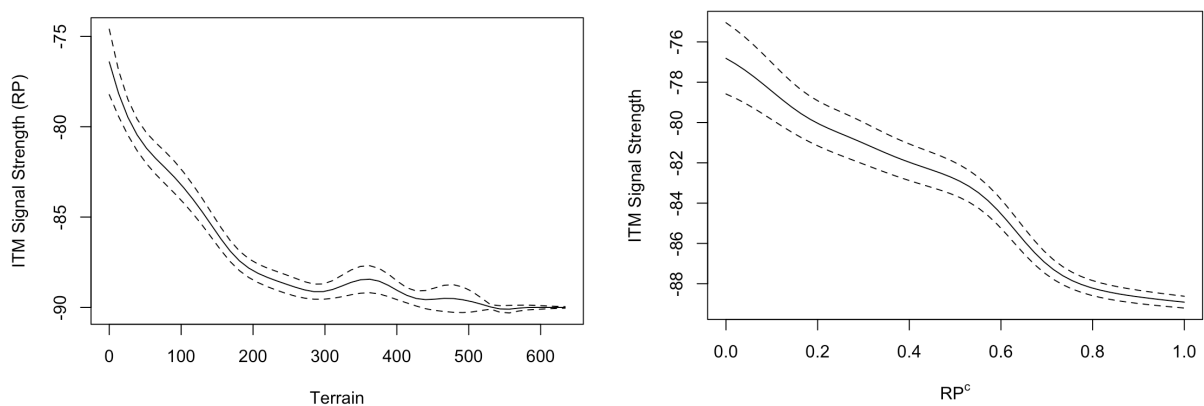


Figure A9: Nonparametric estimates of the relationship between the ITM-based measure of signal strength for each arrondissement and terrain (left panel) and our recentered and normalized measure of radio exposure  $RP_{it}^c$  (right panel). Estimations done with local linear regressions, a bootstrapped error band and a bandwidth that uses Kullback-Leibler cross-validation.

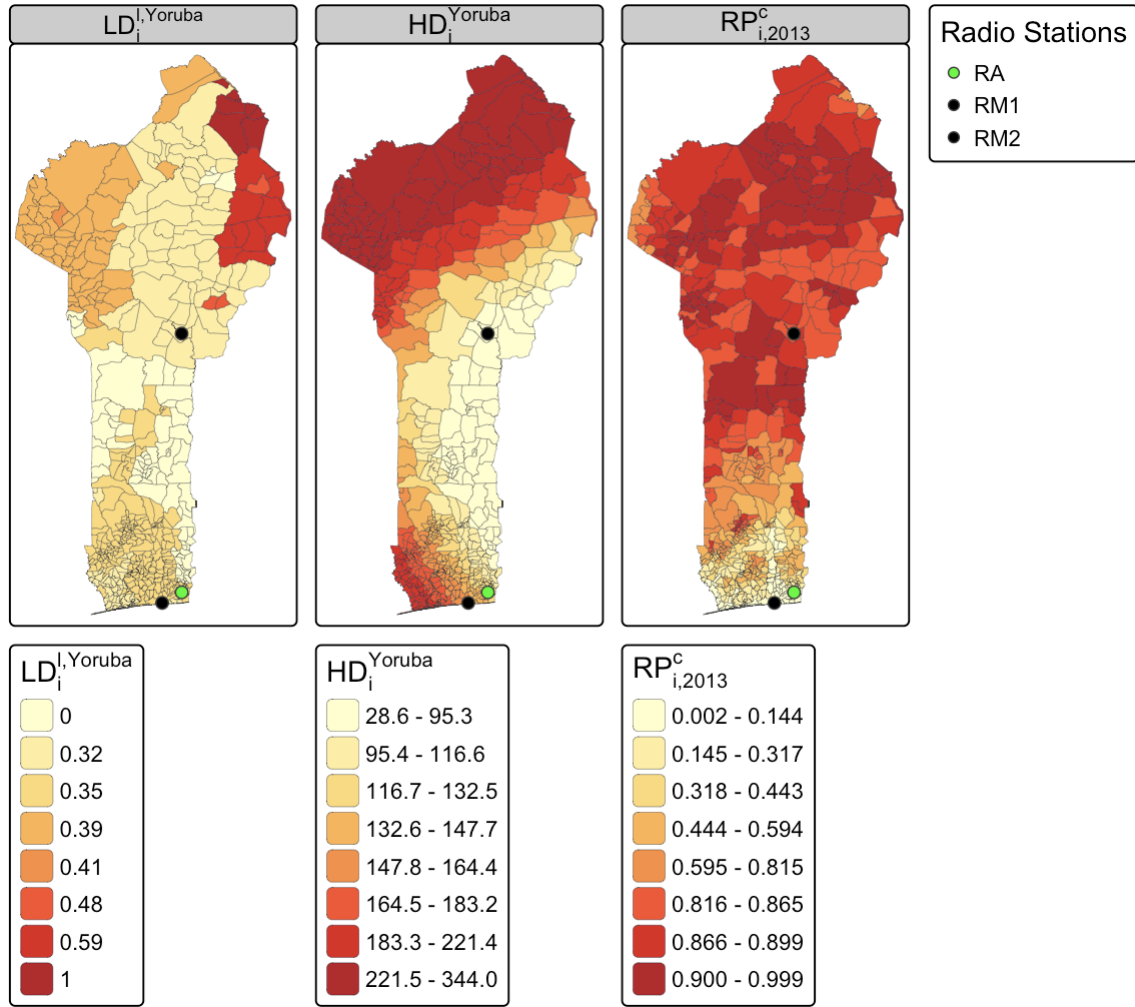


Figure A10: The three sources of exogenous variation used to build the instrument. Left hand side panel shows the linguistic distance of the language  $\ell$  of the arrondissement from the Yoruba language. Middle panel shows the haversine distance of the arrondissement centroid to the Yoruba ethnic homeland. The right panel shows the 2013 recentered residualized signal strength  $RP_{it}^c$ . For all three, higher values are associated with higher ATR adherence. The dot symbol refers to the locations of the transmitters of Radio Maranatha (RM1, RM2) and Radio Alléluia (RA).

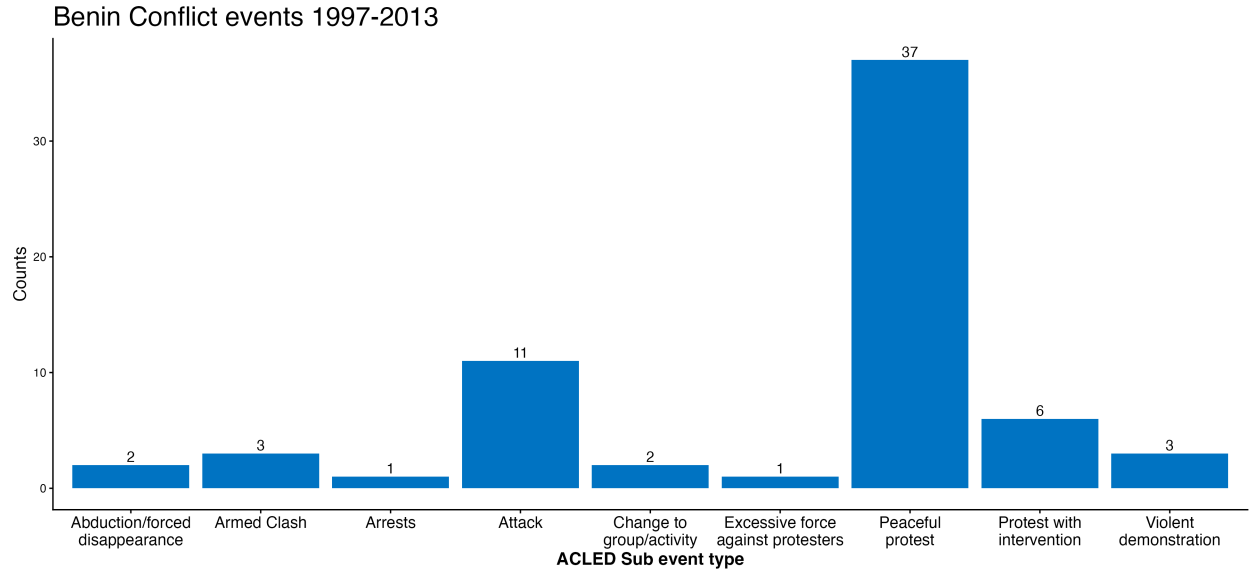


Figure A11: Distribution of ACLED conflict events in Benin between 1997-2013.

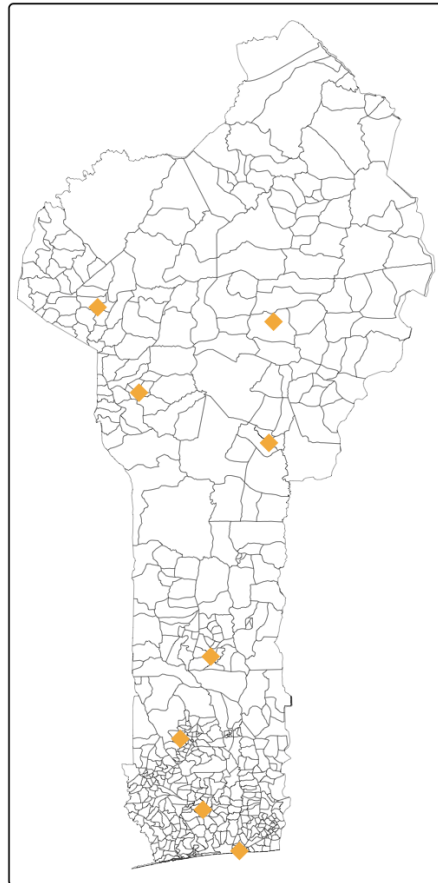


Figure A12: Location of the Radio Immaculée Conception Transmitters based on FMLIST database by Radio Data Center GmbH.

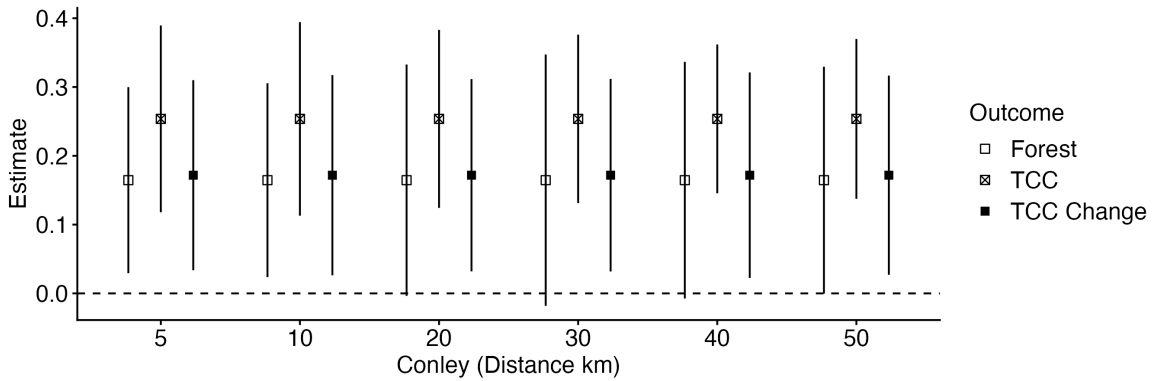


Figure A13: Robustness of the 2SLS estimates to computing Conley standard errors for spatial bandwidth between 5-50 km. The choice of the bandwidth is based on the geographic characteristics of Republic of Benin which is narrow, key-shaped and at its widest measures about 325 km and the narrowest width of the country is the 125 km stretch of its coastline along the Bight of Benin. 90% confidence intervals.

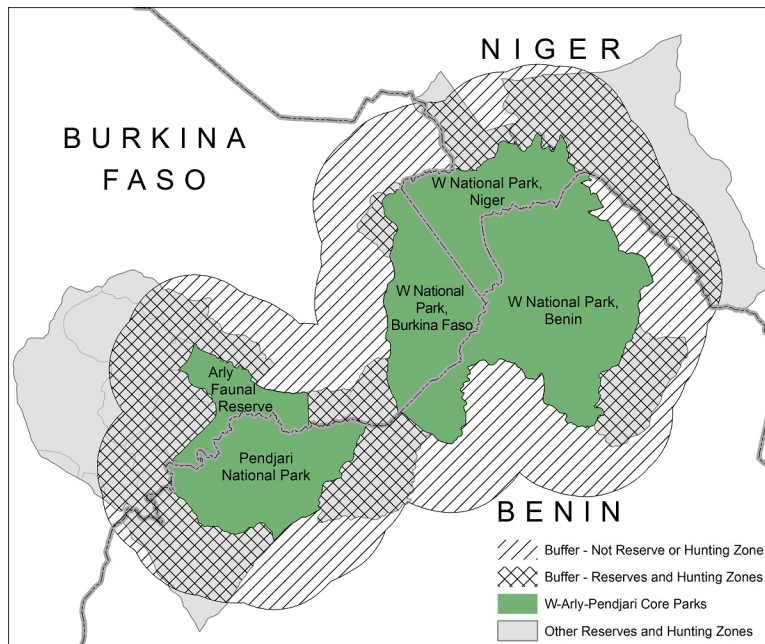


Figure A14: W-Arly-Pendjari complex and surrounding buffer zones.

Source: USGS EROS, <https://eros.usgs.gov/westafrika/case-study/w-arly-pendjari-transboundary-biosphere-reserve>

## B Data Sources

- Climatic variables: Temperature (minimum and maximum) and precipitation are obtained from the Climatic Research Unit (CRU) Time-Series (TS) version 4.08, covering the period 1901-2023.
- Geographic variables: Elevation data is obtained from Advanced Spaceborne Thermal Emission and Reflection Radiometer (ASTER) Global Digital Elevation Model Version 3 (GDEM 003). The longitude and latitude coordinates are the centroids of the Benin arrondissement, administrative division level 3 shapefile obtained from GADM Database of Global Administrative Areas. The agro-ecological zones are taken from [UNDP et MEPN \(2008\)](#).
- Soil suitability: Maize, cassava and cotton soil suitability, rainfed with low inputs has been obtained from FAO GAEZ, where suitability ratings are assigned based on soil qualities influencing crop performance, inputs level and water supply system.
- Population density: The Gridded Population of the World (GPW) collection, version 3 (UN Adjusted) 1995 for the census year 1992 and version 4.11 (UN Adjusted) 2005, 2015 for the census years 2002 and 2013.
- Nighttime lights: Taken from [Li et al. \(2020\)](#) who provide a harmonized global nighttime light dataset using Defense Meteorological Satellite Program (DMSP) and the Visible Infrared Imaging Radiometer Suite (VIIRS).
- Socio-economic variables: The three waves of the Benin population census are used for these variables. Question on “alphabetisation” is used to calculate the rate of illiteracy by taking the share of response “Ne sait ni lire ni écrire/Cannot read or write” per arrondissement. Data on religion is used to calculate percentage of ATR and Catholic adherents, and religious fractionalization. Data on ethnicity is used to calculate ethnic fractionalization. Question on “statut d’occupation / status of occupation” is used to calculate the rate of informal employment by taking the share of response “Occupé secteur informel/Occupied in informal sector” per arrondissement. Share of poorest households is obtained by creating a wealth index based on household characteristics and assets (roof, wall and floor materials, source for electricity, water, waste and wastewater, type of toilet, and cooking fuel used). The index is generated with principal components analysis (PCA) where each household receives a wealth score based on the weights assigned to the different assets and characteristics by the PCA. The household scores are standardized and the household population is divided into five equal groups (quintiles) from the poorest to the wealthiest.
- Environmental outcomes and additional variables : Share of forests, rainfed agriculture and savanna is from the ESA-CCI-LC dataset. This data also permits us to calculate if a cell has transitioned from one land cover (LC) type to another between census waves. See [Table A1](#) for details on LC. For  $SavannaAg_{it}$  we calculate the share of cells in an arrondissement that underwent transition from LC type 120,121,122 to 10 between 1992-2002 and 2002-2013, leaving us with  $t = 2$ . Similarly, for  $ForestAg_{it}$  we calculate the share of cells that underwent transition from LC type 50,60-62,70-

72,80-82,90,100,160,170 to 10. TCC and annual change rate of TCC is from the NASA VCF5KYR dataset. For more information on both datasets refer to Section 3 of the main paper.

- Instrumental Variable:
  - Nigeria exposure: The linguistic distance data is based on the language level dataset provided by [Giuliano and Nunn \(2018\)](#) who use the sixteenth edition of the Ethnologue: Languages of the World. The ethnic homeland boundaries are taken from the Ethnographic Atlas, a world-wide ethnicity-level database constructed by George Peter Murdock ([Murdock, 1967](#)). The data on the number of Pentecostals in Nigeria is obtained from the “Religious Characteristics of State Dataset: Demographics, version 2.0” by [Brown and James \(2018\)](#), available at The Association of Religion Data Archives (ARDA). Finally, Nigeria’s land area, defined as a country’s total area, excluding area under inland water bodies, national claims to continental shelf, and exclusive economic zones, is taken from World Bank data ID: AG.LND.TOTL.K2.
  - Benin Exposure: Radio transmitter characteristics for Radio Maranatha, Radio Alléluia and Radio Immaculée Conception such as location coordinates, frequency, antenna height and effective radiated power (ERP) were been obtained from FMLIST database by Radio Data Center GmbH.

## C Model Setup

Let us first show in detail the reason behind the particular form of coupling we have assumed, the geometric mean  $\exp \mathbb{E}^p[\log X_{it}^q]$ , as with it one can explicitly show the dynamics of the (geometric) average forest cover.

We consider a continuum of individuals, or equivalently a large  $N$ , yielding a mean-field game. Mean-field games are a branch of game theory pioneered by [Lasry and Lions \(2006; 2007\)](#) with increasing applications in both economics and finance literature (see, for example [Lucas and Moll, 2014](#), [Gabaix et al., 2016](#) and [Achdou et al., 2022](#)). To our knowledge, our application of this powerful framework is novel, both in its approach to heterogeneity and pro-environmental beliefs. Our application of this powerful framework introduces two novel features, particularly underexplored in environmental and natural resource economics: first, it successfully couples heterogeneity in beliefs and attitudes with managed ecosystems by means of strategic decision making. Second, it establishes a framework for analyzing the feedback of global environmental dynamics on natural resource policies and their sustainability, which remains eminently tractable and estimable whilst maintaining the essence of the complexity of the problem. Since each individual  $i$  has her own level of exogenous adherence to ATR beliefs  $a_i \in A$ , the forest cover spatial distribution  $p(x, t)$  will depend jointly on the distribution of ATR beliefs, i.e. it should be defined as  $p(x, a, t)$ . This density is equipped with an initial distribution  $p_0(x, a, 0)$ , which is the initial joint distribution of forest cover and ATR adherence. We thus augment our filtration  $\mathcal{F}_t$  to  $\mathcal{F}_t^a$ , which includes the information available to all individuals at time 0 over the initial state of both forest and adherence.

It must therefore be that the beliefs have a marginal distribution

$$\int_x p(dx, a, t) = \int_x p_0(dx, a, 0) := p_0(a),$$

which is the distribution of ATR beliefs among the population. This allows to separate forest cover and beliefs in the joint distribution:

$$p(dx, da, t) = p^a(dx, t)p_0(da) \tag{12}$$

where  $p^a$  is a probability measure in  $x$  for  $p_0$ -almost any  $a$ .

Using (12), we can write the interaction term between agents as

$$\bar{X}_t = \exp \int_{[0, \infty) \times A} \log x p(dx, da, t) = \exp \int_{[0, \infty)} \int_A \log x p^a(dx, t)p_0(da). \tag{13}$$

Note that for a discrete number  $j = 1, \dots, n$  of observations  $x_j$ ,  $p^a(x, t)$  is exactly the empirical measure associated to the realizations  $x_j$  and (13) becomes the familiar expression for the geometric mean  $(\prod_j x_j)^{1/n}$ .

First, a straightforward application of Itô's lemma yields

$$d \log X_t = \left( \mu - \frac{\sigma^2}{2} - q_t \right) dt + \sigma dW_t$$

where  $\bar{W}_t$  is a  $\mathcal{F}_t^a$ -adapted standard Brownian motion. Since all agents face idiosyncratic and independent Brownian motions and  $\mu, \sigma$  are assumed to be the same across the population, and expectations of a Brownian motion are equal to zero, the dynamics of the median forest cover  $\bar{X}_t$  are given therefore by

$$d\bar{X}_t := d \exp(\mathbb{E}[\log X_{it}^q | \mathcal{F}_t^a]) = \left[ \bar{X}_t \left( \mu - \frac{\sigma^2}{2} \right) - \int_A \bar{q}_t p(da) \right] dt. \quad (14)$$

where  $\bar{q}_t = \int q p^a(dx, t)$  is the median deforestation policy for individuals with any adherence  $a$ . The dynamics implied by (14) show clearly how the average state of the forest depends not only on the ecological parameters  $\mu$  and  $\sigma$ , but also on the heterogeneity in beliefs within the population, which shape global deforestation. We now conjecture individual deforestation policies to be linear in  $\bar{X}$ , i.e.  $q_{it} := q(X_{it}, t) = q_{it} X_{it}$  and thus assume  $q_{it} \in [0, 1]$  to be the average fraction of forest consumed by an individual at each  $t$ . This conjecture will be shown to be correct later - getting slightly ahead of ourselves, we begin with this conjecture as it is well-known that a single-agent (or representative) agent's problem with power utility and a geometric Brownian motion yields optimal policies linear in the state variable. Equipped with (14), we can write our problem as shown in Eq. (8) of the paper.

Before delving further in the full solution, let us present the following general (i.e. independent of the choice of utility function) result, showing how for any  $t \in [0, T]$  any optimal deforestation policy  $q_t^*$  in equilibrium changes with ATR adherence according to the following equation:

$$\partial_a q_t^* = \frac{1}{u_{qq}} \mathbb{E}_t^P \int_t^T e^{-\int_t^s (\rho - \mu + \partial_x q_v^*) dv} (D_s \partial_a u_{q\bar{x}} - \partial_a u_x) ds \quad (15)$$

where the  $\mathcal{F}_t^a$ -measurable process  $D_t = (\mu - \sigma^2/2)\bar{X}_t - \int \bar{q}_t^* p(da)$  is the instantaneous median forest change, net of median deforestation. The expectations are calculated with respect to the measure  $P$ , which is induced by the distribution  $p^a(x, t)$  of all individual forest cover processes  $X_{it}$  in equilibrium. The derivation of this Euler-type equation is based on a differentiation of the envelope of the Hamilton-Jacobi-Bellman equation (i.e. at the first-order condition), some straightforward derivations and an application of the Feynman-Kac formula, and is left for the involved reader.

Equation (15) shows how deforestation is determined by the interplay of three forces: individual adherence to ATR, the marginal value of one unit of forest cover for personal use, and the utility the individual assigns to the overall state of the environment via the spatial forest distribution. Furthermore, it shows how the change in deforestation due to a marginal increase in ATR is the sum of two effects discounted over time. One is always negative, and depends on each agent's sensitivity to ATR of the marginal utility of forest cover. This is intuitive: the more valuable for an agent is the stock - not the consumption - of forest left standing, and the more this quantity is sensitive to ATR adherence, the more the agent will

reduce deforestation. The second term depends on the *change* in median deforestation  $D_t$ . An increase in global deforestation reinforces the overall negative effect of ATR adherence on individual deforestation via the pro-environmental attitudes, weighed by the sensitivity to ATR of the mixed second partial derivative of forest consumption and scarcity, which is the key indicator of substitutability between the two. The slope of each individual deforestation policy  $\partial_x q$  determines the (stochastic) discount factor which makes the present value of lifetime marginal utility of forest consumption equal its future expectation (i.e. a martingale).

## D Proof of Proposition 1

Let us now focus on the problem of finding an equilibrium. In the limit of a large amount of individuals, and using (12), the  $\mathcal{F}_t^a$ -measurable deforestation policy in order to be a mean-field equilibrium must solve the following coupled backward/forward system of Hamilton-Jacobi-Bellman and Kolmogorov forward equations given by

$$-V_t + \rho V = \sup_{q \in Q} \left\{ u(q^{g_1(a)} \bar{x}^{g_2(a)}) - qV_x \right\} + \mu x V_x + \frac{\sigma^2}{2} x^2 V_{xx} \quad (16)$$

$$\partial_t p^a(x, t) = -\partial_x [(\mu x - q)p^a(x, t)] + \frac{\sigma^2}{2} \partial_{xx} x^2 p^a(x, t) \quad (17)$$

with the coupling condition

$$\bar{x} = \exp \int_{[0, \infty)} \int_A \log x p(dx, t) p_0(da), \quad (18)$$

under the decomposition (12) and the boundary conditions for the HJB (backwards, so with a final condition)  $V(x, T) = b(T; a)$  and Kolmogorov (forward, so with an initial condition)  $p(x, 0, a) = p_0^a(x_0, 0) p_a(a)$ .

The key feature of this system is the forward/backward dimension, essential characteristic of mean-field games. The Hamilton-Jacobi-Bellman equation (the optimality equation) is obtained backwards, as for all Bellman equations, starting from an endpoint condition. On the other hand, the Kolmogorov forward equation (17) (the probability equation) starts from an initial resource distribution  $p(x, 0)$  which is known to the agents, and transports probability forward by means of the individuals' optimal decisions  $q$  as well as its diffusive part. Starting from this distribution, they observe an endogenously time-evolving distribution  $p(x, t)$  for all  $t$ , which identifies an aggregate forest cover level  $\bar{x}$  via the coupling (18). They then optimize proportionally to the "forest rent"  $V_x$ , since the optimal extraction policy  $q^*$  conditional on the observation of  $p$  for all times  $t$  satisfies the first-order condition  $q^* = u_q^{-1}(V_x)$ . Since  $u$  is increasing and weakly concave in  $q$  for all  $a \in A$ , the optimal policy  $q^*$  is decreasing in the resource rent associated to the "average" forest stock  $V_x$ , increasing in the utility associated to scarcity  $\bar{x}$ , and increasing when  $g_1$  increases.

Using the condition (14), we have thus obtained a closed-form expression for the dynamics of  $\bar{X}_t$  and thus can incorporate the coupling condition of  $\bar{X}$  given by (18) together with the controlled state process

in the extended state space  $(X_t, \bar{X}_t, t)$ , subject to the SDE

$$dX_t = (\mu X_t - q)dt + \sigma X_t dW_t$$

and the ODE (14).

The HJB equation in the extended state space  $(x, \bar{x}, t) \in \mathbb{R}^+ \times \mathbb{R}^+ \times [0, T]$  becomes

$$-V_t + \rho V = \sup_{q \in Q} \left\{ \frac{1}{1-\gamma} \left[ q^{g_1(a)} \bar{x}^{g_2(a)} \right]^{1-\gamma} - q V_x(x, t) \right\} + \mu x V_x(x, t) + \bar{\mu}^a \bar{x} V_{\bar{x}} + \frac{\sigma^2}{2} x^2 V_{xx} \quad (19)$$

with boundary condition  $V(x, \bar{x}, T) = b(x, \bar{x}, T; a)$ . Note that this HJB equation is random, as it depends on the  $\mathcal{F}_t^a$ -measurable distribution of beliefs  $p_0(a)$ .

The supremum is achieved by the optimal policy

$$q^*(x, \bar{x}, a, t) = \left( \frac{V_x}{g_1 \bar{x}^{\nu_{\bar{x}}}} \right)^{-\epsilon_q} \quad (20)$$

where  $\epsilon_q$  is the elasticity of intertemporal substitution for forest use given by

$$\epsilon_q(a) = -\frac{u_q}{u_{qq}} \frac{1}{q} = (1 - g_1(a)(1 - \gamma))^{-1}$$

and  $\nu_q := \nu_q(a) = q \frac{u_q}{u} = g_1(a)(1 - \gamma)$  is the point elasticity of utility with respect to  $q$ , and similarly for  $\bar{x}$ ,  $\nu_{\bar{x}} := \bar{x} \frac{u_{\bar{x}}}{u} = g_2(a)(1 - \gamma)$ . Inserting (20) in the HJB yields the nonlinear PDE

$$-V_t + \rho V = \frac{\bar{x}^{\nu_{\bar{x}}}}{1-\gamma} \left[ \frac{V_x}{g_1 \bar{x}^{\nu_{\bar{x}}}} \right]^{\nu_q \epsilon_q} - \left[ \frac{V_x}{g_1 \bar{x}^{\nu_{\bar{x}}}} \right]^{\epsilon_q} V_x + \mu x V_x + \bar{\mu}^a \bar{x} V_{\bar{x}} + \frac{\sigma^2}{2} x^2 V_{xx}, \quad (21)$$

We now assume *for simplicity* a bequest function of the form  $b = h^{-1/\epsilon_q} \frac{X_T^{\nu_q} \bar{X}_T^{\nu_{\bar{x}}}}{1-\gamma}$ , where  $h := h(a), h' > 0, h : [0, 1] \rightarrow [0, 1]$ . Individuals thus want to leave at end of life  $T$  an amount of forest (both local and global) which depends on their own ATR adherence.

Using as *ansatz* for the value function a time-separable guess  $V(x, \bar{x}, t) = f(t) \frac{x^{g_1(1-\gamma)} \bar{x}^{g_2(1-\gamma)}}{1-\gamma}$  for a continuous function  $f : \mathbb{R}^+ \rightarrow [0, 1]$ , differentiable at least once, that exploits the homothetic and multiplicative form of the objective function. This *ansatz* implies that if an appropriate  $f(t)$  is found, then the optimal deforestation policy is given by  $q^* = f(t)^{-\epsilon_q} x$  for  $p_0$ -almost any  $a$ , which means that this form will apply for each individual, fixed any  $\bar{q}$ . This validates our conjecture of the median deforestation policy being linear in  $\bar{X}_t$ . After some lengthy computations we obtain that the function  $\phi(t)$  needs to solve the ODE

$$f'(t) = -f(t)^{\nu_q \epsilon_q} (1 - \nu_q) - f(t) \left[ \mu \nu_q + \left( \mu - \frac{\sigma^2}{2} - \int_A \bar{q}_t p(da) \right) \nu_{\bar{x}} + \frac{\sigma^2}{2} \frac{\nu_q}{\epsilon_q} - \rho \right]$$

with boundary condition  $f(T) = h^{-1/\epsilon_q}$ . This nonlinear ordinary differential equation has a closed form solution:

$$f(t) = \left[ \frac{\exp(-\epsilon_q(T-t))(1-\nu_q+hC)}{C} \right]^{-\frac{1}{\epsilon_q}} \quad (22)$$

$$C = \mu\nu_q + \left( \mu - \frac{\sigma^2}{2} - \int_A \bar{q}_t p(da) \right) \nu_{\bar{x}} + \frac{\sigma^2}{2} \frac{\nu_q}{\epsilon_q} - \rho, \quad (23)$$

which in turn yields the optimal individual deforestation rate, conditional on observing  $\bar{q}$  and for any  $a$ , given by

$$\frac{q_t^a}{X_t} = \frac{\exp(-\epsilon_q C(T-t))(1-\nu_q+hC)}{C} \quad (24)$$

where  $C$  is again given by (23). The function  $f(t)$ , which is pinned down using the final boundary condition on  $V(x, \bar{x}, T)$ , depends clearly on the individual adherence  $a$ , the bequest  $h$  and continuously on a combination of all model parameters as well as the mean extraction integrated over the whole beliefs distribution. Note that for  $a = 0$  and  $p(a) = 0$  one reverts to a standard consumption problem under uncertainty.

However, (24) is not yet a solution of our problem, because it depends on the median deforestation policy  $\int_A \bar{q}_t p_0(da)$ . What is then now required is to prove the existence of a mean-field equilibrium, and thus solve a fixed point problem. We need to then prove self-consistency of the mean-field equilibrium solution  $q^{MFE}$ . Let  $q_t^*$  be a  $\mathcal{F}_t^a$ -measurable extraction policy for our problem, and assume it to be admissible, such that  $\mathbb{E} \int_0^T |(q_t^*)^2| dt < \infty$ . Let  $\bar{X}_t$  be a  $\mathcal{F}_t^a$ -measurable random variable given by  $\bar{X}_t = \exp(\mathbb{E} \log X_t^*)$ , where  $X_t^*$  is the forest cover associated with the policy  $q_t^*$ . The policy  $q_t^*$  is a mean-field equilibrium if  $q_t^*$  is optimal for each agent upon this choice of  $\bar{X}_t$ , under the consistency condition that  $\bar{X}_t = \exp \int \log x^* p(dx^*, da, t)$  for all  $t \in [0, T]$ . This implies that the equilibrium is associated with a continuum of optimal choices, weighed by each individual adherence, in a framework where essentially each agent in the continuum faces an independently distributed copy of the same optimization problem, based on the initial draw from the beliefs distribution. In other words, the equilibrium happens at the point for which  $\int_A q_t^a/x p_0(da) = \int_A \bar{q}_t p_0(da)$  for all  $t \in [0, T]$ .

This is the case if there exists a function for the population forest consumption averaged over the whole beliefs distribution  $\bar{q}_t^a : [0, T] \rightarrow [0, 1]$  that solves the fixed point relation given by

$$\int_A \bar{q}_t p_0(da) := q_t^a = \int_A \frac{\exp(-\epsilon_q C(T-t))(1-\nu_q+hC)}{C} p_0(da). \quad (25)$$

If this fixed point exists, there exists a mean-field equilibrium where each individual consumes an amount of forest inversely proportional to their *own* individual beliefs  $a$  and to the collective average actions  $\bar{q}_t^a$  of the population, which are defined by the fixed point in (25).

Assuming the right-hand side exists and is bounded, which is equivalent to assuming a reasonably

well-behaving distribution of beliefs  $p(a)$ , we study the map  $Q_A(q_t^a)_t : Q[(0, T)] \rightarrow Q[(0, T)]$  given by

$$Q_A(q^a)_t := \int_A f(t, q_t^a, a) p_0(da)$$

where  $f(t, q^a, a) = \frac{\exp(-\epsilon_q C(T-t))(1-\nu_q+hC)}{C}$ , which is the optimal policy for *any* median policy  $q^a$ . This map is a contraction, since it is defined in  $[0, T] \rightarrow [0, 1]$  and for any  $q_1^a, q_2^a \in Q^A[(0, T)]$  in which  $q_i^a = \int_A q_i p(da)$  (i.e. the dependence on  $a$  has been integrated out) one has

$$\begin{aligned} |Q_A(q_1^a)_t - Q_A(q_2^a)_t| &= \sup_{t \in [0, T]} \left| \int_A f(t, q_1^a, a)^{-\frac{1}{\epsilon_q}} p_0(da) - \int_A f(t, q_2^a, a)^{-\frac{1}{\epsilon_q}} p_0(da) \right| \\ &= \sup_{t \in [0, T]} \left| \int_A \left[ f(t, q_1^a, a)^{-\frac{1}{\epsilon_q}} - f(t, q_2^a, a)^{-\frac{1}{\epsilon_q}} \right] p_0(da) \right| \\ &\leq \int_A \left[ 1 - \nu_q + h \left( \mu \nu_q + \left( \mu - \frac{\sigma^2}{2} \right) \nu_{\bar{x}} + \frac{\sigma^2}{2} \frac{\nu_q}{\epsilon_q} \right) \right] \times \\ &\quad \times \frac{h |q_1^a - q_2^a| \exp(-\epsilon_q \nu_{\bar{x}} |q_1^a - q_2^a| T)}{\nu_{\bar{x}}} p_0(da) \\ &\leq \bar{Q} \|q_1^a - q_2^a\|, \end{aligned}$$

for some constant  $\bar{Q}$  in which  $a$  has been integrated out, since  $a$  is a random variable with bounded support  $A \in [0, 1]$  and all terms  $\nu_q, \nu_{\bar{x}}, \epsilon_q, 1/\epsilon_q$  are bounded for all realisations of  $a \in A$ . Note also that  $\epsilon_q \rightarrow 1$  as  $a \rightarrow 0$ . One then can apply Banach's fixed point theorem which guarantees the existence of a solution  $\bar{q}_t^* := \int_A \bar{q}_t^* p_0(da)$ . There thus exists an equilibrium deforestation rate for all times  $t \in [0, T]$  and adherences  $a \in p_0(a)$ ,  $q_t^{MFE}$ , given by

$$q_t^{MFE} = \frac{\exp(-\epsilon_q C \bar{q}_t^* (T-t)) (1 - \nu_q + h C \bar{q}_t^*)}{C \bar{q}_t^*} \quad (26)$$

$$C \bar{q}_t^* = \mu \nu_q + \left( \mu - \frac{\sigma^2}{2} - \bar{q}_t^* \right) \nu_{\bar{x}} + \frac{\sigma^2}{2} \frac{\nu_q}{\epsilon_q} - \rho, \quad (27)$$

and  $\bar{q}_t^*$  solves (25).

Consider now the infinite horizon case  $T \rightarrow \infty$ . The HJB equation (21) is then solved by setting  $V_t = 0$ , and we have a stationary solution  $q_t^a = q^a$  by using the *ansatz*

$$V(x, \bar{x}) = B \frac{x^{g_1(1-\gamma)} \bar{x}^{g_2(1-\gamma)}}{1-\gamma}.$$

By similar computations as before, we can obtain the individual deforestation policy, conditional on the median policy  $\int_A \bar{q} p_0(da)$  given by

$$q^a = \epsilon_q \left( \rho - \mu(\nu_q + \nu_{\bar{x}}) - \frac{\sigma^2}{2} \left( \frac{\nu_q}{\epsilon_q} + \nu_{\bar{x}} \right) + \nu_{\bar{x}} \bar{q}^a \right) X_t.$$

The equilibrium is achieved by imposing the self-consistency condition

$$\int_A q^a p_0(da) = \int_A \bar{q}^a p_0(da)$$

Integrating the optimal policy over all adherence levels  $a$ , one obtains the equilibrium condition

$$\int_A \bar{q} p_0(da) = \int_A \epsilon_q \left( \rho - \mu(\nu_q + \nu_{\bar{x}}) - \frac{\sigma^2}{2} \left( \frac{\nu_q}{\epsilon_q} + \nu_{\bar{x}} \right) + \nu_{\bar{x}} \int_A \bar{q} p_0(da) \right) p_0(da).$$

One can then use the law of iterated expectations, solve for the equilibrium median policy, and obtain Equation (10) in Proposition 1.

Figure 5 in the paper shows the shape of the stationary deforestation rate  $q^{MFE}$ . The left-hand panel is for a model with only pro-environmental attitudes, where  $g_1 = 0$  for all  $a$ , and ATR adherence affects individual utility only via global scarcity. The panel plots the equilibrium deforestation rate  $q^{pro}$  for three different choices of  $g_2$ , linear ( $g_1 = a$ ), quadratic and cubic, in order to uncover patterns that can then be matched with the data. The interpretation of  $g_2$  is straightforward: the more its convexity increases, and the more individuals will only care about the state of the environment only for “high” levels of ATR adherence. This is directly reflected in the shape of the deforestation policy. The right-hand panel shows the model with both  $g_1, g_2 \geq 0$ , such that individuals care both about their own local forest, via sacralization of their lived environment, and the (average) global state of the forest across the entire population. The panel shows that if local forest consumption and global scarcity are perfect substitutes (i.e.  $g_1 + g_2 = 1$ ), then the optimal deforestation policy is nonlinear even for linear choices for  $g_1, g_2$ , and the two mechanisms of valuing local vs. global environment balance each other except for high levels of ATR adherence. For both scenarios, Figure 5 shows that for high levels of adherence deforestation can switch from unsustainable (above the dashed line, equal to  $\mu - \sigma^2/2$ ) to sustainable, such that one observes a net forest growth even with active deforestation. This switch is not possible if individuals’ adherence affects only local forest use and there are no pro-environmental attitudes at play.

For reference, it is useful to show the more compact expression for the optimal deforestation rate when ATR influences forest utility only via pro-environmental attitudes, i.e. when  $g_1 = 1$  everywhere and assume  $g_2(a) = a^k$ , where  $k \in \mathbb{R}^+$ . This form of  $g_2$  allows to flexibly specify the shape of the ATR-environment nexus, such that the higher is  $k$ , the more individuals care about the environment only for high levels of adherence. We then have

$$q^{\text{pro}} = q_{a=0}^* + \frac{\nu_{\bar{x}}}{\gamma} \left( \mu - \frac{\sigma^2}{2} - \frac{\gamma q_{a=0}^* - (\mu - \frac{\sigma^2}{2})(1 - \gamma)\langle \bar{a}^k \rangle}{1 - (1 - \gamma)\langle \bar{a}^k \rangle} \right) \quad (28)$$

$$q_a^* = \epsilon_q \left[ \rho - \mu \nu_q - \frac{\sigma^2 \nu_q}{2 \epsilon_q} \right] \quad (29)$$

where the quantity  $q_{a=0}^*$  is the optimal deforestation policy (29) when  $a = 0$  everywhere, without any effect played by both ATR adherence and pro-environmental beliefs,  $\langle \bar{a}^k \rangle := \int_A a^k p_0(da)$  is the  $k$ -th raw moment of the ATR adherence distribution across the population and  $q_a^*$  is the optimal deforestation policy without pro-environmental beliefs, i.e. when  $g_2 = 0$  everywhere, there are no interactions and each individual chooses its deforestation policy based only on observing local forest stocks. Note that  $\epsilon_q(0) = \gamma$ , so that in absence of ATR beliefs the elasticity of intertemporal substitution of deforestation is the inverse of risk aversion. Here  $q_0^*$  is essentially an upper bound, and since  $g_2' > 0, \nu_{\bar{x}} < 0 \forall a \in A$ , the deforestation rate with only pro-environmental beliefs is thus a *reduction* in deforestation with respect to the “no ATR, no interactions” rate.

Once equipped with  $q^{MFE}$ , one can integrate in time the equilibrium Kolmogorov equation to obtain the (transition) forest spatial density . We can now use the linearity in  $x$  of (28) for both finite and infinite time and the decomposition (12) to obtain the measure  $p(x, a, t)$ . Using the Kolmogorov forward equation at the optimal control  $q_t^{MFE}$  for the joint distribution  $p(x, a, t)$  we obtain

$$\partial_t p(x, a, t) = -\partial_x \left[ \mu - \frac{\exp(-\epsilon_q C^{\bar{q}_t^*} (T - t)) (1 - \nu_q + h C^{\bar{q}_t^*})}{C^{\bar{q}_t^*}} \right] x p(x, a, t) + \frac{\sigma^2}{2} \partial_{xx} x^2 p(x, a, t).$$

where  $C^{\bar{q}_t^*}$  is given by (27) and is evaluated at the equilibrium median deforestation rate  $\bar{q}_t^*$ . Since  $p_0(da)$  is a probability measure, we can apply the dominated convergence theorem and integrate the PDE over the domain  $A$ , using (12) and the time invariance of  $p_0$ , which yields

$$p_0(a) \partial_t p^a(x, t) = -p_0(a) \partial_x \left[ \mu - \frac{\exp(-\epsilon_q C^{\bar{q}_t^*} (T - t)) (1 - \nu_q + h C^{\bar{q}_t^*})}{C^{\bar{q}_t^*}} \right] x p^a(x, t) + \frac{\sigma^2}{2} p_0(a) \partial_{xx} x^2 p^a(x, t).$$

Integrating in time and using very well-known results, one obtains that solving the above PDE under the normalization condition  $\int p^a(dx, t) = 1$  yields a transition density given by

$$p(dx, da, t) = \frac{p_0(da)}{dx \sigma \sqrt{2\pi t}} \exp \left( -\frac{1}{2\sigma^2 t} \left[ \log(dx) - \left( \mu - \frac{\sigma^2}{2} - \int_0^t \frac{\exp(-\epsilon_q C^{\bar{q}_s^*} (T - s)) (1 - \nu_q + h C^{\bar{q}_s^*})}{C^{\bar{q}_s^*}} ds \right) t \right]^2 \right),$$

with starting condition  $p(x, a, 0) = p_0(a)p_0(x, 0)$ . The reader can now verify that the same applies

without the time integral for the infinite horizon case  $q^{MFE}$  shown in Proposition 1, and that the cross-sectional spatial forest density evolves in time according to the log-normal transition density.

As a more explicit example, the forest cover starting in year  $t_0$  for any individual  $i$  with adherence  $a$  and only pro-environmental beliefs ( $g_1 = 0$  for all  $a$ , assuming an infinite horizon and  $g_2 = a^k$  for  $k$  positive integer) evolves according to the transition density

$$p^a(x, t|x_0, t_0) = \frac{1}{x\sigma\sqrt{2\pi(t-t_0)}} \exp\left(-\frac{1}{2\sigma^2(t-t_0)} \left[ \log\left(\frac{x}{x_0}\right) - \left(\mu - \frac{\sigma^2}{2} - q_0^* + \frac{1}{\gamma} \left[ \nu_{\bar{x}} \left( \mu - \frac{\sigma^2}{2} - \frac{\gamma q_0^* - (\mu - \frac{\sigma^2}{2})(1-\gamma)\langle \bar{a}^k \rangle}{1 - (1-\gamma)\langle \bar{a}^k \rangle} \right) \right] \right] \right)^2\right)$$

where  $\bar{a}^k = \int_A a^k p_0(da)$  is the  $k$ -th raw moment of the beliefs distribution.

An Ito process with (30) as transition density, however, has no stationary distribution, as the cross-sectional variance explodes in time unless deforestation is unsustainable, i.e.  $\mu - \sigma^2/2 - q_t^{MFE} < 0$ , and in such a case it is a degenerate one  $\delta(x=0)$  - no more forest. We therefore exploit the fact that there is a maximum forest area available to the agents  $S$ , identifiable as the total overall geographical area available for the population. We therefore augment (14) with a reflection term  $-dL_t$ , where  $L_t$  is a nonnegative, right-continuous and nondecreasing process that occurs both instantaneously as well as with infinitesimal magnitude (so that the sample paths of  $X_t$  are always continuous) whenever  $X_t = S$ ,  $\mathcal{F}_t^a$ -measurable for all  $t \geq 0$  and thus adapted to  $\mathcal{F}_t^a$  generated by the Brownian motion process together with the adherence distribution. The term  $dL_t$  is of finite variation, and the measure of the time spent on the boundary has Lebesgue measure zero with probability one. This term does not affect the optimal deforestation policy, as it is in feedback form, linear in  $X_t$  and the boundary condition of the HJB equation is one for a final time  $T$ , as well as a natural one  $V(0, t) = 0$  which is easily satisfied by our policy and is unaffected by the upper bound. Furthermore, we have by construction  $dt dL = dW dL = dL dL = 0$  and thus the policy remains the one shown in Proposition 1. It does however affect the transition density: we need to solve the KFE (17) now with an added Robin condition that the conditional probability mass of at the boundary is zero. We evaluate the limit of a very useful result by [Vestraeten \(2004\)](#), using the boundary condition given by

$$\lim_{x \rightarrow S} \frac{\sigma^2}{2} \partial_x x p^a(x, t|x_0, t_0) - \mu^* x p^a(x, t|x_0, t_0) = 0$$

where we define

$$\mu^* := \mu - \frac{\sigma^2}{2} - \int_0^t \frac{\exp(-\epsilon_q C^{\bar{q}_s^*} (T-s)) (1 - \nu_q + h C^{\bar{q}_s^*})}{C^{\bar{q}_s^*}} ds,$$

and obtain the equilibrium transition density with reflections at  $S$  as

$$\begin{aligned}
p^a(x, t|x_0, t_0) &= \frac{1}{x\sigma\sqrt{2\pi t}} \exp\left[-\frac{(\ln x - \ln x_0 - \mu^*(t - t_0))^2}{2\sigma^2(t - t_0)}\right] + \\
&+ \frac{1}{x\sigma\sqrt{2\pi t}} \exp\left[-\frac{2\mu^*}{\sigma^2}(\ln S + \ln x_0)\right] \exp\left[-\frac{(\ln x - \ln x_0 + 2\ln S - \mu^*(t - t_0))^2}{2\sigma^2(t - t_0)}\right] + \\
&+ \frac{2\mu^*}{\sigma^2 x} \exp\left[-\frac{2\mu^*}{\sigma^2}(\ln S - \ln x)\right] \Phi\left(\frac{\ln x + \ln x_0 - 2\ln S + \mu(t - t_0)}{\sigma(t - t_0)}\right)
\end{aligned} \tag{30}$$

where  $\Phi(z)$  is the Gaussian CDF. The stationary distribution  $p^a(x)$  is obtained setting  $\partial_t p^a = 0$  in the KFE, using  $\mu^* \rightarrow \mu^s := \mu - \sigma^2/2 - q^{MFE}$ , and after defining  $y := \ln x$  is obtained by solving

$$0 = -\mu^s \partial_y y p^a + \frac{\sigma^2}{2} \partial_{yy} y^2 p^a$$

with the boundary condition  $p^a(S) = 0$ , and is a power law-type distribution in  $x$  (exponential in  $y$ ) given by

$$p^a(y) = C \frac{\sigma^2}{2\mu^s} \left( S^{\frac{2\mu^s}{\sigma^2}} - e^{\frac{2\mu^s}{\sigma^2} y} \right) \tag{31}$$

where  $C$  is a normalization constant. We note that a very similar result would be obtained by imposing instead a lower reflection boundary  $S$ , i.e. a minimum forest size (one tree, for example), or individual births and deaths, one of many stabilizing forces that can be found in the Appendix of [Gabaix et al. \(2016\)](#) that generate power law-type stationary distributions.

## E Proof of Proposition 2

Assume  $a = 0$ , and hence  $g_1 = 1, g_2 = 0$ . It's then clear that  $q_0^* \geq 0$  since we assumed  $\rho > \mu(1 - \gamma) - \frac{\sigma^2}{2}\gamma(1 - \gamma)$  for the problem to be well-posed. Because of our parametric assumption, then it's easily seen that  $\partial_a q_a^* < 0$  for all  $a$ . Then  $q_1^* = \rho < q_0^*$  and therefore  $q_a^* \geq 0$  for all  $a \in A$ . Since  $g_2' < 0$  by assumption, then if  $\gamma < 1$   $\partial_a \nu_{\bar{x}} < 0$  and one can see that  $\frac{\gamma q_0^* - (\mu - \frac{\sigma^2}{2})(1 - \gamma)\langle a^k \rangle}{1 - (1 - \gamma)\langle a^k \rangle} > \mu - \frac{\sigma^2}{2}$ , and viceversa for  $\gamma < 1$ , so it follows that  $\partial_a q^{pro} \leq 0$  for all  $a \in A$ . Note this is exactly what (15) implies, in a simplified scenario and for our particular choice of  $u$ . One can make the same argument using the same parametric restriction, albeit for a more complicated expression, for the general policy given by Eq. (10) in the paper.

Let us now show the impact on individual deforestation policies of a change in the beliefs distribution in the population. Let  $\mu_a$  be a parameter (or a combination of parameters) that regulates the first-order stochastic dominance between different parametrizations of the beliefs distribution, i.e.

$$\mu_a \text{ s.t. } \frac{d}{d\mu_a} \int_A a \times p_0^{(\mu_a)}(da) > 0. \tag{32}$$

Firstly, since  $p_0(a)$  is a probability measure it is Lebesgue-integrable and so is its cumulative density  $P_0(a)$ . Parametrizing both as  $p_0(a; \mu_a)$  and  $P_0(a; \mu_a)$  and assuming that  $\partial_{\mu_a} p_0, \partial_{\mu_a} P_0$  exist and are bounded (a simple requirement that holds for most non-degenerate parametrized distributions), for any bounded and continuous function  $f(a)$  one can apply the bounded convergence theorem and show that

$$\frac{d}{d\mu_a} \int_A f(a) p_0(da; \mu_a) = \int_A f(a) \partial_{\mu_a} p_0(da; \mu_a).$$

Integrating by parts and using Fubini's theorem we obtain

$$\int_A f(\bar{a}) \partial_{\mu_a} p_0(d\bar{a}; \mu_a) = f(a) \partial_{\mu_a} P_0(a; \mu_a) \Big|_0^{\bar{A}} - \int_A f'(a) \partial_{\mu_a} P_0(da; \mu_a), \quad (33)$$

where  $\bar{A}$  is the upper boundary of the domain of the beliefs distribution. For distributions in a bounded domain, which applies for example such as the uniform and Beta distributions, one has

$$\int_A f(\bar{a}) \partial_{\mu_a} p_0(d\bar{a}; \mu_a) = f(\bar{A}) \partial_{\mu_a} P_0(\bar{A}; \mu_a) - \int_A f'(a) \partial_{\mu_a} P_0(da; \mu_a).$$

Furthermore, by the definition (32) of first-order stochastic dominance, an increase in the parameter that ranks the beliefs distributions in such order must generate a shift to the right of the beliefs CDF, hence  $\partial_{\mu_a} P_0(da) \leq 0$ . Hence, the first term on the right-hand side of the previous expression is zero at its maximum, achieved at  $\bar{A}$ . It immediately follows that  $\int_A f(\bar{a}) \partial_{\mu_a} p_0(d\bar{a}; \mu_a) = f(0) \partial_{\mu_a} P_0(0; \mu_a) - \int_A f'(a) \partial_{\mu_a} P_0(da; \mu_a)$ . Now applying this result to our functional forms, one can see that for (28) we have  $f = g_2$ , and  $g_2(0) = 0$ , so it's easily checked that  $dq^{pro}/d\mu_a \geq 0$ , implying that since global deforestation increases with decreasing global adherence, pro-environmental beliefs imply that individuals react to increasing scarcity with reduced individual deforestation policies. For the general form of the solution given by Equation (10) in the paper, one needs to apply the same result to each term, noting that  $g_1(0) = 1$  and so  $\epsilon_q(0) = \gamma^{-1}$ , and  $\nu_{\bar{x}}(0) = 0$ , and it's easily checked that  $dq^{MFE}/d\mu_a \geq 0$  and  $dq^{MFE}/d\mu_a = 0$  for  $a = 0$  (i.e. when there are no pro-environmental beliefs).

Regarding the switch from unsustainable to sustainable, one first sees immediately that without pro-environmental beliefs ( $g_2 = 0$ ) the optimal deforestation policy can only either be sustainable or unsustainable regardless of adherence, since for  $\gamma < 1$  in order for the problem to be well-defined one must have the forest growth rate  $\mu$  low enough to satisfy the parametric assumption, and hence since  $\partial_a q_a^* \leq 0$  for all  $a$  deforestation will always be unsustainable. Viceversa for sustainable deforestation, which occurs if  $\gamma > 1$ . Now, if one introduces back pro-environmental beliefs and  $g_2 \neq 0$ , Then, noting that  $\nu_{\bar{x}}(0) = 0$  and that for  $\gamma > 1$  we have  $\nu_{\bar{x}} < 0$  for all  $a$ , then one can see immediately that for  $\gamma > 1$  there exist  $\mu, \sigma, \mu_a$  such that  $q^{pro} < \mu - \frac{\sigma^2}{2}$  for some  $a \in A$ . Then since  $g_1, g_2$  are continuous functions of  $a$ , because of the intermediate value theorem there exists an  $\underline{a} \in A$  such that  $q^{pro}(\underline{a})$  switches from unsustainable to sustainable.

Proposition 2 describes the key characteristics of the equilibrium deforestation policy. The first char-

acteristic, as also evidenced by the reduced form, implies that a greater individual adherence yields a lower deforestation rate. One can observe in Equation (10) in the paper that the equilibrium individual deforestation rate is determined by the interplay of individual adherence to ATR and the median forest cover across the population, which is determined continuously by the median deforestation rate  $\tilde{q}^*$ , whose heterogeneity is driven by the global distribution of ATR beliefs. A decrease in first-order stochastic dominance for the ATR distribution, therefore, yields a global average increase in deforestation, since there are “less adherents” across the population with less pro-environmental concerns, which yields a higher aggregate deforestation and lower aggregate forest cover. In turn, individuals with nonzero adherence which have not been personally affected by the change in ATR population distribution (i.e. it wasn’t them who changed adherence) observe this change and as a response decrease in  $dt$  their own deforestation policy based on their own preferences (i.e. their own adherence  $a$ ), the “average“ deforestation policy across all levels of adherence (the mean field) adjusts and the system remains in equilibrium.

## F Estimation of the model parameters

We first estimate the beliefs distribution  $p_0(a)$  from the data. We first focus on the 2013 cross-section of our data, and normalise adherence in terms of the “representative adherent”, shown by the percentage of ATR adherence for each arrondissement in Benin. Given that our adherence measure is between 0 and 1, a natural candidate for its distribution is the Beta distribution, parametrised with the positive parameters  $\alpha, \beta$  such that the distribution mean is given by  $\frac{\alpha}{\alpha+\beta}$ . We start with an initial guess of  $\alpha = \hat{\mu}_a(1 - \hat{\mu}_a)/\hat{s}_a^2 - 1$  and  $\beta = (1 - \hat{\mu}_a)(\hat{\mu}_a(1 - \hat{\mu}_a)/\hat{s}_a^2) - 1$ , where  $\hat{\mu}_a, \hat{s}_a$  are the mean and standard deviation of the observed ATR beliefs in the data, and estimate the parameters via maximum likelihood. We obtain that a Beta distribution with  $\alpha = 0.553$  (s.d. 0.028) and  $\beta = 2.251$  (s.d. 0.151) is an excellent fit for our data (see Figure F1).

We estimate the “untouched” growth parameter  $\mu$  as follows. We first obtain the forest cover data for areas of WAP falling within Benin corresponding to the W and Pendjari national parks. The forest cover grid cells that we keep for our estimates yield the Core Park area shown in Figure A14. Suppose  $p(X_{it}, t|X_{it-1}, t-1; \Theta)$  is the transition probability density of the area. The Markov property of Eq. (6) of the paper implies a log-likelihood function for the discrete sample given by  $l_{TD}(\Theta) = \log(p(X_{it}, t|X_{it-1}, t-1; \Theta))$  where  $\Theta = [\mu, \sigma]$ . The resulting estimator will be consistent, asymptotically normally distributed and asymptotically efficient under the usual regularity conditions for maximum likelihood estimation in dynamic models. To perform exact ML estimation, one needs a closed form expression for  $l_{TD}(\Theta)$ . It is a well-known result that an uncontrolled geometric Brownian motion, via solving its corresponding Kolmogorov equation, admits a closed form, log-normal transition density:

$$p^{WAP}(x, t + dt|x_0, t; \Theta) = \frac{1}{x\sigma\sqrt{2\pi dt}} \exp\left(-\frac{1}{2\sigma^2 dt} \left[\log\left(\frac{x}{x_0}\right) - \left(\mu - \frac{\sigma^2}{2}\right)t\right]^2\right). \quad (34)$$

Equipped with (34), the likelihood function can be easily constructed using the  $n$  available observations

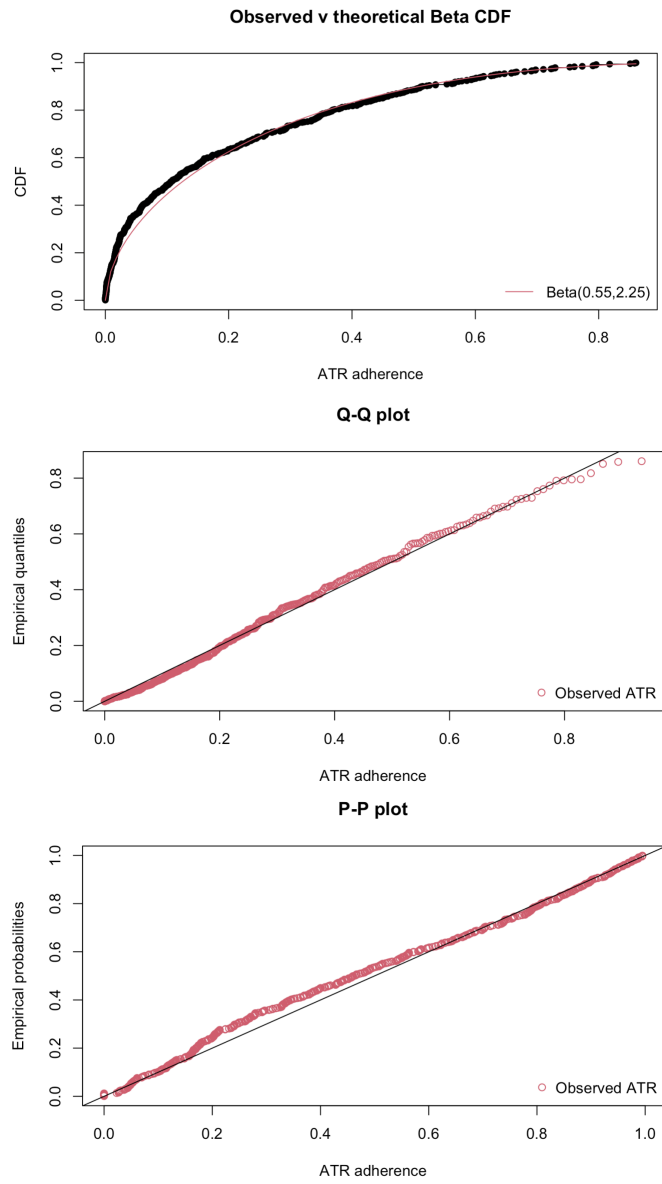


Figure F1: Maximum likelihood estimation of  $p_0(a)$ : Observed v theoretical Beta CDF (top), Empirical v theoretical quantiles (middle) and estimated probabilities (bottom).

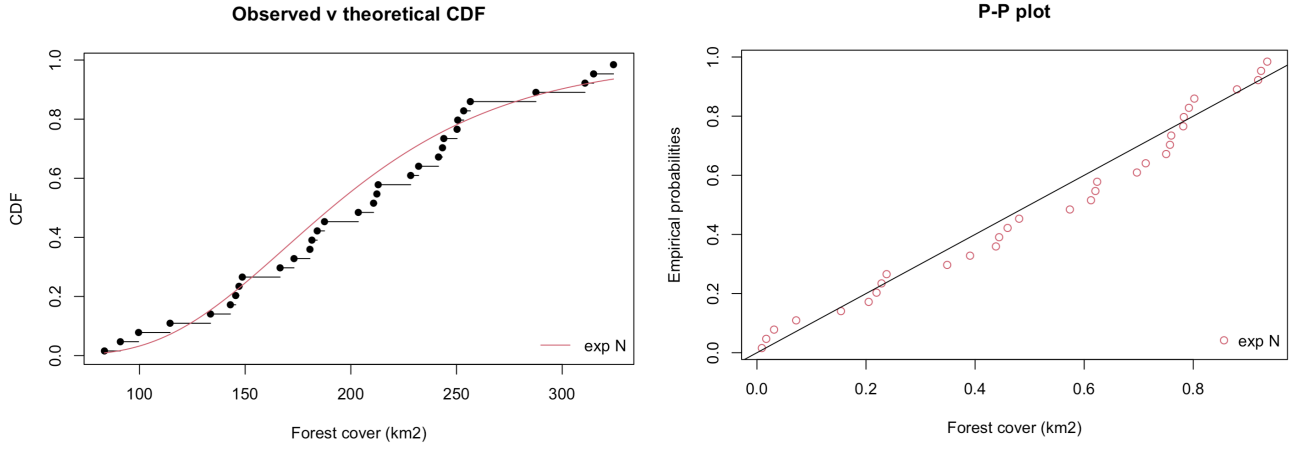


Figure F2: Maximum likelihood estimation of  $p(X_{it}|X_{it-1}, \theta)$  as the log-normal transition density (34)

in  $T$  as

$$L_n(\Theta) = \prod_{i=1, t=1}^{n, T} p^{WAP}(X_{it+\Delta t}, t + \Delta t | X_{it}, t; \Theta) p^{WAP}(X_{i,0}). \quad (35)$$

Setting all  $p^{WAP}(X_{i,0}) = 1$  as typically done (its weight decays quickly with observations), the log-likelihood to be maximized is

$$\ell_n(\Theta) = \log L_n(\Theta) = \sum_{i=1}^n \sum_{t=1}^T \ell_i(\Theta) \quad (36)$$

$$= \sum_{i=1}^n \sum_{t=1}^T \log p^{WAP}(X_{it+\Delta t}, t + \Delta t | X_{it}, t; \Theta). \quad (37)$$

The discretization of the time grid has to be equivalent to the yearly frequency of the data, and thus we fix  $\Delta t = 1$ . Estimation is obtained by bootstrapped maximum likelihood, and we obtain  $\mu = 0.0482$  with a standard deviation of 0.003. The data seems to be in good agreement with a log-normal transition density fit, as shown by Figure F2. In order to obtain  $\sigma^2$  we use the entirety of Benin's forest cover, and exclude the top 1%-sized not to have our estimates driven by outliers. We obtain a ML estimate of the drift of 0.018 (std. dev. 0.047), statistically not significant, which is a reassuring result given that using the entirety of Benin data yields a drift estimate net of deforestation and thus not allowing to estimate  $\mu$ , as described in the main text. The estimate of  $\sigma$  is not statistically different if estimated on WAP data (0.346 with std. dev. 0.045, the lower bound of a 95% CI is 0.26), but is noisier as it's evaluated over a substantially smaller area.

Estimation of the moment condition shown in Equation (11) of the paper is done using  $\mathcal{F}_t^a = \sigma\{X_{it}, \Delta t\}$  as the  $\sigma$ -field generated by the  $\Delta t$ -sampled observations until  $X_{it}$ . We rewrite the moment condition as

$$\mathbb{E} \left[ \frac{X_{it+\Delta t} - X_{it}}{X_{it}} - \hat{\mu} - q^{MFE}(a_i) \middle| \mathcal{F}_t^a \right] = 0,$$

which identifies the required parameter  $\gamma$  over the sampled discretized processes in  $\Delta t$ . However, it is well-known that the conditional moments of a discretized diffusion process do not necessarily coincide with the conditional moments of its continuous-time equivalent. What we want to obtain is to simply condition on the  $a_i$ , which is the entire sample variation on ATR adherence. In other words, we want to switch from conditional to unconditional moments. This is not a trivial change: however, we exploit the fact that  $q^{MFE}$  is stationary and only dependent on  $a_i$ . We therefore exploit space (the measured ATR adherence across arrondissements and years) rather than time for identification. We stack each increment of  $\frac{X_{it+\Delta t} - X_{it}}{X_{it}}$ , over the 3 survey years, write it as  $\Delta X_i / X_i$  and can then write

$$\mathbb{E} [\Delta X_i / X_i - \hat{\mu} - q^{MFE}(a_i)] = 0. \quad (38)$$

Equation (38) is therefore an unconditional moment condition. By exploiting the spatial variation over the sample periods of ATR, we bypass this difficulty and obtain consistent estimates of  $\gamma$ . Estimation is then done over the condition (38) using a standard two-step GMM procedure.

Lastly, in order to validate our modeling choices for estimation, Figure F3 shows the estimated non-parametric relationship between ATR adherence and tree canopy growth implied by our model  $\Delta X_i = f(a_i) + \epsilon_i$  for the three stacked observed years  $t = \{1992, 2002, 2013\}$ . The linearity validates our choice of  $k = 1$ , even though changing the functional shape of  $g_2(a) = a^k$  via  $k$  does not affect our results significantly as we have shown in the main text. We allow for different year intercepts (year dummies), due to the census sampling different individuals across each of the 10-year intervals that separates each wave, and estimate the function  $g$  using straightforward local linear regression methods, a bootstrapped error band and a bandwidth that uses Kullback-Leibler cross-validation.

We also obtain an identical estimate of 2.35 (std. dev. 0.86) when estimating  $\gamma$  ( $k = 1$ ) using the moment condition shown in Eq. (11) of the paper, together with the condition

$$\mathbb{E} \left[ \left( \frac{X_{it+\Delta t} - X_{it}}{X_{it}} - \mathbb{E}_{p_0}[(\hat{\mu} - q^{MFE}(a_i))\Delta t] \right)^2 \middle| \mathcal{F}_t^a \right] - \sigma^2 X_{it} \Delta t = 0,$$

with the p-value of the J over-id test failing to reject with more than 99% confidence. These two robustness results dampen potential concerns that the estimation of  $\gamma$  might be over-sensitive to the choice of  $g_2$  or of moment condition.

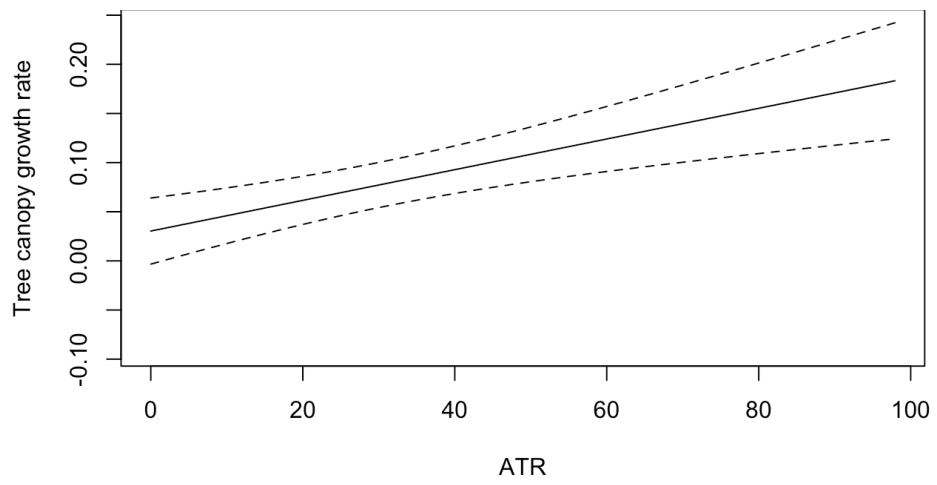


Figure F3: Estimated nonparametric relationship between  $\Delta X_i/X_i$  and  $a_i$ .